PETROGENESIS

OF THE

ESHOWE MELILITITES

BY

ELIZABETH ANNE COLGAN

Thesis submitted in the fulfillment of the requirements for the degree of Master of Science in the Department of Geochemistry, University of Cape Town. February 1992.

DECLARATION

I hereby declare that all the work presented in this thesis is my own, except where otherwise stated in the text.

Signed by candidate

Signature Removed

E.A. Colgan
February 1992

TABLE OF CONTENTS

CHAPTER FOUR : MINERALOGY

CHAPTER FIVE : MINERAL CHEMISTRY

CHAPTER SIX : WHOLE ROCK GEOCHEMISTRY

CHAPTER SEVEN : PETROGENESIS

LIST OF TABLES

LIST OF FIGURES

LIST OF PLATES

ABSTRACT

The Eshowe melilitites intruded marginal cratonic crust at approximately 80my. Their intrusion followed after a long period of extensive rift tectonism associated with the breakup of Gondwanaland. The intrusives represent the final phase of alkaline and basaltic magmatism that commenced at about 200my. This magmatism was probably related to mantle processes responsible for the continental fragmentation and was controlled by a fluctuating mantle thermal regime. The Eshowe melilitites intrude an area of attenuated crust in an essentially rift valley setting.

Petrological, and chemical evidence suggest that the Emtilombo melilitite does not represent crystallisation of a primary magma. The magma was generated in the asthenosphere but reacted with incompatible element and probably CO_2 and H_2O enriched lithosphere and perhaps crustal sources on its way to the surface. The Emtilombo melilitite contains microxenoliths of mantle derived spinel peridotite and of a suite of dunitic rocks that are believed to be high pressure cumulates of earlier alkaline magmas. These latter trapped melts would have introduced metasomatising agents into the lithosphere. The dunitic melts are believed to represent earlier intrusions related to the Eshowe alkaline volcanism. The chemistry of the olivine phenocrysts and microphenocrysts and complex zonation patterns on olivine xenocrysts (macrocryst and some

complex phenocrysts) suggest the Emtilombo magma formed by mixing of several batches of melt. The 'parental magmas' to the Eshowe occurrences are therefore considered to consist of a mixture of asthenospheric and lithosperic components and a variety of different melts. The 'parental magma' to the Emtilombo dyke was an incompatible element enriched ultramafic melt that contained microxenoliths of spinel lherzolite and the dunitic suite of rocks.

Changing oxygen fugacities are believed to be controlled by a loss of volatiles at relatively shallow depths in the mantle or lower crust. These changes are reflected by the spinel chemical trends and perovskite crystallisation. The change occurred after complex zonation patterns had developed on the olivines. The microphenocryst olivines are believed to be the only population of grains that crystallised from the Emtilombo 'parental magma'.

Mode of emplacement of the melilitites is probably influenced by the nature and volume of magma in the intrusion, its volatile content, and to some extent the nature of the country rock. The Eshowe melilitites show a wide variety of intrusive modes and also demonstrate how late stage processes, possibly during or post consolidation, influence the geochemistry of the rock type.

CHAPTER ONE

INTRODUCTION

1.1 GENERAL INTRODUCTION

Six olivine melilitites occur near the town of Eshowe in northern Natal, on the east coast of South Africa. The occurrences were located as surface ilmenite anomalies during routine heavy-mineral loam sampling by De Beers prospecting teams in 1978 to 1980. A further four ilmenite anomalies occur in the area suggesting that more occurrences of this nature are present. These anomalies were not followed up as the associated intrusives have no economic potential.

1.2 PRESENT STUDY

Very little previous work has been done on the Eshowe melilitites. Location and petrography of the intrusions were briefly described in the Third International Kimberlite Conference Abstracts (Colgan 1982). A more detailed description of the occurrences, their geological and tectonic setting and petrogenesis was presented at the Fourth International Kimberlite Conference and a paper published in the Conference Volumes (Colgan et al. 1989). Apart from this no further published information is available.

The Eshowe intrusives occur in an area of complex basement that has undergone a long history of recurrent extensional tectonism. This tectonism is believed to be related to build-up of tectonics culminating in fragmentation of Gondwanaland. It is suggested that mantle processes that triggered fragmentation were also responsible for volcanicity in the area. The timing, spatial distribution and nature of the magmatism along the southern African east coast all suggest a close relationship to the tectonic development of the region.

The aim of this study is essentially to describe and characterise the Eshowe melilitites, establish their petrogenesis and determine their relationship to the basement setting and to other intrusives in the area. The project was therefore tackled with four main objectives in mind:

1. Describe the geological and tectonic setting of the Eshowe melilitites.
2. Describe geology, petrography, mineralogy and chemistry of the Eshowe melilitites.
3. Determine their petrogenesis.
4. Establish the relationship of the occurrences to their geological and tectonic setting and to other alkaline intrusives present in the area.

1.3 METHODOLOGY

Data for this study was obtained from detailed petrography and

matrix mineral, concentrate mineral, whole rock and isotope chemistry. Field work was undertaken by the author during several short visits (each visit was approximately 1 week long) to examine and, where possible map the occurrences, observe local geology and setting, collect samples and supervise a core drilling program on the Emtilombo dyke. Additional geological information was obtained from internal (De Beers) field reports and maps supplied by A.W. Robertson.

Petrography, matrix mineral chemistry and preparation of whole rock powders for geochemical investigations was undertaken by the author. Microprobe analyses of concentrate minerals were obtained by G.W. Hutchinson formerly of Anglo American Research Laboratories (AARL), whole rock analyses by J. Eastell (AARL) and isotope chemistry was done by T. Clark of the Bernard Price Institute (BPI), University of the Witwatersrand. Interpretation of data is by the author unless stated otherwise.

Details of samples collected, sample treatment and analytical techniques are outlined in Appendix 1.

CHAPTER TWO

GEOLOGICAL SETTING AND TECTONICS

2.1 GENERAL INTRODUCTION

The Eshowe olivine melilitites straddle the boundary of the 3.0 Ga Kaapvaal craton and the 1.0 Ga Natal Structural and Metamorphic Province (NSMP). The presence of melilitites in a cratonic environment is unusual, however, evidence for extensive tectonism in the region is apparent and the nature of the volcanism suggests that considerable lithospheric attenuation occurred. It was, therefore, considered important to review the basement setting and tectonic development of the area to establish how much control these factors have over volcanism and, in particular, the nature of alkaline magmatism. As sedimentary deposits in the area record the tectonic history they are described in some detail.

2.2 GEOLOGICAL AND TECTONIC SETTING

Two of the Eshowe olivine melilitites occur within the inferred southern margin of the Kaapvaal craton and four intrude the Northern Marginal Zone (nomenclature of Tankard et al. 1982) of the NSMP. This Precambrian basement is overlain by sedimentary deposits of the Natal Group and Karoo Sequence

which generally mask the craton boundary in the area. It is, however, possible to extrapolate the boundary across from eastern to western basement exposures (Charlesworth 1981, Figure 2.1). To the north of the occurrences are the Lebombo volcanics which may delineate the boundary between the craton and the Pan African Mozambique Belt (Eales et al. 1984).

Tectonic development of the region is largely associated with extensional tectonism interacting with the three basement terranes present: the Kaapvaal craton, the NSMP and the Mozambique Belt, inferred to have been present to the east in Gondwana times. Tectonism took place over a long period of time, some 400 Ma, and is considered to be related to build up to tectonics associated with and following break up of Gondwanaland.

2.2.1 PRECAMBRIAN BASEMENT

The southern Kaapvaal craton consists of granitoid basement and widely spaced greenstone belts of the Nondweni Group unconformably overlain by thick volcano-sedimentary sequences of the Nsuze Subgroup, Pongola Group (Matthews 1981a). Granitic-gneisses with calc-alkaline affinities (Charlesworth 1981, Harmer 1981) and volcano-sedimentary sequences of the NSMP have been thrust northwards over this craton (Matthews 1972, 1981a and b).

The Northern Marginal Zone of the NSMP consists of a major thrust belt and nappe complex. The thrust belt is considered by Matthews (1981a) to define the front of the mobile belt against archaean craton. This is corroborated by a change in metamorphic and structural style across the boundary. The NSMP is characterised by a general east/west structural trend, relatively high grade polyphase metamorphic overprinting and steep dips while archaean basement cover rocks, Nsuze Subgroup, are characterised by little deformation and low temperature metamorphism (Matthews 1981a, Charlesworth 1981, Matthews and Charlesworth 1981). Further evidence is provided by geochronology. Ages of 3090 Ma to 3150 Ma have been obtained from Nsuze lavas (in Matthews 1981a) and ages of 3177 Ma to 3199 Ma from granitoid gneisses of pre-Nsuze basement near the mobile belt front (Charlesworth and Matthews 1981). Ages of 900 Ma to 1194 Ma have been obtained from various localities in the NSMP (in Matthews 1981a) and Charlesworth and Matthews (1981) reports two ages of 1067 Ma and 1218 Ma from the northern front of the NSMP.

Matthews (1981a) suggests that at least 100km of overthrusting onto archaean craton occurred. If this is the case the true craton edge was about 100km south of the thrust belt at the time of formation of the NSMP. Subsequent erosion of basement exposed rocks of a deep crustal level and Matthews (1981a) estimates about 20 to 25km of cover rocks have been removed. This means that the true craton edge is now considerably less than 100km south but it is still to the south of the Eshowe

melilitites. The melilitites, therefore, all intrude Kaapvaal craton; two occur on the craton, as we see it now, and four in "over-thrust" craton (Figure 2.1).

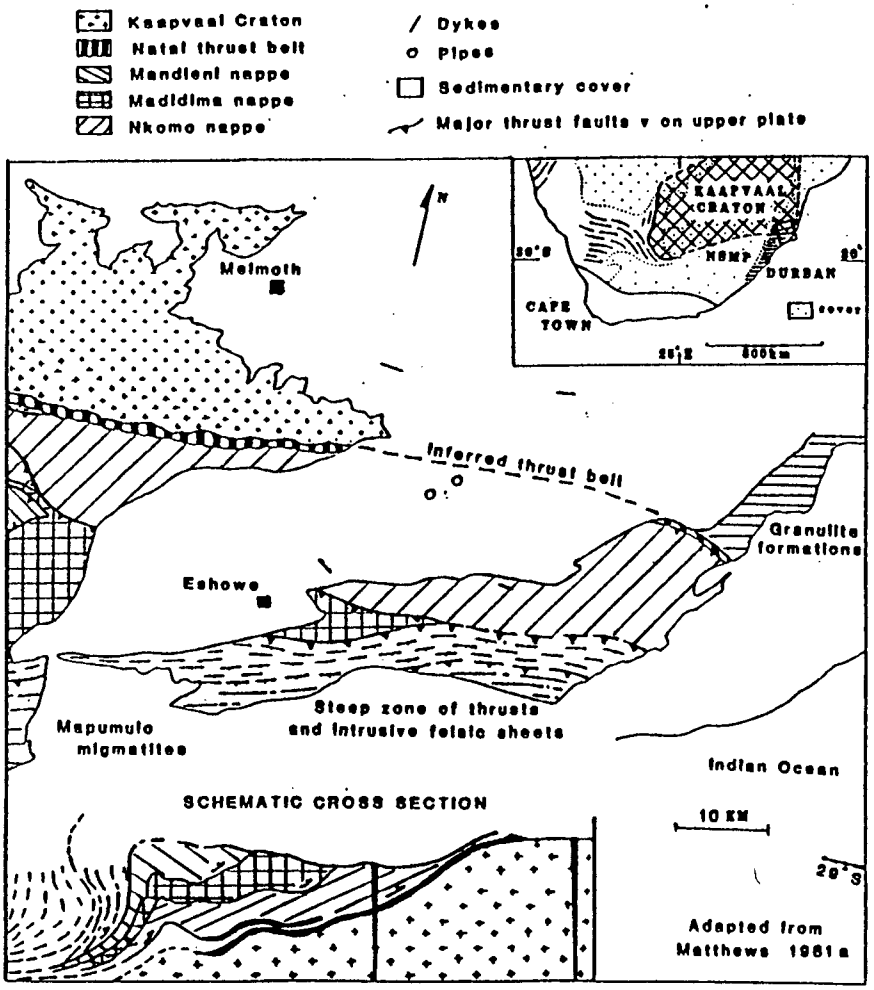

FIGURE 2.1
FRONTAL REGION OF THE NATAL STRUCTURAL AND METAMORPHIC PROVINCE (NSMP)

2.2.2 TECTONO-SEDIMENTARY HISTORY

2.2.2.1 THE MOZAMBIQUE BELT

Following formation of the NSMP structural development of the east coast shows a long history of tensional tectonics. At approximately 500 Ma the Pan African Mozambique Belt developed

(Tankard et al. 1982). This was orientated north/south and probably extended through Mozambique and across the present coastline southwards into Antarctica (Figure 2.2). Groenewald et al. (1988) suggest metamorphic terranes in Dronning Maud Land, Antarctica were continuous with the Mozambique Belt and the NSMP. The belt is, therefore, inferred to have been present to the east of Natal prior to Gondwana fragmentation. This belt represents an ancient suture zone between east and west Gondwanaland and appears to have initiated the zone of weakness along which the Super-continent eventually split.

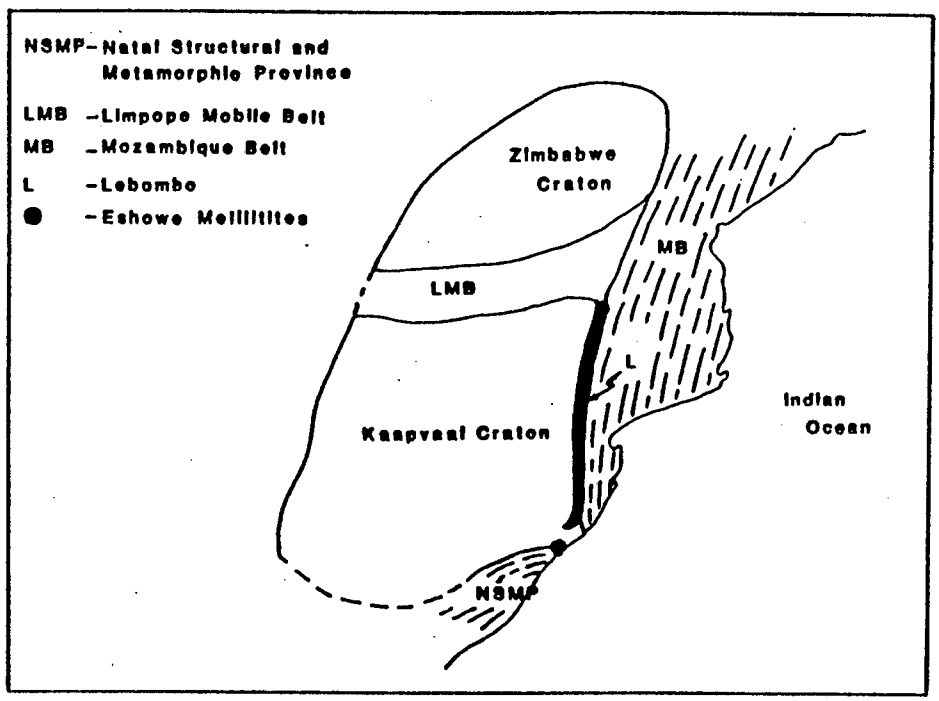

FIGURE 2.2

SCHEMATIC DIAGRAM OF THE BASEMENT STRUCTURAL UNITS

2.2.2.2 CAPE SUPERGROUP

Most of the erosion of Precambrian basement must have taken place prior to deposition of Cape Supergroup sediments. The eroded surface of the NSMP and Kaapvaal craton then formed the basement for deposition of these sediments.

Sediments of the Cape Supergroup (the Natal Group) were deposited in an elongate, down faulted trough, the Natal Embayment (Tankard et al. 1982). This was orientated roughly north-northeast, parallel to the orientation of the Mozambique Belt and sub-parallel to the present coastline. Isopach lines at the base of the Natal Group strike north-northeast in the northern sector of the Embayment but turn sharply northwest in the vicinity of Harding (Kingsley 1975). Kingsley (1975) suggests this change in direction may have been due to the influence of an east/west trending basement ridge. A ridge is present to the west of Kokstad and it possibly extends eastwards to the coast. Nixon et al. (1983) note the presence of a large fault at Matatiele, down thrown (240m) to the north. This fault extends westwards into Lesotho and may represent the western extent of the basement high. Alternatively, the latter is an imposed feature due to removal of sediment during Dwyka glaciation (Kingsly 1975).

Sedimentation into the trough was from the uplifted Northern Zululand highlands southwards into a narrow marine embayment and deposits grade from terrestrial in the north to marine in the south (Tankard et al. 1982, Hobday and Mathew 1974,

Kingsley 1975). Sediments were deposited over an undulating topography with granitic hills providing some local sources for sedimentation (Kingsley 1975).

The Natal Embayment formed as a result of abortive rifting related to approximately east/west orientated tension. Down faulting was contemporaneous with sedimentary deposition (Matthews 1961). Slump structures within sediments indicate tilting to the southeast and appear to be concentrated in the eastern part of the Embayment, perhaps indicating more extensive movement near the trough axis and where the sedimentary load was thicker. Kingsley (1975) describes three major marine transgressions. These may be related to three periods of major down faulting or, alternatively, to eustatic changes in sea level, or a combination of both. Matthews (1961) noted that the hingeline of tilting "indicated by the most western slumped beds is almost coincident with the axis of the post Karoo monoclinal flexure in this part of Natal."

Rifting resulting in formation of the Natal Embayment occurred in early Palaeozoic. On the basis of limited fossil evidence from the southern extent of the Natal Group the sediments are thought to be the time equivalent of the Witteberg Group and not pre-Devonian in age (SACS 1980). The sediments are, therefore, possibly about 400 Ma old.

2.2.2.3 KAROO SEQUENCE

Deposition of the Karoo Sequence sediments followed deposition of the Natal Group. The Natal Embayment was reactivated twice, once in late Carboniferous/early Permian (Dwyka) and once in the Permian (Ecca) to form the Natal Trough (Tankard et al. 1982). The Trough was widened westwards and extended northwards relative to the earlier Embayment and was parallel to the present Natal and Lebombo flexure (Stratten 1970). It is uncertain how far north the Trough extended during Dwyka times. Kostlin and De Gasparis (pers. comm.) using geophysical evidence outlined an "ancient zone of weakness" that extends from approximately 26° 15'S to 28°S. It occurs next to and parallels Lebombo faulting and the Rooi Rand dyke swarm, indicating extensive tensional faulting, occurs within this area (Armstrong et al. 1984). It seems possible that the area represents the faulted basin of the Natal Trough initiated during Ecca and possibly Dwyka deposition.

Dwyka glaciation followed deposition of the Natal Group in late Carboniferous/early Permian, possibly in the region of about 300 Ma. Direction of movement of ice sheets in Natal was generally southwards and Matthews (1970) suggests this was due to topographic deflection. If this is the case the reactivated Natal Embayment was largely responsible for controlling movement of the ice. Deposition of glacial debris was onto a highly irregular surface (Von Brunn 1977, Von Brunn and Gravenor 1983).

A marine incursion at the end of Dwyka glaciation, extending as far north as Tugela Rand, led to conformable deposition of Ecca sediments (Von Brunn and Gravenor 1983). Marine sediments provided a blanket cover that smoothed out major irregularities in the underlying Dwyka topography (Hobday 1973).

The Natal Trough was reactivated during deposition of Ecca sediments (at possibly about 270 Ma). Some evidence for an unstable basement in early Ecca comes from the presence of marine flysch deposits in lower Ecca sediments in Transkei (Truswell and Ryan 1969). During the middle Ecca basinal subsidence appears to have been gradual. Sediments were deposited as a series of cyclical prograding delta fronts (Hobday 1973, Hobday et al. 1975, Mason and Tavener-Smith 1978, Tavener-Smith 1979, Christie and Tavener-Smith 1979) and sedimentation more or less balanced subsidence (Hobday 1973, Whateley 1980). Subsidence within the Natal Trough appears to have been variable with localised areas showing relatively greater subsidence (eg. the Nongoma graben) and others a relatively more stable environment characterised by slower subsidence (eg. Vryheid). Further irregularities within the Trough were probably created by upfaulted areas such as the Ngoya horst. Bristow (1976) suggests the latter may represent an old basement high formed prior to intrusion of the Lebombo basalts. Middle Ecca sedimentation ended with more stable fluvial deposition followed by regional subsidence, a marine transgression and deposition of upper Ecca mudstones (Cadle

and Hobday 1977, Whateley 1980). This was followed by deposition of lower Beaufort sediments.

Little is known about deposition of the younger, Triassic, Karoo sediments (Beaufort to Stormberg Groups) along the Natal coast. In general, limited erosional outliers of Beaufort Group sediments are present, however, in some down faulted blocks, in the interior of Natal and along the Kwazulu coast parts of the sedimentary record are preserved (geological maps series 2831 DA to DB). Evidence from these deposits suggests a more stable platform sedimentation with Upper Karoo sequences thinning from the main basin northwards and eastwards over the earlier Natal Trough (Tankard et al. 1982, Dingle et al. 1983). It is inferred that sediments wedged out to the east, over Antarctica. Dingle et al. (1983) suggest that deposits thinned from a depth of about 7km in the vicinity of Grahamstown to 1km on the east coast. Spreading of sediments from the main Karoo basin over the Natal Trough, a distinct basin during Natal Group, Dwyka and middle Ecca deposition, was probably related to the regional downwarping of the continental interior and uplift along the present coast which occurred at this time.

Karoo volcanism associated with voluminous outpouring of basaltic magma along the Lebombo line was initiated at about 190 Ma (Bristow 1980), just prior to the breakup of Gondwanaland. This was related to the main phase of tensional tectonics. Intrusion of the Eshowe melilitites followed after

major rift tectonics and after basaltic magmatism (Section 7.5).

2.2.3 GONDWANA AND POST-GONDWANA TECTONICS

2.2.3.1 GONDWANA FRAGMENTATION AND DRIFT

The style of Gondwana fragmentation interacting with pre-existing crustal structures has influenced structural development of the African east coast (Figure 2.3). At approximately 140 Ma Antarctica split away from Africa by east/west tensional parting with oceanic crust developing from north to south (Dingle et al. 1983).

This was followed at between approximately 121 Ma and 129 Ma by the parting of South America and Africa (Eales et al. 1984, Dingle et al. 1983). On the east coast of Africa the Agulhas/Falkland Plateau moved away by northeast/southwest shearing with oceanic crust developing from north to south. Simultaneously the west coast of Africa separated from South America by east/west orientated tensional parting with oceanic crust developing parallel to the coastline and extending from south to north.

The Eshowe melilitites occur at the junction of these two styles of parting: the east/west tensional parting of Africa and Antarctica and the northeast/southwest shearing of the Agulhas/Falkland Plateau (Figure 2.3).

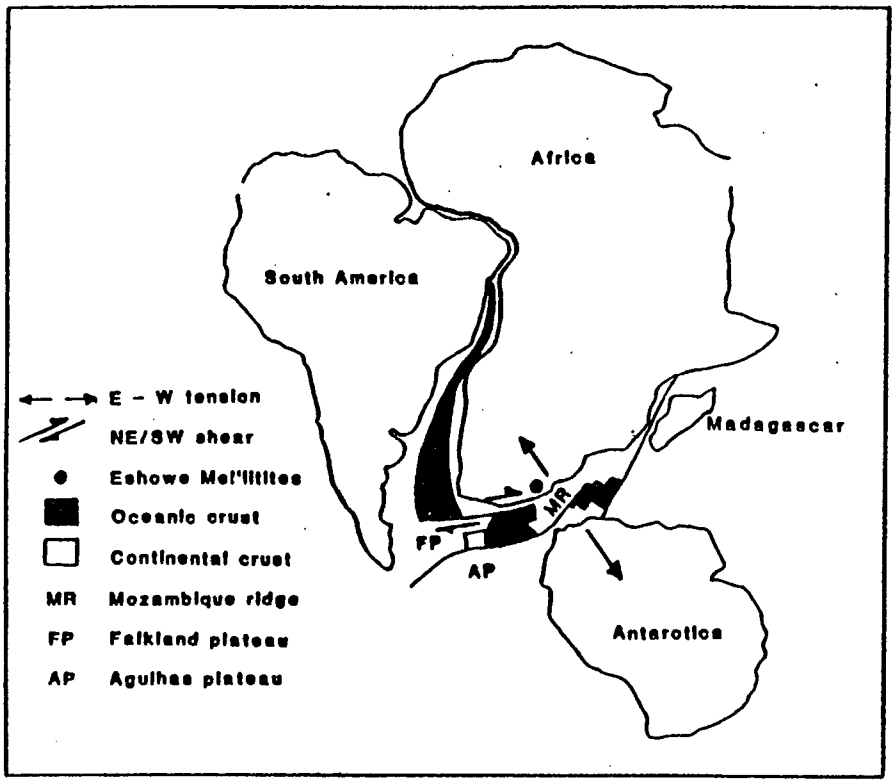

FIGURE 2.3

STYLE OF GONDWANA FRAGMENTATION

2.2.3.2 GONDWANA TECTONICS

Three distinct structural units occur on the east coast (Dingle et al. 1983): a northern region characterised by rifts; a southern region by a long straight continental edge and; at the juncture of the two, in Natal, are two zones of arcuate faulting (Figure 2.4).

represented in Antarctica (Dingle et al. 1983), however, parts of the limb may have been destroyed by crustal fragmentation, sea-floor spreading and drift (Bristow pers. comm.). Parts of the western limb are preserved in the ocean floor. This is represented by the northern Natal Valley, a graben, and the Mozambique Ridge, a horst. On the basis of gravity and seismic data the structures both consist of thinned continental crust, approximately 15 and 20km thick respectively (Dingle et al. 1983) and Eales et al. (1984) suggest basalt, intersected in a drill hole, on the Mozambique Ridge represents the upper part of an essentially continental sequence of crustal rocks.

Basement control on rifting is also apparent. Rifts parallel the Pan African Mozambique belt and probably occur at the mobile belt/archaean craton boundary (Bristow 1976).

The main phase of tensional tectonics, related to Gondwana fragmentation, probably commenced at about 190 Ma. Proto-rift formation, however, probably started prior to 200 Ma (Bristow 1980). This rifting ended when the Lebombo magmatism ceased, at 133 Ma (Bristow 1980), following Antarctica drift. Some movement along faults did continue until 100 Ma (Dingle et al. 1983).

2.2.3.2.2 THE SOUTHERN REGION

The long straight continental edge to the south of about 30° S

is a vertical shear fault formed by the movement of the Falkland and Agulhas plateaus to the southwest (Figure 2.4). The fault truncated all pre-drift structures such as the Transkei Swell, the eastern part of the Karoo basin and the Outeniqua basin (Dingle et al. 1983) and forms the western boundary to the southern Natal Valley. The latter is bounded on the east by the Mozambique Ridge. The southern Natal Valley differs in character from its northern extension in that it is not a graben structure but consists of oceanic crust. Gravity and seismic data indicate a basement thickness of 9km, in addition, depth of seawater above basement is more than 5km while that above the northern Natal Valley is 3 to 4km (Dingle et al. 1983).

2.2.3.2.3 THE NATAL FAULT ZONE

The Natal Fault Zone occurs between approximately 29° to 33° S and consists of two zones of arcuate faulting, a northern and southern zone (Dingle et al. 1983). These fault zones are probably related to a complex interaction of forces and to basement control (Figures 2.2 to 2.4). The complex of forces developed as a result of east/west tension, associated with fragmentation of Antarctica, interacting with the tensional systems (orientated northeast and northwest) and a shear component related to movement of the Falkland Plateau (Bristow 1976).

On the continent the northern arcuate fault zone occurs at the

juncture of the archaean craton and the NSMP and appears to truncate the Lebombo rifts. Faults swing to the east near the coastline and are approximately aligned with the Naude Ridge which may represent the seaward continuation of landward faulting (Dingle et al. 1983). The southern arcuate fault zone appears to truncate the northern faults and again swings east across the coastline to align with the Tugela Ridge. The latter is believed by Dingle et al. (1983) to represent the continent-ocean boundary between thinned continental crust of the northern Natal Valley and oceanic crust of the southern Natal Valley.

Faulting in the Natal Fault Zone is characterised by tilted and step-faulted blocks and associated horst and graben structures (Figure 2.4). In general faults trend north-northeast and swing, in the southern extension of each zone, to north/south and in the northern extensions through northeast to east/west. Downthrow is generally on the outer convex side of fault arcs and the dip is inland to the west and northwest. In the core of the arcs downthrow is on the concave side and the dip is to seaward, southeast, (Maud 1961). The throw on faults varies from a few metres to a thousand metres. In general, step-faulted cores have relatively small throws while longer convex faults have larger throws. Beater and Maud (1960) suggest a throw of about 1200m to 1500m for the Eteza fault while McCarthy (1988) suggests 6000m against the Southern Lebombo extrusives.

The major phase of faulting associated with Gondwana fragmentation occurred in the Jurassic. Movement of faults in the northern arcuate zone ceased in the late Jurassic (Frankel 1960) while fault movement of the southern zone is believed to have stopped in the mid-Cretaceous (Maud 1961).

Faulting in the Natal Fault Zone was associated with uplift along the present day coastline. Uplift occurred spasmodically from lower Triassic to upper Tertiary and appears to have been localised events. ie. not a uniform regional uplift but occurring at different times and amplitudes and resulting in development of the "coastal arch" (De Swardt and Bennet 1974). This resulted in different centres of uplift: the Transkei Swell (consisting of the Port Shepstone and Port Alfred arches), the Natal Arch and the Vryheid Arch.

Uplift of the Port Shepstone Arch was initiated in the lower Triassic, and of the Port Alfred Arch in the post Triassic (Dingle et al. 1983). Timing of uplift of the Natal and Vryheid arches is uncertain but they appear to be intimately associated with the arcuate faults (De Swardt and Bennet 1974). They are, therefore, probably, at least, Jurassic in age. This uplift is probably largely responsible for the thinning of Upper Karoo sediments over this part of Natal. From about the mid-Cretaceous faulting associated with uplift ceased and uplift was associated with continued seaward tilting of the coastal zone (Dingle et al. 1983). De Swardt

Swardt and Bennet (loc. cit.) suggest the latter uplift and tilting was related to erosion of uplifted areas and deposition into newly created, generally oceanic, sedimentary basins. It seems probable however that further magmatic activity was responsible for this uplift. Fission track dating of apatites suggest an extensive heating event occurred at about 95my along the east coast (R. Brown pers com.).

The Eshowe melilitites occur within the northern zone of arcuate faulting (Figure 2.4).

CHAPTER THREE

GEOLOGY AND PETROGRAPHY

3.1 GENERAL INTRODUCTION

The olivine melilitites are located to the northeast of Eshowe, approximately 100km northeast of Durban and 30km west of the coastline (Figure 3.1). The intrusions comprise four dykes; Tembani Ranch, Ndundulu, Umgoya and Emtilombo, and two pipes; Cowards Bush and Nqoleni. They have an unusual box like distribution with Ndundulu and Tembani Ranch making up the most northerly corners, Umgoya and Emtilombo the most southerly and Cowards Bush and Nqoleni within the centre.

The extensive vertical tectonism along the Natal coast has influenced development of the drainage and relief resulting in a highly dissected terrane. Highlands related to uplifted horsts occur in the northwest (northern horst) and south (Ngoya horst). These are separated by the northeast trending generally lower lying, gently undulating countryside of the Nkwaleni graben that occurs in the centre of the area and forms the Mhlatuze River valley (Figure 3.2). The total relief in the area is 640m (2081 feet). The dykes, with the exception of Tembani Ranch, are located on the horsts and the pipes are in the graben.

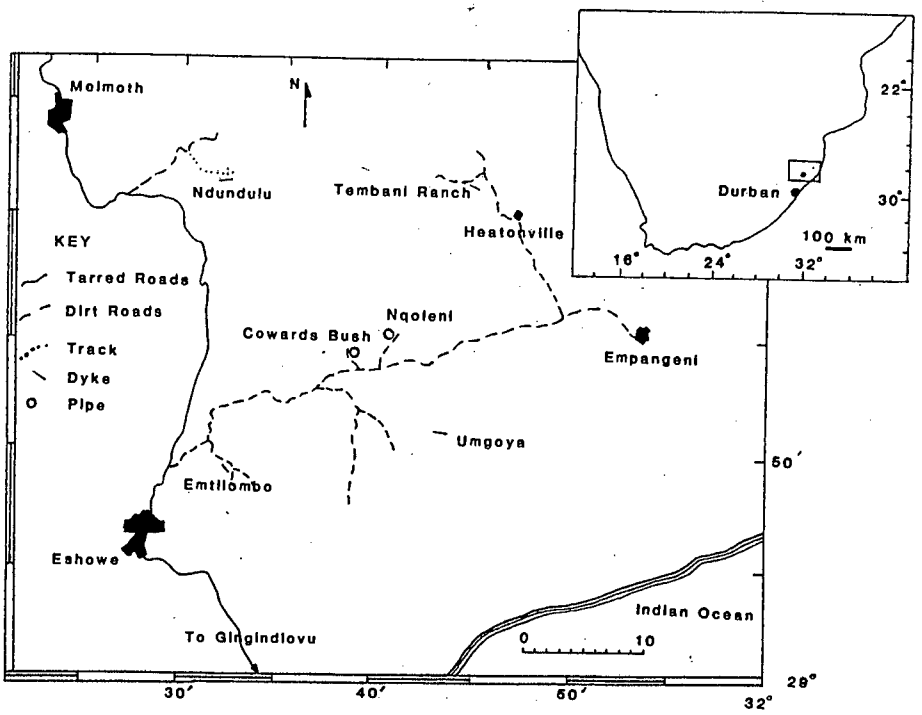

FIGURE 3.1

LOCATION OF THE ESHOWE MELILITITES

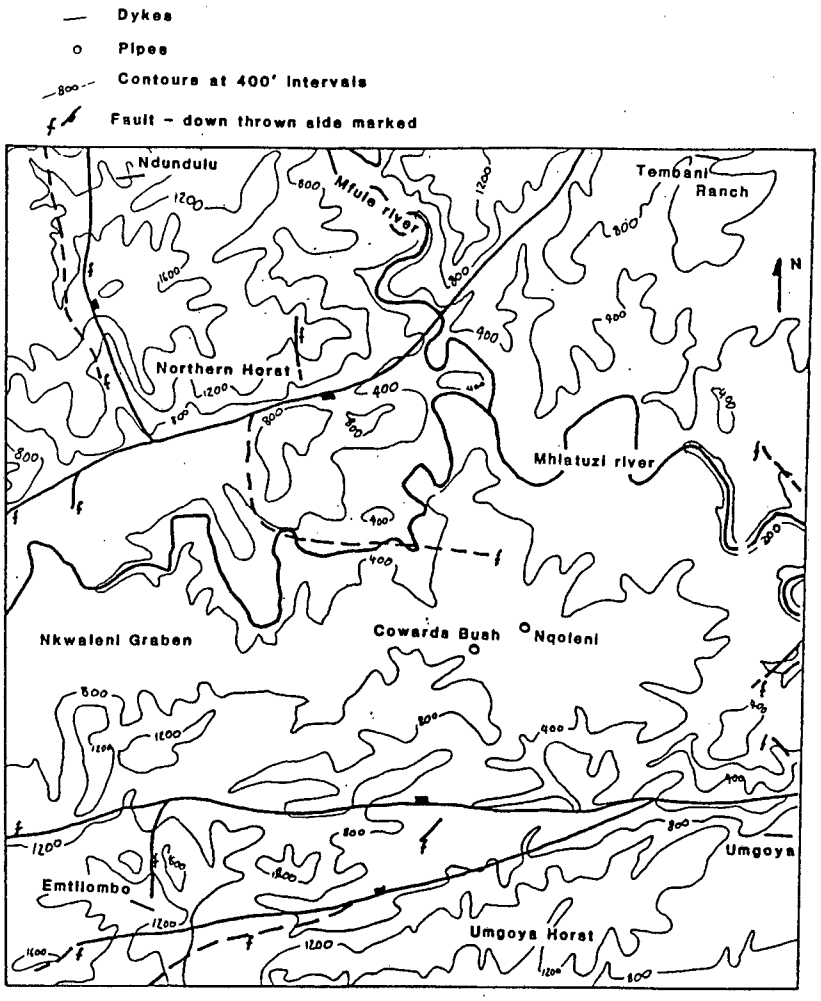

FIGURE 3.2

TOPOGRAPHY AND STRUCTURE

Access into the area is via the N2 South Coast and Eshowe - Melmoth national roads and the old Empangeni main road (dirt), which follows the trend of the Nkwaleni graben. Most of the occurrences are readily accessible and the only difficulties encountered are in the rugged highlands. Here access is generally via small tracks that lead from rural roads to schools, churches and trading stores.

As the occurrences have no economic potential little work has been done on outlining them. Geological descriptions are based on a combination of field observations, information from pits, trenches, drilling, surficial spread of heavy minerals (ilmenite) and ground magnetometry. Surface exposures of the Eshowe olivine melilitites are rare and where present consist of extremely weathered micaceous clay material. Borehole core obtained from Tembani Ranch and Emtilombo dykes and Cowards Bush and Nqoleni pipes was suitable for petrographic investigation. The freshest specimens are from Emtilombo and it is on these that the petrological study of the Eshowe melilitites is based. No fresh material is available from Ndundulu and Umgoya dykes and as samples collected from trenches are too altered for meaningful petrographic interpretation they are excluded. Locality and geological details of the occurrences are summarised in Table 3.1.

TABLE 3.1
LOCATION AND GEOLOGY OF THE ESHOWE MELILITITES

	DYKES				PIPES	
LOCALITY	TEMBANI RANCH	EMTILOMBO	NDUNDULU	UMGOYA	COWARDS BUSH	NQOLENI
LONGITUDE-E	31° 44' 43"	31° 32' 32"	31° 32' 18"	31° 43' 23"	31° 38' 57"	31° 40' 53"
LATITUDE -S	28° 38' 09"	28° 50' 45"	28° 38' 13"	28° 48' 45"	28° 45' 28"	28° 44' 43"
WIDTH	0.15 to 0.35m	0.6 to 2.0m	-	-	1.2ha	0.25ha
LENGTH	-	375m	-	-	-	-
STRIKE	120°	127°	~80°	~110°-120°	-	-
CONCENTRATE	Ilmenite	Ilmenite, chromite	Ilmenite, garnet, clinopyroxene.	Ilmenite	Ilmenite	Ilmenite, garnet, clinopyroxene
COUNTRY ROCK	Karoo Siltstone. Dolerite	Arkosic sandstone. Dolerite	Arkosic sandstone	Basement gneiss	Karoo siltstone	Karoo siltstone, dolerite
SETTING	Graben	Horst	Horst	Horst	Graben	Graben

TABLE 3.2
TERMINOLOGY

TERM	DESCRIPTION
XENOCRYST	Anhedral extensively corroded olivines characterised by mosaic re-crystallisation textures (neoblasts). Other minerals, eg. pyroxene and spinel, commonly associated with peridotite microxenoliths.
MACROCRYST	Terminology of Clement (1982). Large anhedral olivine grains of uncertain paragenesis. Also used to refer to all minerals of uncertain paragenesis.
COMPLEX PHENOCRYST	Refers specifically to euhedral to subhedral olivine with unusual primary morphology. They consist of parallel growth aggregates, growth aggregates, sharp re-entrant and other resorption features and hopper olivines.
PHENOCRYST, MICROPHENOCRYST	Early formed crystals with simple euhedral to subhedral morphology. Phenocrysts >=0.5mm. Microphenocrysts <0.5mm in longest dimension.
CRYSTALLINE	Generally with respect to carbonate morphology - the term refers to carbonate occurring as coarse anhedral plates or euhedral to subhedral rhombs.
CRYPTOCRYSTALLINE	Minerals occurring as clusters of minute, microscopically indiscernible, granules - generally refers to carbonate or serpentine in the groundmass.
MACROCRYSTIC	Macroscopic texture - Olivine (mainly) macrocrysts are relatively abundant and conspicuous in a macroscopically fine-grained and uniform groundmass (Clement and Skinner 1985).
SEGREGATIONARY	Segregations of later crystallising minerals, usually calcite and serpentine (in kimberlites), calcite and zeolites in melilitites (this study) into irregular shaped pools within the earlier crystallised groundmass (based on terminology of Clement and Skinner 1985).
GLOBULAR-SEGREGATIONARY	Extreme segregation where the earlier crystallised minerals segregate into 'globular' spheroids and these are set in a base of the later crystallising calcite, serpentine and/or zeolites (the latter is prevalent in the Eshowe melilitites). Based on the terminology of Clement and Skinner 1985.
VOLCANICLASTIC	Terminology of Fisher and Schmincke 1984. A non-genetic term for pyroclastic and epiclastic eruptive volcanic deposits.

TABLE 3.3
PETROGRAPHIC CLASSIFICATION OF THE ESHOWE MELILITITES

LOCALITY	TEXTURAL-GENETIC CLASSIFICATION	MINERALOGICAL CLASSIFICATION[2]
TEMBANI RANCH[1]	Hypabyssal facies porphyritic melilitite with a uniform groundmass texture.	Carbonatised opaque mineral-rich olivine-clinopyroxene phlogopite-melilite melilitite. Some varieties are apatite-rich.
EMTILOMBO[1]	UNIFORM MELILITITE - Hypabyssal facies, macrocrystic melilitite with a trachytic groundmass texture. Groundmass minerals have a uniform distribution. Rare varieties have a segregationary or globular-segregationary groundmass texture.	Predominant variety - Opaque mineral-rich olivine calcite-phlogopite-melilite melilitite. Micaceous variety - Opaque mineral-rich phlogopite-melilite melilitite.
	CLINOPYROXENE MELILITITE - Hypabyssal facies, macrocrystic melilitite with a globular-segregationary groundmass texture.	Contaminated olivine calcite-analcite-melilite-clinopyroxene melilitite.
	MELILITITE BRECCIA - Hybabyssal facies, globular-segregationary melilitite breccia.	Altered (carbonate and clay minerals), opaque mineral-rich olivine serpentine?-melilite melilitite.
COWARDS BUSH	Volcaniclastic[3] breccias and fine-grained lapilli volcaniclastic deposits.	Based on the mineralogy of the lapilli - Altered (clay minerals and carbonate) olivine melilite melilitite.
NQOLENI	Volcaniclastic[3] breccias and fine-grained lapilli volcaniclastic deposits.	Based on the mineralogy of the lapilli - Altered (clay minerals and carbonate) olivine phlogopite-melilite melilitite

1 = Based on the textural-genetic classification used for kimberlites (after Clement and Skinner 1985).
2 = Based on the mineralogical classification scheme used for kimberlites (Skinner and Clement 1979).
3 = Terminology of Fisher and Schmincke 1984.

Intrusion morphology and textures of the rock types are in some cases similar to those observed in kimberlites. Textural-genetic and descriptive terms, used in kimberlite terminology are therefore used or adapted for description and classification of the melilitites. All terms used are defined in Table 3.2. The petrographic classifications of the Eshowe melilititites are summarised in Table 3.3.

3.2 DYKES

3.2.1 NDUNDULU AND UMGOYA

Ndundulu is located 28km north-northeast of Eshowe within the rugged northwestern highlands. The highest point in the area, 702m (2281 feet), is 3km northwest of the dyke which is at an elevation of 500m. Ndundulu occurs within a small, gently sloping, grass covered valley. The dyke does not outcrop but ilmenite macrocrysts are conspicuous in the sandy soil above and in the vicinity of the intrusion. A small stream in the valley (a tributary of the Hlambanyati River) is believed to cut across the dyke as large ilmenite macrocrysts are present in the drainage downstream of the occurrence but no outcrop was observed. Coarse-grained, pebbly, arkosic sandstone country rock of the Eshowe Formation (Natal Group) outcrops along the stream bed.

Umgoya dyke, at an elevation of 246m, is located 21km east-northeast of Eshowe. It occurs on the side of a steeply sloping spur in the foothills of the Ngoya highlands. The

dyke, again, does not outcrop but conspicuous phlogopite and ilmenite are present in the red soil directly above and down slope of the intrusion. A small stream cuts across the intrusion but no outcrop was observed. Granite-gneiss and quartz vein material is conspicuous over the hill slope and outcrops extensively in the stream bed. The Umgoya dyke intrudes a granitic-gneiss unit within the Tugela Nappe Zone of the NSMP and is the only locality that intrudes basement rocks. The remainder of the occurrences intrude sedimentary cover rocks.

Access to both dykes is difficult and a four wheel drive vehicle is advisable. Once off the main roads the dirt tracks are indistinct and several diverging tracks can lead to confusion. In places tracks are badly eroded, particularly where they ascend steep slopes, or are very indistinct.

Little is known about Ndundulu and Umgoya. The strike of the ilmenite anomaly above Ndundulu is approximately east/west and is about 120m in extent. The dyke has an apparent near vertical dip. Umgoya is 1.4m wide, strikes approximately 110° to 120° but its strike length is not known (Internal Field Report, October 1980). Trenches into the occurrences intersected very weathered, clay-mineralised material at about 2m depth (Robertson pers com). Extensive alteration precludes a positive identification of the rock types and textures but material is similar to the weathered rock above Emtilombo and mica and ilmenite macrocrysts are conspicuous in both dykes.

3.2.2 TEMBANI RANCH

Tembani Ranch dyke is located 38km to the northeast of Eshowe on the farm Tembani Ranch, in the Heatonville area. It occurs in relatively lower lying hilly terrane, north of the Mhlatuze valley and within the Nkwaleni graben, at an elevation of 246m. It is located at the top of a steeply sloping hill which is covered by black, loamy soil and a relatively dense vegetation of grass and trees. No outcrop was observed. The melilitite intrudes a dolerite sill and shales of the Emakwazini Formation (lower Beaufort Group). The dyke is readily accessible as it is close to a well defined farm track.

Tembani Ranch strikes 120° and has an apparent dip of 86.5° southwest. Its strike length is unknown but it appears to have a restricted surface extent. It is a narrow, 30 cm wide, dyke. Near surface it pinches out upwards, probably as a result of alteration and compression by weathered shale, until it is present as a narrow sinuous band of lateritic nodules (Internal Field Report June 1978). Alternatively this could be a primary feature and the occurrence may narrow near surface. At 27.5m depth the dyke splits into a 40cm and 15cm wide intrusion, separated by 15cm of shale. These rejoin to form a single 30cm wide intrusion at 52m depth (Internal Field Report July 1978).

Tembani Ranch dyke is essentially mineralogically and texturally similar throughout. At about 2m depth the rock

type is fairly hard but extensively weathered while at deeper levels (27.5m and 52m) it is harder and relatively fresher but is still altered. The dyke consists of a pale to dark brownish-grey porphyritic rock type in which a sub-parallel flow orientation of the elongate phenocrysts is discernible.

In thin section the rock type is seen to consist of altered olivine, melilite, and fresh clinopyroxene phenocrysts, and very rare, small, altered olivine and phlogopite macrocrysts (<1 vol %) set in a fine-grained groundmass (Plate 3.1). Macrocrysts and phenocrysts are commonly less than 2mm in size although rare melilite and phlogopite laths up to 3mm and 4.5mm, respectively, are present. The groundmass comprises abundant altered melilite, fairly abundant phlogopite, carbonate and opaque minerals, accessory apatite, clino-pyroxene and perovskite and rare rounded ghost relicts of possible sodalite all set in an isotropic analcite? base. In some samples apatite is relatively more abundant and becomes a conspicuous groundmass phase (Table 3.4 and Plate 3.2).

Crystalline carbonate occurs as an irregular network throughout the matrix and as rafts rimming small, irregular analcite filled 'pools'. The groundmass texture varies from uniform to segregationary as these 'pools' increase in abundance. Sub-parallel orientation of melilite laths gives rise to a trachytic sub-texture and minor small, rounded 'globular-segregations' are scattered randomly throughout this matrix. The latter commonly comprise a kernel of olivine

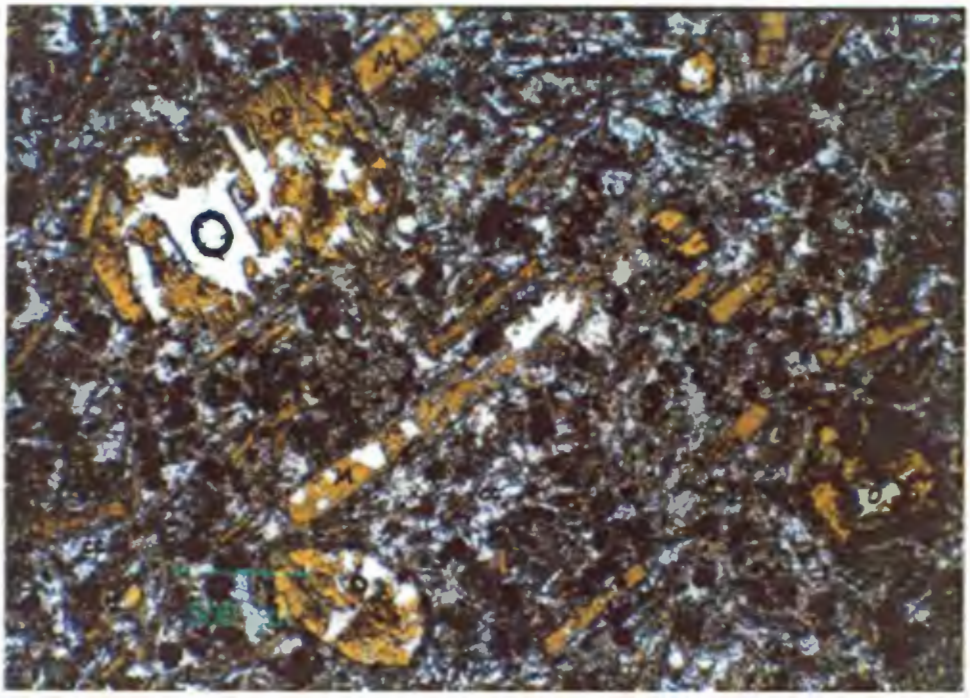

PLATE 3.1
TEMBANI RANCH MELILITITE - TEXTURE

Altered olivine (o) and melilite (M) phenocrysts set in a finer grained opaque mineral rich groundmass. Altered groundmass melilite (m) and calcite (cc).

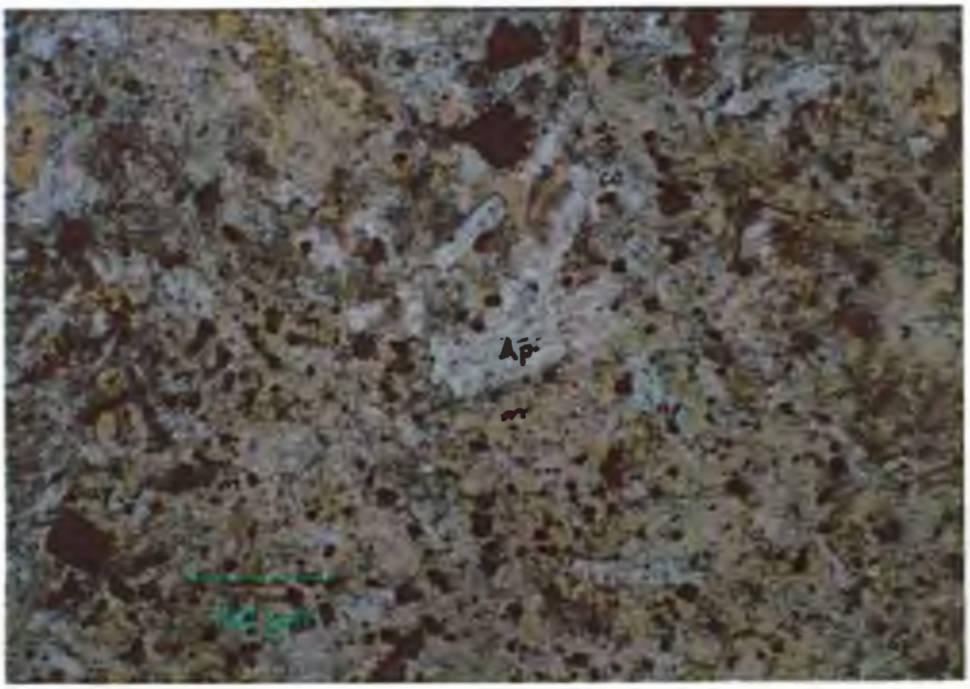

PLATE 3.2
TEMBANI RANCH MELILITITE - GROUNDMASS

Altered melilite (m), coarse (Ap) and fine (ap) apatite, interstitial phlogopite (p), emerald green clinopyroxene (cpx), calcite (cc) and opaque minerals (black).

rimmed by concentrically arranged melilite and apatite laths. Turbid, cryptocrystalline carbonate is ubiquitous throughout the matrix of the specimens and replaces much of the groundmass mineralogy, in particular, melilite. Secondary alteration to clay is also ubiquitous in the specimens.

3.2.3 EMTILOMBO

Emtilombo dyke is located 7km northeast of Eshowe. The dyke occurs in the relatively gently undulating highlands of the Eshowe plateau (Ngoya horst), at an elevation of 323m. It is to the south of the Mhlatuze valley and in the headwaters of the small Mlalazi River drainage basin. The dyke strikes across the lower slopes of a hill and is cut by tributaries of the Emtilombo Stream (a tributary of the Mlalazi River) at its southeastern and northwestern extent. The intrusion outcrops in banks and beds of the streams at both sites, where it occurs as extremely weathered, friable, yellowish to greenish micaceous clay. Outcrops in the stream beds have been destroyed by pitting and subsequent flooding of streams has infilled these pits with black clay. The weathered material, in stream banks, grades downwards into harder but still altered, greenish-grey rock and pits excavated in stream beds intersected hard, relatively fresh melilitite at about 1m depth (Figure 3.3). No outcrop is discernible on the hill slope which is covered by deep, loamy soil and dense grass and occasional shrub vegetation. Relict outlines of three infilled trenches mark the location and strike of the dyke on

the hill slope. The country rock is coarse-grained pink, pebbly, arkosic, Eshowe Formation, sandstone which outcrops extensively along the drainage and in the lower slopes of the hill towards the northwest. Strongly developed jointing is clearly discernible in the country rock and Emtilombo dyke parallels the direction of the jointing. The dyke contacts with the sandstone are sharp and clean. Access to the occurrence is relatively simple and is along well defined roads for most of the way.

Emtilombo is the only occurrence that has been studied in detail and Figure 3.4 shows an idealised diagram of the intrusion geology. The dyke narrows from 2m in the southeast to 1.5m (at surface) and 0.6m (at depth) in the northwest. Most of the dyke consists of dark-grey macrocrystic melilitite that appears to be mineralogically and texturally uniform throughout. There is, however, a restricted zone with a distinct globular-segregationary distribution of groundmass minerals (Figure 3.4) in the central/northwestern end of the dyke. Country rock xenoliths are rare in the macrocrystic melilitite and where present are small, generally less that 2cm in size. Towards and at the southeastern end of the dyke a 20cm to 30cm wide zone of a pale-grey, xenolith-rich rock type occurs, at either contact, between country rock and macrocrystic melilitite. This rock type consists of abundant pink, sandstone fragments that range from less than 1cm up to 23cm in size and are set in a fine-grained 'globular-segregationary' matrix. The contact between the macrocrystic

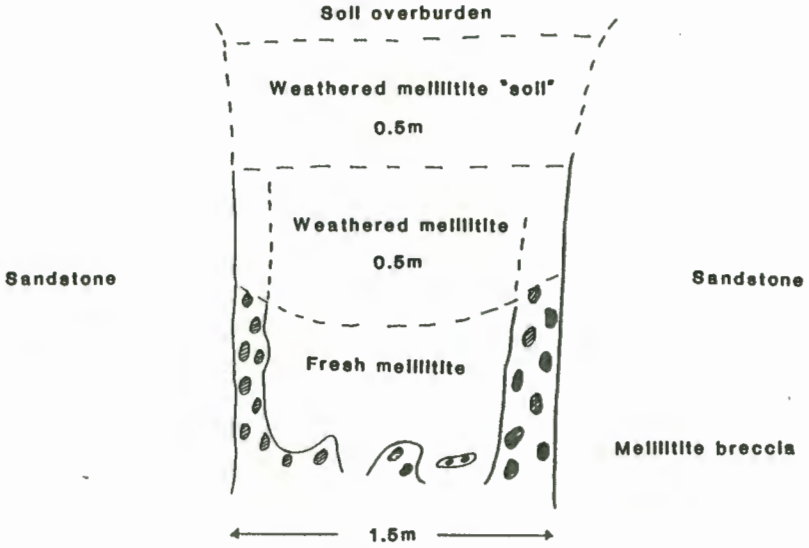

FIGURE 3.3
EMTILOMBO DYKE PIT PROFILE

FIGURE 3.4
EMTILOMBO DYKE GEOLOGY

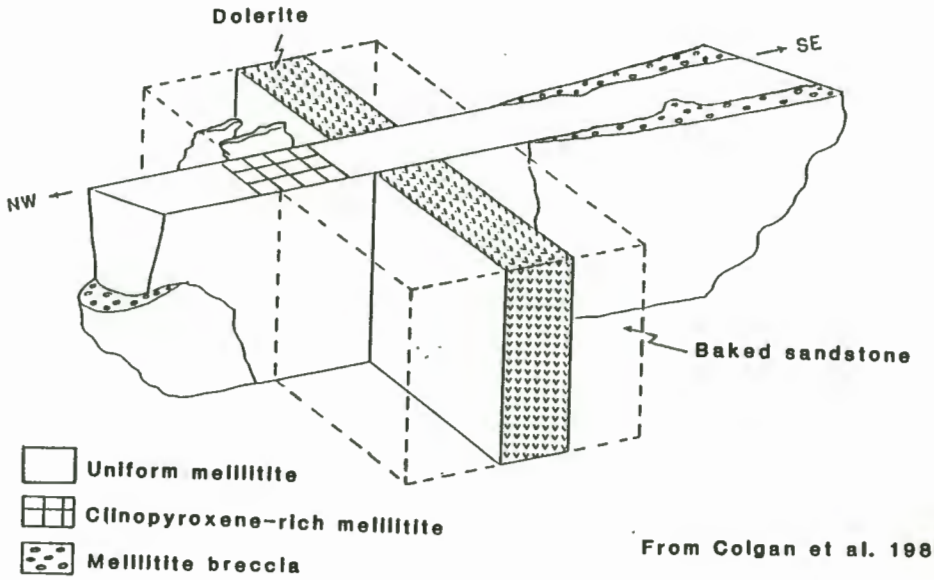

From Colgan et al. 1989

TABLE 3.4
TEMBANI RANCH AND EMTILOMBO MELILITITE
MODAL PROPORTIONS (VOL%)

SAMPLE NUMBER		PK1	PK3/A	PK3/B	PK3/C	PK3/D
XENOLITHS		-	TRACE	TRACE	TRACE	3.7[5]
CLINOPYROXENE MACROCRYSTS		4.1[3]	TRACE	TRACE	TRACE	TRACE
PHLOGOPITE MACROCRYSTS		TRACE	TRACE	TRACE	TRACE	1.5
OLIVINE MACROCRYSTS		TRACE	8.0	9.0	10.4	10.0
OLIVINE PHENOCRYSTS		6.6	16.8	13.2	13.4	7.8
MELILITE PHENOCRYSTS		2.9	-	-	-	-
GROUNDMASS	MELILITE	30.7	27.6	31.8	21.4	11.9
	PHLOGOPITE	12.4	2.0	15.9	10.2	6.0
	OPAQUE MINERALS	11.0	6.0	9.9	11.2	6.2
	PEROVSKITE	3.1	1.2	4.2	5.3	2.8
	APATITE	4.5	0.8	1.4	2.0	1.6
	CARBONATE	15.5	15.2	1.5	10.7	7.0
	CLINOPYROXENE	4.9	-	1.0	0.2	21.9[6]
	INTERSTITIAL[1]	4.3	6.0	2.7	9.2	7.2
	MATRIX[2]	-	16.4[4]	9.4	6.0	12.4
TOTAL POINTS COUNTED		1500	250	1800	2050	900

PK1 = TEMBANI RANCH MELILITITE (PK001/3, PK001/5 AND PK001/8)
PK3/A = EMTILOMBO GLOBULAR SEGREGATIONARY MELILITITE (PK003/8)
PK3/B = EMTILOMBO MICACEOUS MELILITITE (PK003/55 AND PK003/56)
PK3/C = EMTILOMBO UNIFORM MELILITITE (PK003/58 AND PK003/59)
PK3/D = EMTILOMBO GLOBULAR SEGREGATIONARY AMPHIBOLE-RICH MELILITITE (PK003/64, PK003/66 AND PK003/67)
1 = UNIDENTIFIED INTERSTITIAL BASE
2 = UNIDENTIFIED GROUNDMASS (SODALITE?)
3 = PHENOCRYSTS
4 = ALTERED MATRIX IN GLOBULAR SEGREGATIONS
5 = MANTLE XENOLITH 3.3 VOL%
6 = AMPHIBOLE

melilitite and the melilitite breccia is sharp and the latter appears to cut irregularly through the former (Figure 3.3 and 3.4). At the northwestern end of the intrusion this breccia is again present but it occurs at depth and no macrocrystic melilitite is present. Two narrow, approximately 30cm and 50cm wide, melilitite stringers are present next to the main dyke in the central/northwestern end.

Phlogopite and ilmenite macrocrysts are ubiquitous throughout the dyke. As are numerous narrow (up to 0.5cm wide), dominantly vertical to sub-vertical, calcite-filled veinlets. Calcite also veins the contact between melilitite breccia and macrocrystic melilitite. Rare large, centimetre wide, open veins (or vugs?) characteristically lined by calcite rhombs are also present.

Emtilombo comprises essentially three petrographically distinct rock types (Figure 3.4): uniform melilitite, clinopyroxene-rich melilitite with a globular-segregationary texture and melilitite breccia. Mineral modal abundances of the various types are listed in Tables 3.4 and 3.5.

3.2.3.1 UNIFORM MELILITITE

Uniform melilitite (Plate 3.3) is the most common rock type in Emtilombo dyke. It consists of fairly abundant olivine and rare clinopyroxene and phlogopite macrocrysts and abundant olivine phenocrysts all set in a fine-grained, uniform,

predominantly trachytic textured groundmass. Rare translucent spinels, orthopyroxene and olivine xenocrysts and very rare ilmenite macrocrysts are also present. Occasional microxenoliths that consist of various combinations of olivine, clinopyroxene, orthopyroxene and/or translucent or opaque spinel are observed in thin section. The groundmass comprises abundant melilite, scattered opaque minerals and perovskite, randomly distributed patches of interstitial phlogopite, minor small apatite and rare clinopyroxene set in an interstitial matrix of granular clusters of a colourless mineral in an amorphous analcite? base. These clusters consist of subhedral, rounded grains that are characterised by low relief and are isotropic. This mineral is thought to be a feldspathoid, possibly of the sodalite group. Small interstitial 'pools' of possible analcite and minor crystalline carbonate occur within this matrix. Secondary alteration of, predominantly, melilite and sodalite? to cryptocrystalline carbonate and/or clay minerals is evident in some samples. This alteration is sometimes extensive, masking much of the groundmass mineralogy and altering the larger constituents (particularly olivine).

The relative abundances of the different minerals vary within and between specimens resulting in a number of closely related mineralogical and textural varieties (Table 3.4). A phlogopite-rich rock type occurs in the central area of the dyke and patches within this are characterised by the presence of conspicuous and relatively abundant, emerald-green clino-

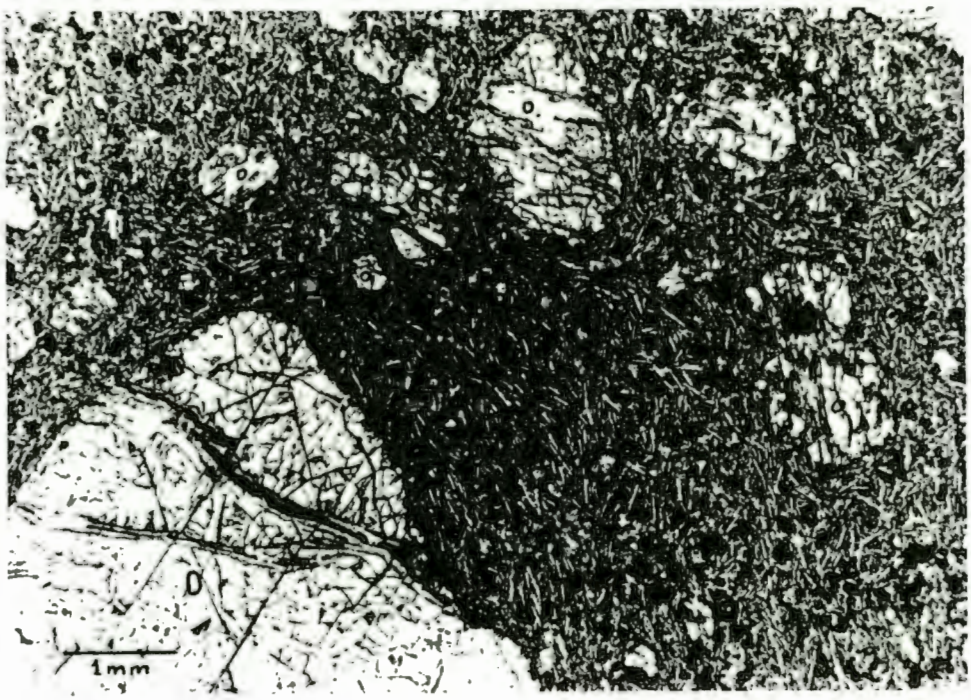

PLATE 3.3
EMTILOMBO UNIFORM MACROCRYSTIC MELILITITE

Olivine macrocrysts (O) and phenocrysts (o) set in a trachytic textured base of abundant fine melilite laths. Relatively abundant opaque minerals (black) are scattered throughout this base.

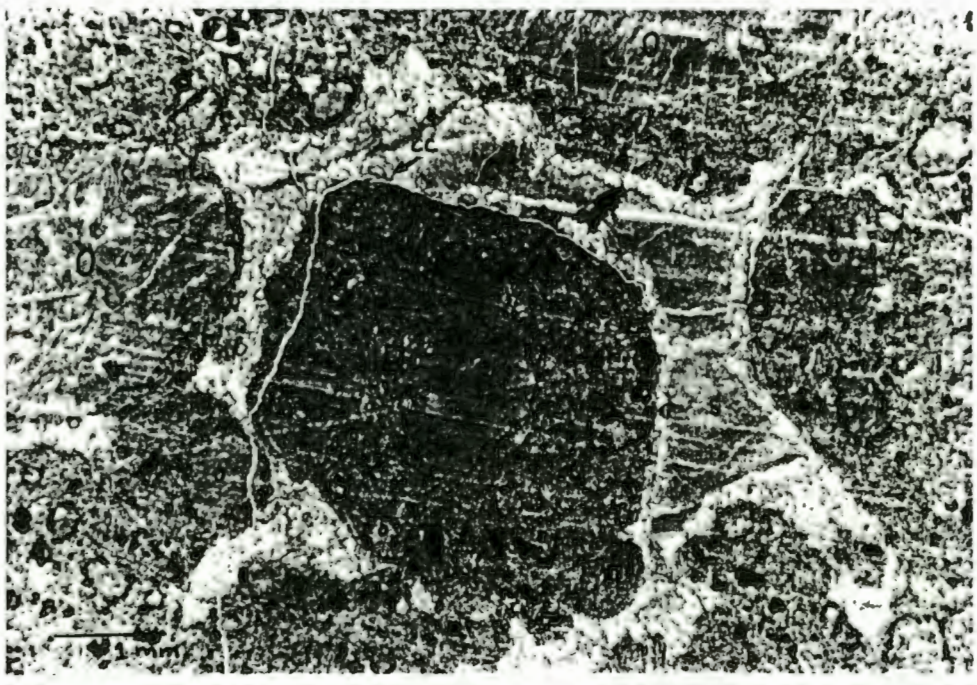

PLATE 3.4
EMTILOMBO GLOBULAR SEGREGATIONARY MELILITITE

Globular segregations consist of altered olivine macrocrysts (O) and phenocrysts (o) in a similar groundmass to that in Plate 3.3. The segregations are set in an intersegregationary base of altered serpentine? (s) rimmed by calcite rhombs (cc).

pyroxene. Apatite is generally a minor phase but was observed to be fairly abundant in one sample. An increase in the size and abundance of segregated serpentine? and carbonate 'pools' results in the development of segregationary to globular-segregationary textural varieties. These occur as restricted millimetre to centimetre size pockets within the uniform melilitite and both rock types are gradational into the latter. The globular-segregationary textural variant was observed in one specimen from the southeastern end of the dyke (Table 3.4, Plate 3.4) and would therefore appear to have a very restricted distribution while the less extreme segregationary texture occurs randomly throughout the uniform melilitite.

3.2.3.2 CLINOPYROXENE-RICH MELILITITE

The clinopyroxene-rich melilitite appears to be almost entirely confined to the central/northwestern end of the dyke where it occurs across the entire width of the intrusion. It is uncertain how extensive it is along strike or in depth. The rock type consists of globular to irregular shaped segregations of the earlier crystallised groundmass minerals (melilite, phlogopite, opaque minerals, perovskite, etc.) set in an intersegregationary matrix of abundant pale green, clinopyroxene laths and interstitial analcite?, serpentine?, zeolites and rare crystalline carbonate (Table 3.4, Plate 3.5). Some, rare, corroded fragments of a felsic rock type, consisting of quartz and feldspar, are present and are

associated with the clinopyroxene-rich matrix. One specimen from the southeastern end of the dyke contains abundant clinopyroxene-rich segregations which are again associated with small splinters of resorbed, altered felsic xenoliths.

3.2.3.3 MELILITITE BRECCIA

The melilitite breccia consists of macrocrysts and phenocrysts of altered olivine, abundant rounded 'globular-segregations', xenoliths and xenocrysts of country rock, minor phlogopite and rare ilmenite macrocrysts all set in a base of turbid brownish, clay mineralised serpentine? and cryptocrystalline and minor crystalline carbonate (Table 3.5A). Extensive alteration to clay minerals and carbonate masks much of the primary mineralogy but relict textures are well preserved and it is possible to identify a large proportion of the original mineralogy.

The serpentine? base makes up a relatively small proportion of the rock, 19 vol.%, while xenoliths, xenocrysts and 'globular-segregations' account for 81 vol.%. As a result the rock type is characterised by a close packed, fragmental texture (Plate 3.6).

'Globular-segregations' occur as rounded spheroids ranging from 0.1mm up to 4mm in diameter. They consist of small phenocrysts of altered olivine set in a groundmass of generally concentrically arranged melilite pseudomorphs and

PLATE 3.5
EMTILOMBO CLINOPYROXENE-RICH MELILITITE

Globular segregations with concentrically arranged melilite (small laths) and olivine phenocryst (o) kernels, corroded country rock xenoliths (X), patches of clinopyroxene (turbid grey areas) and occasional pools of analcite (an).

PLATE 3.6
EMTILOMBO GLOBULAR SEGREGATIONARY MELILITITE BRECCIA

Globular segregations are similar to those in Plate 3.2. The 'inter-globular' groundmass consists of xenocrysts (x) and xenoliths (X) and minor carbonate (cc) in an altered base.

granular, altered, possible sodalite?, scattered opaque minerals, minor interstitial phlogopite and rare perovskite. Small carbonate-filled 'pools' that appear primary, are present in some of the segregations. Olivine macrocrysts and the larger phenocrysts, rare phlogopite macrocrysts and very rare, small, country rock fragments occur as kernels within some of the 'globular-segregations' (Table 3.5B).

Most of the xenoliths and xenocrysts are found in the inter-globular matrix. Xenoliths occur as angular fragments and elongate splinters of arkosic country rock while xenocrysts consist of, disaggregated, quartz and altered feldspar. No corrosion of the included fragments is evident and no clino-pyroxene appears to be present in the rock type.

3.3 PIPES

Cowards Bush and Nqoleni are both small pipes, approximately 1.2ha and 0.5ha in area, respectively. The rock types are similar in that they are xenolith-rich and are extremely fragmental in appearance. Abundant mica and ilmenite macrocrysts are again conspicuous in both melilitites. They differ, in detail, in the degree of alteration, texture and mineralogy of the rock types and the size and nature of included xenoliths. Both pipes are readily accessible as they are located next to well defined dirt roads.

3.3.1 COWARDS BUSH

Cowards Bush pipe is 21km northeast of Eshowe. It occurs in flatter lying, undulating countryside on the southern flank of the Mhlatuze valley, at an elevation of 215m. The pipe is located on the side of a gently sloping hill and extends into a small valley. It is covered by deep, loamy soil and relatively dense tree vegetation but outcrops in a large donga that is about 2m deep. An extensive trenching program was carried out over the body and relict outlines of infilled trenches mark its location and approximate size. Some outcrops of Karoo siltstone and sandstone (Emakwazini Formation) are present further down slope away from the pipe and numerous dolerite dykes (Effingham dykes, Bristow et al. 1984) occur throughout the area.

Cowards Bush is an irregular, elliptical shaped body approximately 150m long by 77m wide with the long axis trending east-northeast. A narrow dyke-like extension occurs at the eastern end of the pipe and trends approximately east/west (a strike similar to that of Ndundulu dyke). The rock type in the pipe is extensively altered to 162m depth: it grades from a friable, yellowish-brown, clay-mineralised breccia at surface to a hard, greyish-cream, clay-mineralised and carbonatised breccia at depth. From surface outcrop, trenches and core information xenoliths appear to be randomly distributed throughout and narrow finer-grained zones are present within the coarser material providing some evidence for bedding. From about 63m downwards juvenile lapilli are

conspicuous in the inter-xenolith matrix. Xenoliths comprise black, carbonaceous shale, siltstone, sandstone and minor dolerite(?) and range from a few centimetres up to 12m in longest dimension. These inclusions comprise predominantly Karoo sediments.

Extensive alteration masks the primary mineralogy and textures of all specimens collected from Cowards Bush pipe and hampers detailed petrographic interpretation of the rock type. Macroscopically the primary texture and some relict mineral morphologies are clearly discernible. In thin section these textures are generally only vaguely distinguished through a turbid grey to brownish-grey mask of secondary clay minerals and carbonate.

In thin section most specimens consist of abundant, country rock xenoliths and disaggregated xenocrysts, altered pseudomorphs after olivine macrocrysts and phenocrysts, phlogopite macrocrysts, indistinct juvenile lapilli and turbid grey possible accretionary lapilli set in an altered, murky, fine powdery base (Table 3.5A, Plate 3.7). Rare, minute, possible clinopyroxene microlites are discernible in the interstitial base of some specimens and they occasionally occur within the groundmass of the lapilli. The abundance and size of the different constituents varies from sample to sample resulting in a variety of textural types. Country rock xenoliths occur as angular to subangular fragments and shards and in some samples are extremely abundant. In the latter

case, parts of the matrix in thin section are characterised by a coarse, clast supported texture with minor, altered, fine-grained and disrupted melilitite material forming the interstitial base. The predominant texture in most of the thin sections is of matrix supported clasts. A few specimens are characterised by much finer-grained constituents and vague layering. These rock types consist of essentially the same mineralogy as the coarser varieties described above but country rock fragments are small and rare and juvenile lapilli are small and very closely packed (Plate 3.8). These constituents are set in a base of crystal fragments, in particular melilite, and turbid fine powder. It is uncertain whether this powder is finely comminuted ash or an artefact of secondary alteration. Distribution of the 'powder' (described below) suggests that it could represent altered ash particles.

Phlogopite macrocrysts generally occur as ragged, disrupted laths although a few do not show any signs of distortion. Olivine occurs as indistinct carbonate pseudomorphs after euhedral phenocrysts and fragmented macrocrysts.

Juvenile lapilli occur as elongate oval and irregular shaped patches or as rounded spheroids (Plate 3.9). They range from less than 1mm up to 13mm in diameter. The larger lapilli consist of small altered olivine phenocrysts in a groundmass of abundant ghost relict melilite pseudomorphs, opaque minerals, altered perovskite and rare interstitial phlogopite all set in a turbid base of secondary carbonate and minor clay

TABLE 3.5
COWARDS BUSH VOLCANICLASTIC BRECCIA AND EMTILOMBO MELILITITE BRECCIA

3.5A
LARGE CONSTITUENTS MODAL PROPORTIONS (VOL%)

SAMPLE NUMBER	PK002/3[1]	PK002/5(I)[1]	PK003/1[2]
CLASTS	62.9	5.6	34.8
MATRIX	27.4	40.8	19.6
LAPILLI/GLOB. SEGS	2.2	49.6	45.6
PHLOGOPITE MACROCRYSTS	0.4	0.8	-
OLIVINE	7.1	3.2	-
TOTAL POINTS COUNTED	550	250	500

3.5B
JUVENILE LAPILLI AND GLOBULAR SEGREGATIONS MODAL PROPORTIONS (VOL%)

SAMPLE NUMBER		PK002/5(I)[1]	PK003/1[2]
CLASTS/CRYSTAL FRAGMENTS		14.7	1.8
PHLOGOPITE MACROCRYSTS		3.4	TRACE
OLIVINE MACROCRYSTS		3.4	2.6
OLIVINE PHENOCRYSTS		2.0	5.8
GROUNDMASS	MELILITE	18.1	41.2
	OPAQUE MINERALS	9.9	4.8
	PEROVSKITE	-	0.4
	PHLOGOPITE	1.4	0.6
	CLINOPYROXENE	0.3	-
	APATITE	0.3	-
	CLAY MINERALS	26.3	9.2
	CARBONATE	20.2	1.8
TOTAL POINTS COUNTED		293	250

1 = COWARDS BUSH VOLCANICLASTIC MELILITITE BRECCIA
2 = EMTILOMBO MELILITITE BRECCIA

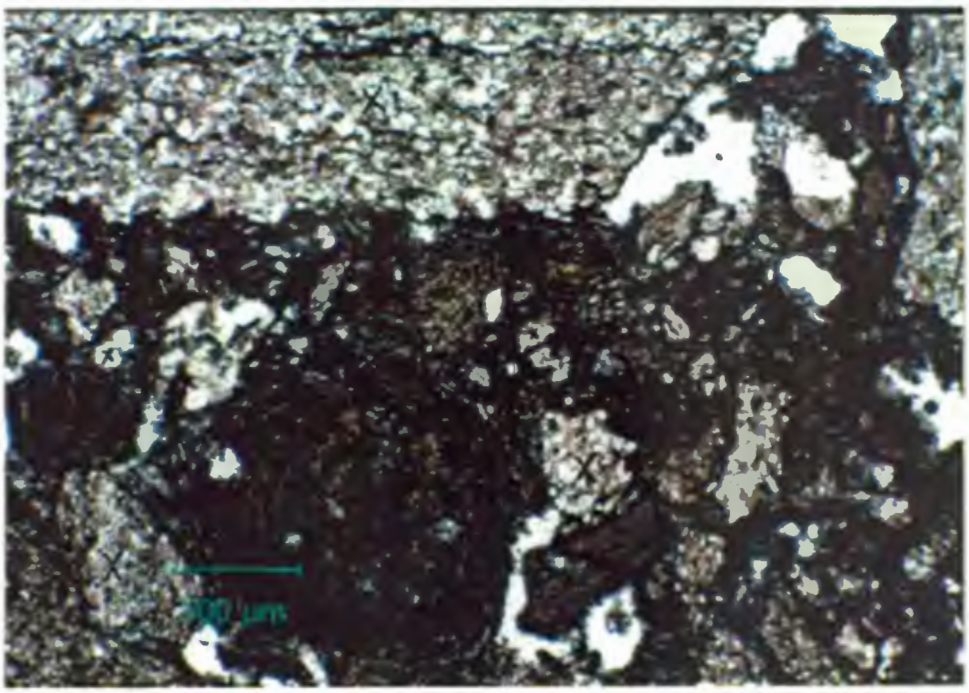

PLATE 3.7
COWARDS BUSH VOLCANICLASTIC - COARSE BRECCIA

Juvenile lapilli (L), xenoliths (X) and xenocrysts (x) set in a fine grained turbid grey base of possible ash particles. Holes in the thin section (white areas).

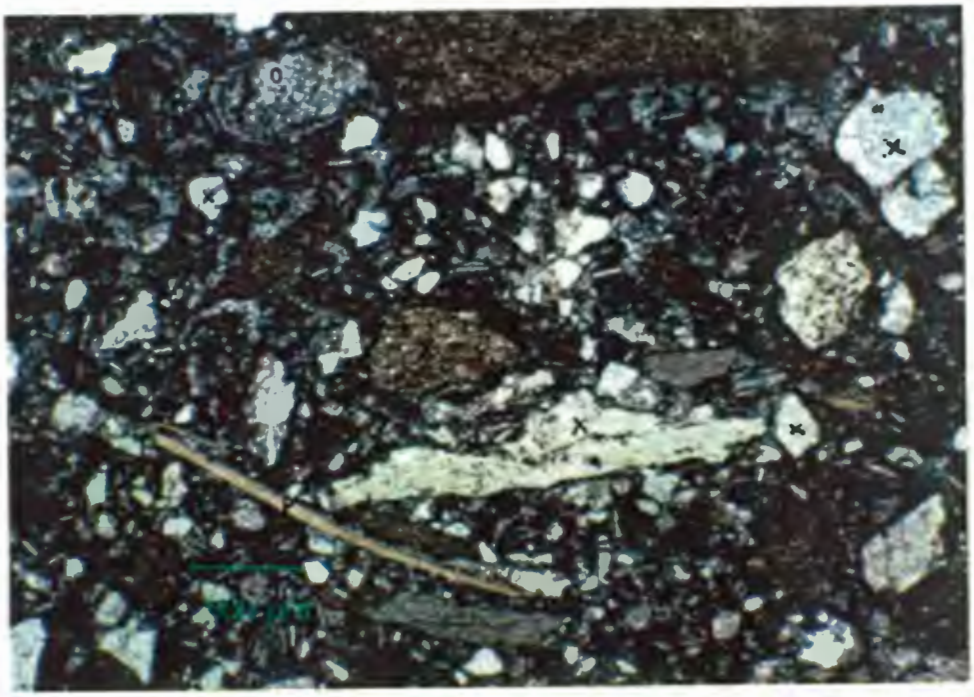

PLATE 3.8
COWARDS BUSH VOLCANICLASTIC - FINE BRECCIA

Indistinct juvenile lapilli (L), phlogopite macrocrysts (P), altered olivine (o) and xenolithic fragments (x) in a turbid grey ash? base. Note parallel bedding alignment.

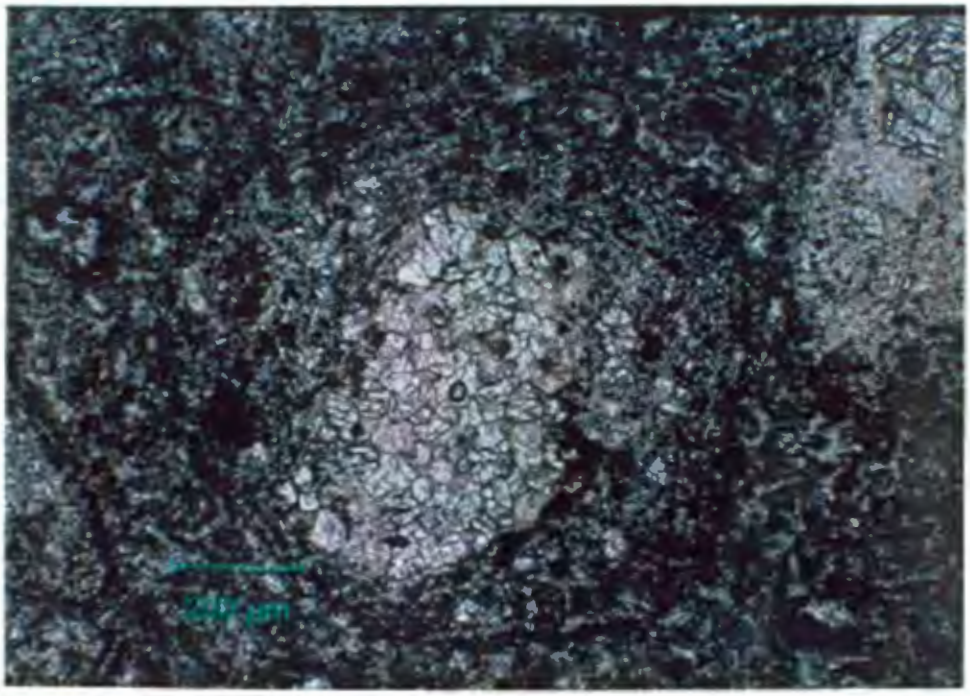

PLATE 3.9
COWARDS BUSH VOLCANICLASTIC - JUVENILE LAPILLI

Indistinct rounded juvenile lapilli consisting of an altered olivine phenocryst (o), vague melilite laths (small white laths) and altered opaque minerals (black). Note turbid grey rim of possible ash.

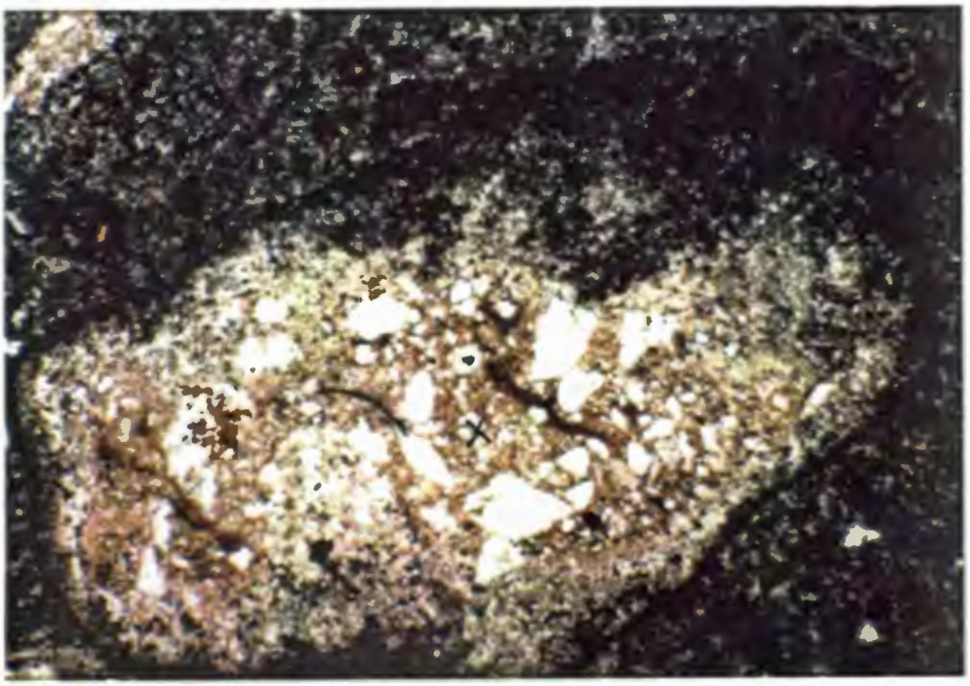

PLATE 3.10
COWARDS BUSH VOLCANICLASTIC - ACCRETIONARY LAPILLI

An accretionary lapilli consisting of finely comminuted particles (turbid grey) around a country rock xenolith (X).

minerals (Table 3.5B). Melilite laths are commonly concentrically orientated within the lapilli. Olivine macrocrysts occur as kernels within some of the larger lapilli.

Accretionary lapilli are generally small and commonly irregular or oval in shape (Plate 3.10). They consist of aggregates of fine, turbid grey, possible ash or as rims of turbid grey material around country rock xenoliths, xenocrysts, juvenile lapilli or melilite laths.

3.3.2 NQOLENI

Nqoleni pipe is 24km to the northeast of Eshowe and 3.4km northeast of Cowards Bush. It is located at the top of a rounded, gently sloping, dolerite capped hill, at an elevation of 154m. The occurrence is covered by loamy soil and dense euphorbia vegetation and does not outcrop but it does produce a surface vegetation anomaly, namely, a conspicuous, almost circular relatively vegetation-free area. Soil over the intrusion contains abundant phlogopite and ilmenite macrocrysts and country rock xenoliths are conspicuous. Xenoliths are largely derived from the basement being granite-gneiss and amphibolite although some siltstone and dolerite are also present. A relatively steep, approximately 1m high, slope on the northwestern side of the anomaly probably defines the rim of the pipe. The outline of an infilled pit is discernible and greenish, clay-mineralised, micaceous breccia

is present in the associated spoil heap. The melilitite intrudes Emakwazini Formation sediments and a dolerite sill.

Little is known about Nqoleni pipe. From the surface vegetation anomaly it appears to be approximately 50m in diameter. The rock type is a hard, greenish, breccia to 75m depth and again there is some evidence for bedding: it consists of a relatively coarse sequence of very xenolith-rich material with some thinner, interbedded, finer-grained zones. Near surface it is weathered but still relatively hard. Xenoliths are smaller than those observed in Cowards Bush and range from less than 1cm up to about 20cm in size. The most conspicuous features of the occurrence are the abundance of dolerite and basement xenoliths and the hardness of the rock type. Basement xenoliths were not observed in any of the other melilititites in the area. The Nqoleni intrusion appears to be relatively fresher than that of Cowards Bush.

In thin section the coarser grained variety comprises country rock xenoliths, disaggregated xenocrysts, various macrocrysts and phenocrysts, abundant rounded devitrified glass fragments and minor indistinct juvenile and accretionary lapilli all set in a colourless, generally amorphous probable analcite base (Plate 3.11). Abundant amphibole and minor clinopyroxene needles are ubiquitous throughout this base (Plate 3.12) and minor relatively coarsely crystalline carbonate and occasional zeolite and apatite laths are also evident.

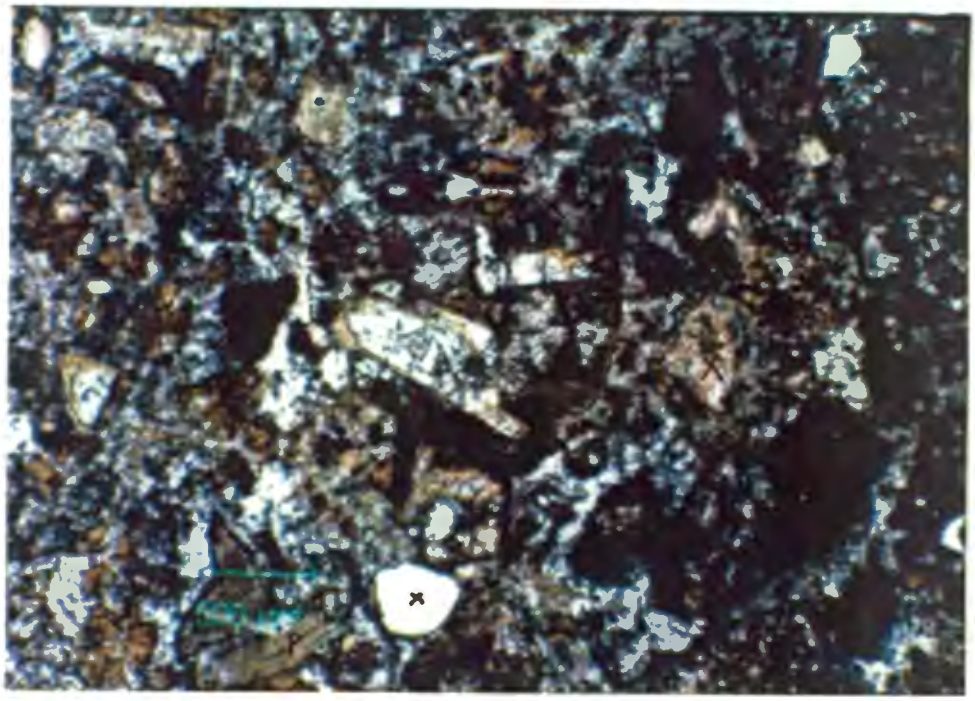

PLATE 3.11
NQOLENI VOLCANICLASTIC - TEXTURE

Fragmental texture. Indistinct juvenile lapilli (outlined), glass spheroids (brown), phlogopite (P), xenoliths (X) and xenocrysts (x) in a cement of amphibole (turbid grey), analcite and carbonate.

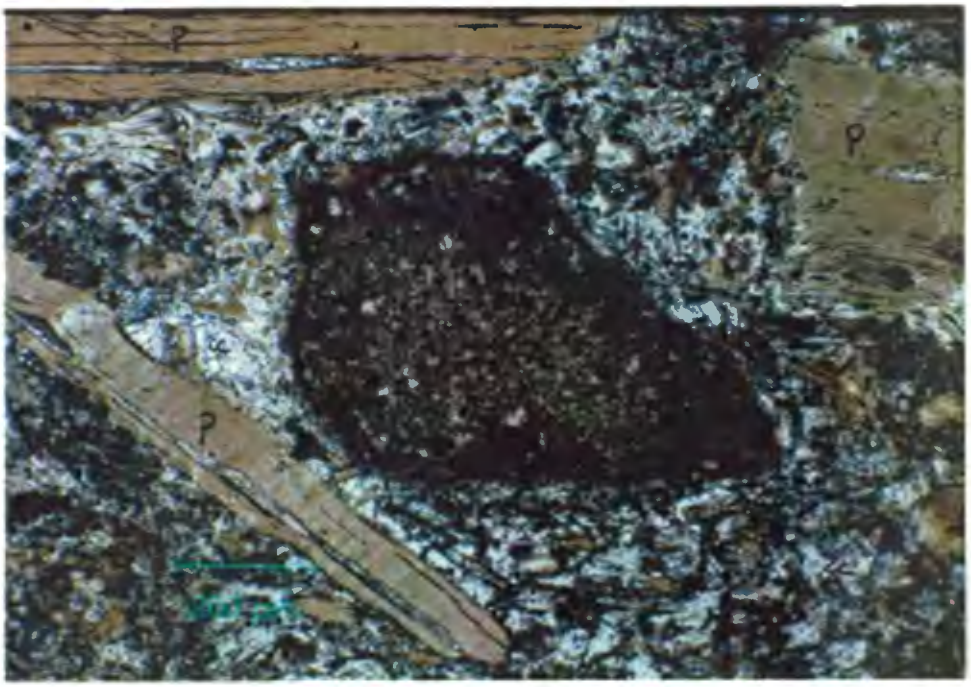

PLATE 3.12
NQOLENI VOLCANICLASTIC - ACCRETIONARY LAPILLI

Accretionary lapilli consisting of finely comminuted ash? particles. Phlogopite macrocrysts (P), glass (brown), amphibole (blue) and carbonate (cc).

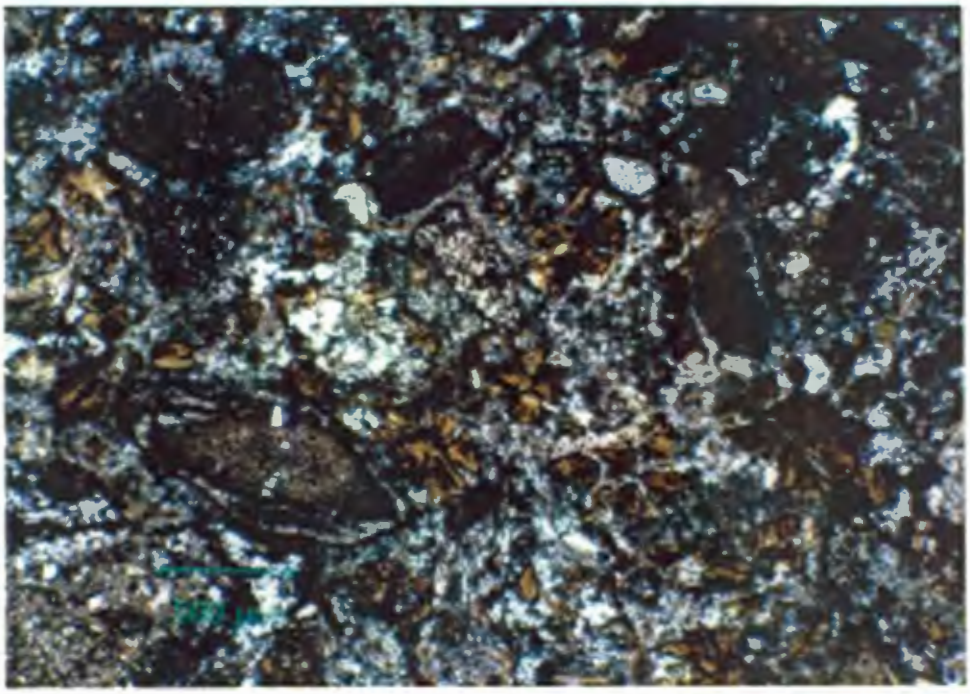

PLATE 3.13
NQOLENI VOLCANICLASTIC - GLASS

Glass spherulites (brown) showing bow-tie structures and crystallites.

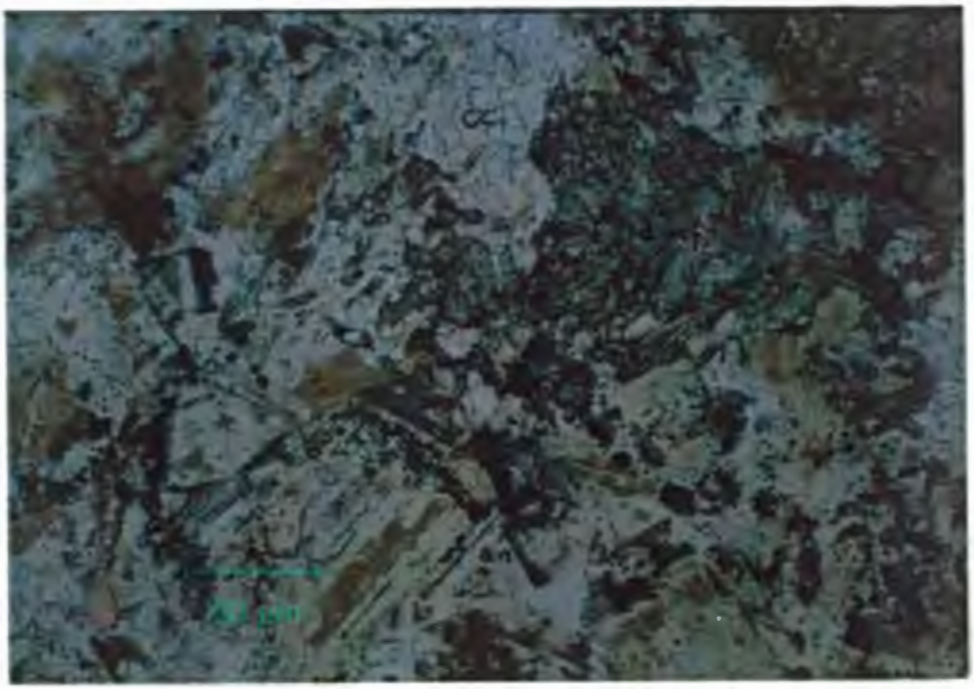

PLATE 3.14
NQOLENI VOLCANICLASTIC - CEMENT

Amphibole (amf), carbonate (cc) and analcite (an) in the cement base.

The xenoliths consist of dolerite, siltstone, fine-grained sandstone and felsic crustal rocks while disaggregated xenocrysts are mainly feldspar and quartz and lesser amphibole. Carbonate pseudomorphs that resemble the shape of olivine phenocrysts and rare partially altered clinopyroxene and phlogopite macrocrysts occur disseminated within the matrix of the sample. These latter minerals probably represent crystal fragments from the melilitite magma.

Juvenile lapilli occur as indistinct irregular shaped blebs of largely indeterminate mineralogy. Small altered (carbonate) olivine phenocrysts, phlogopite, altered melilite phenocrysts and groundmass laths and small opaque minerals are occasionally discernible within the matrix of some pellets.

Accretionary lapilli (Plate 3.13) occur as irregular shaped aggregates of finely comminuted material (country rock and melilitite) and as turbid grey rims of fine particles on country rock fragments, xenocrysts, glass and juvenile lapilli. In the larger lapilli two or three zones of layering are apparent.

Abundant orange-brown, isotropic blebs occur randomly distributed throughout these samples. They are typified by rounded shapes and conchoidal fractures and, where this 'fracturing' is extensive, 'bow-tie' like shapes. A radial arrangement of feathery, darker brown crystallites? is present within most of these blebs (Plate 3.14). The shape,

appearance and isotropic nature of these structures resembles descriptions of devitrified glass fragments (Cas and Wright 1987).

Constituents in the finer-grained zones are characterised by a distinct almost parallel orientation (bedding). The rock type is made up of essentially the same mineralogy, clasts and mineral fragments as the coarser volcaniclastic material but the mineralogy of the pellets is better preserved, disaggregated phlogopite macrocrysts more abundant and some fragments of magmatic rock are also present. Both juvenile lapilli and fragments consist of occasional altered olivine macrocrysts and phenocrysts, altered melilite phenocrysts and phlogopite and rare clinopyroxene macrocrysts set in a groundmass of altered melilite laths, phlogopite, opaque minerals, altered perovskite and rare apatite. Carbonate is more abundant than analcite in the interstitial base. Amphibole is an abundant and conspicuous mineral throughout this base and is also present in the lapilli and melilitite fragments.

CHAPTER FOUR

MINERALOGY

4.1 GENERAL INTRODUCTION

Mineral morphologies and their textural relationships are useful criteria for establishing the probable parageneses of minerals, order of crystallisation of the primary magma, reaction processes, phase relations and the nature and extent of alteration. With this view in mind the mineralogy of the Eshowe melilitites is described in detail in order to aid the petrogenetic evaluation of mineral and whole rock chemistry.

Several populations of minerals have been recognised on the basis of grain size, mineral associations and morphology. Terminology used to classify each of the groups is defined in Table 3.2. In general, five populations of minerals are present in the melilitites. These are: xenocrysts, macrocrysts, phenocrysts, microphenocrysts and groundmass. *Xenocrysts* are believed to be derived from disaggregated mantle xenoliths and as such detailed descriptions of these minerals are included in Section 4.8 in conjunction with the microxenoliths. The term *macrocryst* is based on the terminology of Clement (1982) and refers, in particular, to olivines characterised by a generally large grain size and

anhedral morphology. It is a non-genetic term introduced because of uncertainty as to whether the grains represent large corroded phenocrysts, or xenocrysts from disaggregated xenoliths. The term is also used with reference to all minerals of uncertain paragenesis. *Phenocrysts* and *microphenocrysts* are generally characterised by simple euhedral or subhedral morphologies and are believed to have crystallised at an early stage from the melilitite magma. The terms are purely descriptive in that they distinguish between essentially macroscopically and microscopically discernible grains respectively. An arbitrary boundary of 0.5mm in longest dimension has been used: phenocrysts are considered to be larger than and equal to 0.5mm while microphenocrysts are less than 0.5mm in size. *Groundmass* minerals make up the bulk of the fine-grained matrix of the melilitites and represent the later crystallising minerals.

4.2 OLIVINE

Five morphological groups of olivines are present in all of the Emtilombo rock types. These are: xenocrysts, macrocrysts, complex-phenocrysts, phenocrysts and microphenocrysts.

In Tembani Ranch dyke olivine occurs as altered, yellowish-brown (clay-minerals, serpentine, calcite and/or dolomite) pseudomorphs with relict subhedral to euhedral morphology (Plate 3.1). They range from 0.1mm up to rare 3.6mm grains. Rare, small (approximately 2mm or less in size), rounded,

anhedral grains are present and may represent pseudomorphs after olivine macrocrysts. The fine-grained, porphyritic nature of the dyke suggests that, although olivine morphologies are well preserved, they may not be representative of all groups that were originally present; the macrocrysts and larger phenocryst populations could have been removed by, for example, magma or crystal fractionation.

Modal abundance analyses of olivine morphological groups was estimated from the Emtilombo uniform melilitite as this is the predominant rock type at this locality. Olivine accounts for an average 24 vol.% of the uniform melilitite (range 20 to 25 vol.%). Macrocrysts account for 8 vol.% (range 5 to 10 vol.%) and phenocryst populations, including the microphenocrysts, 16 vol.% (range 12 to 20 vol.%). Complex-phenocrysts are commonly the dominant phenocryst type making up 10 vol.% (range 7 to 12 vol.%) of the rock while phenocrysts and microphenocrysts make up 6 vol% (range 5 to 6 vol.%). In terms of the olivine populations a ratio of 8:10:6, macrocrysts (33%) : complex-phenocrysts (42%) : phenocrysts and microphenocrysts (25%) is evident. More microphenocrysts were probably originally present but extensive late stage resorption by residual potassic-rich liquids has masked their presence.

4.2.1 MACROCRYSTS

Macrocrysts occur as discrete grains. They, in general, make

up the larger size fraction of the olivines, commonly occurring within the 3mm to 6mm size range. Grains as small as 0.5mm and as large as 1cm are, however, present. The mean grain size is about 4mm.

Macrocrysts are elongate to rounded or tabular, anhedral or pseudo-subhedral grains (Plates 4.1 and 4.8). No distinct original crystal boundaries are preserved but a few grains have some indistinct straight edges which may represent slightly corroded relicts of original euhedral, or subhedral, morphology. Alternatively it may represent imposed morphology either due to selective corrosion along a crystallographic plane or to later overgrowth. This grain morphology has therefore been termed pseudo-subhedral. Grain boundaries that show definite corrosion are characterised by relatively large concave indentations and rare, sharp re-entrant features. The indentations are filled with groundmass minerals, the most conspicuous of which are phlogopite and opaque spinels. Phlogopite appears to have a reaction relationship with olivine and is a common mineral associated with corroded crystal faces of all morphological groups. Small perovskites and some small opaque spinels cluster along rims outlining grain morphologies.

Macrocrysts, in general, show very little evidence of strain although a few do have undulose extinction and most of the grains are extensively fractured. The latter could be due to depressurisation expansion. Alternatively Deer et al. (1982)

suggest this feature is typical of the more iron-rich olivines. Secondary alteration to a yellowish-brown, possible serpentine-chlorite mixture and/or calcite is ubiquitous along these fractures and around grain rims.

Inclusions in these olivines are rare. Small opaque minerals <0.01 up to 0.04mm are enclosed predominantly near the grain boundaries of most macrocrysts although a few of the larger opaques are enclosed well within grains. Small, ±0.01mm, perovskite inclusions are also present but are rare and occur only within macrocryst rims.

Minute (<< 0.01mm) rounded to elongate blebs and trails of blebs are conspicuous in all macrocrysts. These are believed to represent small fluid inclusions and annealed fractures respectively (Moore 1979). Rare oval to rounded, largely calcite filled "fluid inclusions" (0.06 up to 0.2mm in diameter) are present within some of the grains. These inclusions appear to be primary features, however, they commonly occur within grain fractures or at the intersection of fractures. As a result the original "fluid" is no longer preserved but represents secondary or deuteric material similar to that observed in fractures.

4.2.2 PHENOCRYSTS

4.2.2.1 COMPLEX-PHENOCRYST

The term complex-phenocryst is a sack term and includes all

morphologically unusual olivines. The most distinctive feature of these olivines is their unusual primary morphology (Plate 4.2). The grains are euhedral to subhedral but they occur as growth aggregates, "hopper" and unusually shaped grains characterised by sharp embayments, or re-entrant features. The latter features appear to represent primary crystallisation morphology and not later resorption. Growth aggregates occur as both parallel and knee shaped aggregates. These phenocrysts, generally, range from 1mm up to 2mm, although rare grains down to 0.23mm in size are present. They have an average size of 1.6mm. All grains show some evidence of corrosion by the magma which ranges from slight to extreme. In extreme cases it is difficult to determine olivine paragenesis and these grains are included in the complex phenocryst group. Slight corrosion of grain margins is evident as small, cusp shaped, phlogopite filled embayments.

Complex phenocrysts are similar to macrocrysts in several respects: they are generally fairly fractured, have vague undulose extinction, perovskite and opaques cluster along grain boundaries and minute blebs, trails of blebs and small rounded fluid inclusions, are present. The grains differ from macrocrysts in size and shape, some grains show strain slip and the small opaque inclusions within grain rims are, in general, slightly larger and more abundant. Small perovskite grains occur as inclusions within olivine, near grain boundaries and are sometimes more abundant than the opaques.

4.2.2.2 PHENOCRYSTS AND MICROPHENOCRYSTS

Olivine phenocrysts and microphenocrysts are discrete crystals with "simple" morphology. Phenocrysts range from 0.5mm up to 1.41mm and have a mean of about 0.78mm in size. The microphenocrysts are the smallest olivine size fraction present. They range from less than 0.05 up to 0.48mm and have a mean size of 0.22mm.

Phenocrysts are generally characterised by euhedral grain shapes with extended development of pyramid faces on half of the grain. This gives rise to in-equant crystals (Plate 4.3) which are morphologically unusual with respect to those observed in most kimberlites. In the latter phenocrysts are generally equant. There is some evidence for strain as individual grains show vague undulose extinction and, in some cases, strain slip is apparent as a change in extinction angle across a clear cut line. Grains are again fairly fractured. Trails of minute blebs are present within phenocrysts but are not as abundant as in macrocrysts. In general perovskite and opaque minerals cluster conspicuously along grain boundaries and the latter are relatively more abundant and larger than those observed rimming the complex-phenocrysts. Small opaques and very rare perovskite(?) occur as inclusions within olivine, again near grain margins.

Microphenocrysts are predominantly equant and, in some cases, elongate. They generally show no evidence of strain as extinction is uniform. Trails of minute blebs are generally

absent or rare. Many of the smaller microphenocrysts are characterised by irregular subhedral shapes because grains partially enclose relatively large euhedral opaque minerals (Plate 4.4). In some cases these opaques completely rim the microphenocrysts giving rise to apparently distorted, anhedral olivine grain shapes.

Some resorption of the grain margins of both olivine populations is evident as small jagged, triangular indentations or again as small cusp shaped embayments. Many of the smaller microphenocrysts show almost completely replacement by, in particular, groundmass phlogopite. Some phlogopite patches in the matrix contain a ring of opaque minerals and perovskite and could represent replaced microphenocryst olivines.

4.3 CLINOPYROXENE

Five morphologically distinct groups of clinopyroxenes have been recognised: macrocrysts, phenocrysts, microphenocrysts, inclusions and groundmass. All populations are present in the Emtilombo melilitites and with, the exception of the groundmass clinopyroxenes, are rare. Macrocrysts have only been observed in the Emtilombo uniform melilitite while the phenocryst populations occur in the micaceous melilitite and in the clinopyroxene-rich melilitite. Groundmass clinopyroxene is the most abundant and conspicuous phase in the Emtilombo clinopyroxene-rich melilitite where it accounts for

22 vol.% of the rock. It occurs in minor and trace amounts in the micaceous variety and the uniform melilitites.

Tembani Ranch melilitite differs from Emtilombo in that clinopyroxene phenocrysts and microphenocrysts are relatively abundant (4 vol.%), groundmass clinopyroxene is conspicuous but is a minor phase (5 vol.%) and no macrocrysts or inclusions were observed.

4.3.1 MACROCRYSTS

Clinopyroxene macrocrysts occur as discrete, anhedral, corroded grains that range from 1.0mm up to 5.2mm in size. They vary from elongate to almost tabular or wedge shaped but in many cases a vague suggestion of relict original euhedral or subhedral shape is preserved in the matrix by the orientation of melilite laths. Corroded outlines consist of concave indentations filled by matrix minerals. In some cases corrosion is extreme giving rise to irregular shaped grains and occasional relict islands of clinopyroxene which remain in the melilite matrix next to larger remnants of the original grain (Plate 4.5). This corrosion appears to be crystallographically controlled as it is concentrated predominantly along cleavage traces. Rare grains partially enclose anhedral opaque minerals that are up to 0.45mm in size.

Macrocrysts commonly consist of a core of clear, very pale greenish clinopyroxene and a generally colourless, turbid,

spongy or blocky textured rim. Cleavage traces are distinct in cores as are numerous, narrow (<0.01mm) curvilinear zones that consist of abundant minute blebs. These trails of blebs do not appear to follow cleavage traces and although they are distinct zones, contacts with clear clinopyroxene are diffuse. They are similar to the trails of blebs that occur in the olivines. The cores of some grains show strained extinction. Cores are commonly irregular in shape and have sharp contacts with the turbid rims.

Rims generally range from 0.02 to 0.28mm in width but rare grains consist entirely of turbid clinopyroxene. Rim clinopyroxene is disrupted by an abundance of small, crystallographically orientated blebs which occasionally form an interlinking network. The blebs are irregular pipe-like or rounded features which in general contain a low birefringent, indeterminate mineral and lesser calcite or phlogopite. Clear patches of clinopyroxene occur as fine needle-like laths, rounded or irregular shaped grains and/or relict cleavage blocks. The latter gives rise to the blocky texture.

Clinopyroxene in the rims appears to be optically continuous with that in the core but, in addition to colour differences, generally has a different extinction angle to the latter.

4.3.2 PHENOCRYSTS AND MICROPHENOCRYSTS

In Tembani Ranch the clinopyroxene phenocrysts and micro-

phenocrysts occur as pale-green, pleochroic, subhedral to euhedral grains. They range from 0.3 up to 3mm in size. These grains are darker in colour than the Emtilombo macrocrysts but also show evidence of corrosion and are generally surrounded by a rim of colourless, spongy clinopyroxene (Plate 4.6). The spongy material consists of a mixture of zeolites?, calcite, phlogopite and groundmass clinopyroxene interspersed amongst relict patches of the phenocryst clinopyroxene. The patches of 'groundmass material' within the spongy zone are much broader and better developed than in the Emtilombo macrocrysts. Cores are again clear, cleavage traces are distinct and some trails of minute blebs are present. Some cores are zoned and very fine exsolution lamellae are discernible.

Clinopyroxene phenocrysts in the Emtilombo melilitites range from 0.45mm up to 2mm in size and are characterised by a variety of colours: colourless, very pale green, pale yellow or pinkish brown. Some grains are strongly pleochroic greenish to pale pinkish brown but most are weakly pleochroic pale green to pale yellowish. Vague zoning and strained extinction are evident in some grains and trails of minute blebs are again present in these clinopyroxenes. The grains are generally anhedral and corroded by matrix minerals but relict grain shapes are well preserved by the presence of melilite laths orientated parallel to the original grain boundaries (Plate 4.7). One grain shows clear, parallel twin lamellae. Some small perovskite and opaque minerals occur at

and are partially enclosed by grain rims.

The spongy textured rims prevalent on the macrocrysts do not appear to be present on the Emtilombo phenocrysts but extensive reaction with and replacement by groundmass minerals is evident on all grains. The groundmass minerals consist of phlogopite, calcite, serpentine and zeolites?. Patches of darker, olive-green groundmass clinopyroxene occur in some of these reaction zones.

4.3.3 INCLUSIONS

Rare inclusions of clinopyroxene occur within olivine macrocrysts and complex-phenocrysts and phlogopite macrocrysts (Plate 4.8). They occur as oval shaped, colourless or very pale brownish inclusions in olivines where they range from 0.11 up to 0.23mm in size. Contacts with the host olivine are clean and sharp. One clinopyroxene is associated with a minute opaque mineral.

Two small clinopyroxene inclusions, one elongate and one oval in shape occur in a phlogopite macrocryst. They are approximately 0.06 and 0.03mm in longest dimension. Both are colourless. One inclusion has sharp contacts with the macrocryst and does not appear to be associated with any other minerals. The second grain may be associated with a groundmass incursion into the macrocryst.

4.3.4 GROUNDMASS

Groundmass clinopyroxene in the Emtilombo clinopyroxene-rich melilitite is coarse relative to that in the other rock types. The mineral occurs as pale greenish to faintly pleochroic pale olive to pale emerald green, laths and basal sections. The grains range in size from relatively broad laths, up to 0.13mm in length, to fan-like aggregates of fine needles. They occur predominantly as a felty mesh within analcite and calcite 'pools' (Plate 4.9).

Groundmass clinopyroxene in the Emtilombo micaceous melilitite is olive to emerald-green and is deeper in colour than that in the clinopyroxene-rich melilitite. It occurs as euhedral, blade-like prisms, coarse irregular shaped plates, narrow fine laths with flat terminations and broad laths with irregular terminations. Laths range from less than 0.02 up to 0.13mm in length. These grains are most commonly associated with patches of phlogopite which are either randomly distributed in the interstices between melilite or associated with reaction rims around olivines (Plate 4.10). Occasional clinopyroxene occurs scattered in the melilite groundmass. Birefringence of the grains is masked by their colour but it appears to range from first order greys to yellow and sometimes appears anomalous (berlin blue). Similar clinopyroxene is present in the phlogopite-poor uniform melilitite but is extremely rare. Groundmass clinopyroxene in Tembani Ranch has a similar colour, morphology, size and distribution to that in the micaceous Emtilombo rock type.

Minute possible clinopyroxene microlites are associated with melilite in the Tembani Ranch rock type. The microlites occur at melilite rims and either jut inwards from or are orientated parallel to grain rims (Plate 4.13).

4.4 PHLOGOPITE

4.4.1 MACROCRYSTS

Phlogopite macrocrysts occur in trace amounts in all of the Eshowe melilitites. In the Emtilombo dyke they appear to be more abundant in the clinopyroxene-rich melilitite than in the other varieties. The macrocrysts occur as subhedral to anhedral, yellowish-brown to pale brown basal sections and ragged laths or laths with rounded terminations (Plate 4.11). Pleochroism is normal and strained extinction is evident. The laths range from 0.5mm up to 4.5mm, in Tembani Ranch, and 9mm in Emtilombo. Some grains, particularly those in Tembani Ranch, are distorted by calcite which has invaded along cleavage traces.

Some of the Tembani Ranch macrocrysts are zoned. Zoned laths consist of an irregular either paler coloured core and darker brown euhedral rim, both with normal pleochroism, or a darker core and paler rim. Pleochroism in the paler rim is reversed. An overgrowth of orange-brown groundmass phlogopite with weak normal pleochroism also occurs on many of the Emtilombo phlogopite macrocrysts and is associated with an abundance of very fine opaque minerals (Plate 4.11).

4.4.2 GROUNDMASS

Groundmass phlogopite is present in all of the Emtilombo rock types. It is similar in appearance throughout but varies in abundance. It has a patchy distribution and occurs as euhedral stubby laths and subhedral to irregular shaped interstitial plates that range in size from 0.01mm up to 0.14mm with a mean size of about 0.05mm. The mineral sub-ophitically and poikilitically encloses apatite, melilite, opaque minerals, perovskite, sodalite? and clinopyroxene. Phlogopite cores are characterised by yellow- or orange-brown to pinkish-brown weak normal pleochroism and distinctive deeper reddish coloured rim (Plates 4.12, 4.14). The rims show strong reversed pleochroism.

Groundmass phlogopite in Tembani Ranch is similar in appearance to that in Emtilombo but is paler in colour and appears to lack the darker rim. It occurs as weakly pleochroic (reversed), pale yellow-brown to pale brown, stubby laths, 0.01 to 0.06mm in length, and as subhedral to euhedral basal sections. In a few samples the mica occurs as relatively coarse-grained laths up to 0.17mm in length. The mineral has a similar patchy distribution to that in the Emtilombo melilitites.

4.5 MELILITE

4.5.1 PHENOCRYSTS

Melilite phenocrysts in Tembani Ranch melilitite occur as

slender, elongate laths that make up a conspicuous proportion of the phenocryst population. The mineral occurs as yellowish pseudomorphs that are completely altered to clay minerals and minor calcite (Plate 3.1). Laths range from 0.5 up to 3mm in length and have a length:breadth ratio of 10:1. Apatite laths and basal sections occur as inclusions within many of the phenocrysts but are most commonly partially enclosed by and orientated parallel to the melilite rims (Plate 4.13).

Melilite phenocrysts are present in the Nqoleni volcaniclastic breccia where they occur as stubby altered laths. No phenocrysts appear to be present in the Emtilombo or Cowards Bush melilitites.

4.5.2 GROUNDMASS

Melilite is the most abundant primary groundmass mineral in all of the Eshowe melilitites with the exception of the Emtilombo clinopyroxene-rich rock type.

In the Emtilombo rock types melilite occurs as colourless, euhedral to subhedral, elongate laths that range from less than 0.03mm up to rare 0.42mm grains but are generally about 0.08mm in length (Plates 4.12 and 4.14). Very fine needles of apatite (<<0.01mm width) occur either as inclusions within or juxtaposed parallel to grain rims of many of the melilite laths. A very narrow zone of alteration occurs at the rims of most of the laths. The alteration product is unidentified.

In Tembani Ranch the mineral occurs as indistinct yellowish- to turbid-brown pseudomorphs (Plate 3.2). They occur as vague, elongate laths that range from less than 0.06 up to 0.17mm in length. Alteration and colour are similar to that in the phenocrysts.

4.6 OPAQUE MINERALS AND PEROVSKITE

Opaque minerals are an abundant and ubiquitous phase scattered randomly throughout the groundmass of the Emtilombo and Tembani Ranch rock types. They occur in two size ranges: as a coarse population, 0.11mm to 0.34mm which grades down into a later crystallising, finer grained population (Plate 4.14). The latter range from a fine groundmass speckling up to 0.1mm in size. Both populations display euhedral to subhedral, predominantly equant morphologies and they occur as small aggregates and discrete grains. Perovskite is often associated with these aggregates and is generally partially enclosed by the opaques. In rare cases this relationship is reversed and perovskite partially encloses opaques (Plate 4.14). Opaque minerals characteristically occur in clusters rimming translucent spinel xenocrysts (Plate 4.27) and olivine grains, particularly the smaller microphenocrysts (Plate 4.4). Many of the opaques in the groundmass of the Tembani Ranch and Cowards Bush samples are oxidised to a spongy, brown limonite.

In reflected light the opaque minerals are characterised by a brownish-grey reflectance which is characteristic of titano-

magnetite. No obvious zonation is evident. Small, granular aggregates and slightly larger subhedral to euhedral cubic grains or irregular veinlets of a sulphide mineral (pyrite) are present. Rare sulphide grains have nucleated on the rims of the titano-magnetites but in general they occur scattered within the groundmass. Sulphides grade from minute pinhead sized granules up to rare 0.03mm sized grains and 0.23mm aggregates. Titano-magnetites are the most abundant and conspicuous opaque minerals present with sulphides making up a minor proportion of opaque mineral population.

Perovskite is a common mineral throughout the groundmass of all the dyke rock types. In the Emtilombo melilitites two generations of perovskite are present: a coarse earlier population and finer-grained later crystallising grains. The coarser grains are rare and occur as discrete, anhedral to subhedral, translucent, pale purplish crystals up to 0.13mm in size (Plate 4.9). The second generation of perovskites have a similar colour to the former but are predominantly euhedral to subhedral and occur as discrete grains and clusters. They grade from a fine groundmass dusting up to 0.1mm in size although they are generally less than 0.06mm (Plates 4.4 and 4.14). These grains occur in clusters with opaque minerals, as described above, and as partial rims around olivines. The Tembani Ranch perovskites have a similar morphology, colour, size and distribution to the Emtilombo perovskites but no coarse first generation grains were observed. Alteration is more extreme than in the latter locality and the mineral is

sometimes altered to a turbid yellowish-brown material.

4.7 OTHER GROUNDMASS MINERALS

4.7.1 CARBONATE

Carbonate is an abundant and ubiquitous phase in all the melilitites examined and occurs in both crystalline and cryptocrystalline forms. Calcite is the predominant carbonate in the Tembani Ranch dyke but minor dolomite is also present (the carbonates were identified with alizarin red S stain).

In Tembani Ranch dyke crystalline calcite accounts for about 6 to 8 vol.%. It occurs within irregular segregationary 'pools', within veins, that cut through the melilitite matrix, and as a secondary alteration product replacing olivine. Dolomite similarly occurs associated with calcite within veins and as a crystalline phase replacing olivine. Groundmass phlogopite, clinopyroxene and apatite are commonly associated with calcite in the 'pools'. Crystalline carbonate in the Emtilombo melilitites has a similar morphology and distribution to that in the Tembani Ranch rock type and is probably predominantly calcite. In the segregationary and globular-segregationary varieties it occurs as small rhombs that have nucleated on the earlier crystallised silicate groundmass and rim the serpentine? filled pools (Plate 3.4). Carbonate in veinlets occurs as euhedral rhombs and relatively coarse, anhedral interlocking plates and is closely associated with a variety of feldspathoids and zeolites (Plate 4.15). In

clinopyroxene-rich melilitite carbonate occurs as large, interstitial, anhedral plates associated with clinopyroxene and zeolite filled segregations. Crystalline carbonate in the Nqoleni melilitite has a similar morphology and association with zeolites and is again interstitial (Plates 3.11 and 3.14).

In the Tembani Ranch melilitite cryptocrystalline calcite and lesser dolomite replaces much of the primary groundmass mineralogy and is probably mainly after melilite. The minerals are turbid-brownish in appearance and are extremely abundant with an estimated minimum of 6 to 10 vol.% being present in the samples. These figures represents the volume of carbonate replacing unrecognisable constituents (recognisable pseudomorphs were counted as the original primary phases). This is borne out, to some extent, by comparing modal analyses of extensively altered and relatively fresher specimens. In the former melilite makes up 24 vol.% of the matrix and total carbonate (crystalline and cryptocrystalline) recorded is 18 vol.%, while in the latter, melilite accounts for 40 vol.% and total carbonate is less abundant, 11 vol.%. Cryptocrystalline carbonate is much less abundant in the Emtilombo melilititites. In most cases it replaces the silicate groundmass in the vicinity of the crystalline segregations and appears to emanate from these 'pools'. Carbonate in the Coward Bush melilitite is present as a ubiquitous turbid-grey, cryptocrystalline mask but rare colourless crystalline rhombs do occur.

4.7.2 SERPENTINE

Serpentine was not positively identified in any of the Eshowe melilitites but a mineral similar in appearance and distribution to serpentine in kimberlites occurs in some of the Emtilombo rock types. The mineral is amorphous has a very pale brownish-buff colour and a speckled appearance in polarised light. It is possibly altered to clay minerals. This phase is present in interstitial pools in the segregationary and globular-segregationary varieties of the uniform melilitite and in the melilitite breccia (Plates 3.4 and 3.6).

4.7.3 APATITE

Apatite is ubiquitous in the magmatic dyke rocks, is present in Nqoleni melilitite but was not recognised in the Cowards Bush specimens. The mineral is most abundant in the Tembani Ranch melilitite where it makes up 5 vol.% of the rock. In the latter it is generally euhedral to subhedral and occurs as conspicuous colourless, coarse laths up to 0.3mm in length and a finer grained population that grades down in size to small needles that are less than 0.03mm long. It also occurs as distinctive hexagonal basal sections. The coarser laths are discrete grains that are randomly distributed throughout the groundmass (Plate 3.2) They, in some cases, poikilitically enclose small opaque minerals and perovskite. The smaller apatite population occurs as discrete grains or fan-like clusters of needles and are most commonly associated with

with analcite and calcite filled 'pools'. As mentioned above apatite also occurs as inclusions in or in close association with melilite phenocrysts (Plate 4.13).

Apatite is not as abundant in the Emtilombo melilitites as it is in Tembani Ranch and the coarse population is absent. The morphology and distribution of the apatites is similar to that observed at the latter locality. The mineral occurs as relatively broad, equant to fine, elongate needle-like prisms. The latter commonly occur juxtaposed on and parallel to or partially enclosed within the rims of melilite laths. Rare apatites occur as inclusions within the melilites. These prisms are up to 0.06mm in length.

4.7.4 FELSPATHOIDS AND ZEOLITES

Analcite is abundant in the interstitial base of the magmatic dyke rocks (Plates 4.12 and 4.14), Nqoleni melilitite and possibly in Cowards Bush. It occurs as a colourless, amorphous isotropic phase and is most noticeable in veinlets that transect the magmatic rock types (Plate 4.15), segregations in the Emtilombo clinopyroxene-rich melilitite (Plate 4.9) and in the base of the Nqoleni volcaniclastic breccia (Plate 3.14).

Sodalite(?) is most conspicuous in the groundmass of the Emtilombo uniform melilitite but is also present in the other melilitite varieties and in the Tembani Ranch rock type. It

occurs as randomly distributed, granular clusters of rounded euhedral to subhedral colourless, isotropic grains and is interstitial to melilite (Plate 4.14). The grains range from less than 0.03mm up to 0.17mm in diameter but they are generally small, about 0.03mm or less in size. Rare minute fluid inclusions are present in the larger grains but in general they are inclusion free. It is also a conspicuous mineral in veinlets where it is commonly associated with zeolites and carbonate (Plate 4.15).

Nepheline(?) is rare and occurs as colourless, anhedral grains in small interstitial 'pools' in the groundmass of the uniform melilitite. The mineral was identified optically but this identification was not positively confirmed. It is characterised by a relatively higher relief than analcite and sodalite.

A number of zeolites that have not been identified are present in the Eshowe melilitites. These occur as fibrous, feathery needles in radial aggregates and as colourless, tabular or wedge shaped laths also commonly in fan-like aggregates. Both zeolite types have low first order birefringence. Again these minerals occur in 'pools' and are conspicuous in veinlets. They commonly occur in association with the feldspathoids.

4.8 XENOLITHS AND XENOCRYSTS

Xenocrystic minerals present in Emtilombo rock types consist of olivine, clinopyroxene, opaque and translucent spinel, orthopyroxene, and ilmenite. In all cases these minerals are rare. No large xenoliths were found in any of the Eshowe melilitites but a number of small microxenoliths are present in thin sections from the Emtilombo dyke rocks. These microxenoliths consist of combinations of one or more of the above minerals, with the exception of ilmenite. Ilmenite occurs as rare, discrete macrocrysts within the matrix of the melilitites and is prominent in heavy mineral concentrates from all of the Eshowe melilitites. The mineral was observed to occur as lamellae in one clinopyroxene xenocryst.

The most abundant microxenoliths present consist predominantly of olivine and various combinations of clinopyroxene, orthopyroxene and/or rare translucent spinel. Similarities in, for example, the morphology, grain size and textures of minerals within these fragments suggests they belong to a single suite of lherzolitic nodules. These microxenoliths make up about 54% of the xenolith population present in the Emtilombo dyke. Other rock fragments present comprise: a coarse olivine-rich, dunitic, rock type (34% of the xenolith population); a clinopyroxene-rich variety (8%); and a phlogopite-clinopyroxene nodule fragment (4%).

4.8.1 LHERZOLITE SUITE

The lherzolite microxenoliths are characteristically small, elongate, rounded or wedge shaped and extensively corroded. They are, on average, 2.3mm by 1.7mm in size but range from 5.0mm down to 0.4mm in longest dimension (Plates 4.16 to 4.18). The texture, where discernible, is equant granuloblastic (Harte 1977).

Olivine is the most abundant mineral present and occurs as anhedral, equant grains that range from 0.14mm up to 3.6mm but are, on average, 1.6mm in size (Plate 4.16). A large proportion of the olivines, nearly 50%, are completely altered to yellowish clay minerals (Plates 4.17 and 4.18). Most of the fresh grains show evidence of deformation. This varies from vague undulous to distinct parallel, subgrain, extinction lamellae. The latter are generally rare and occur as broad lamellae with only one or two subgrains present in a single olivine. One olivine was seen to contain a minute (0.02mm) translucent brick-red spinel.

Clinopyroxene is an accessory mineral and occurs as anhedral elongate, rounded or irregular shaped grains that are interstitial to olivine and orthopyroxene (Plates 4.16 and 4.17). The mineral is colourless to very pale green or brownish and is sometimes very weakly pleochroic. Individual grains range from 0.14mm up to 1.9mm in size. A turbid, spongy alteration rim, similar to that associated with discrete macrocrysts, is present where grains are in contact

with the melilitite groundmass. Clinopyroxene appears to have been preferentially corroded, compared to olivine, by the melilitite magma. The larger clinopyroxenes show evidence for deformation as they are characterised by undulous strained extinction. Trails of minute blebs are evident in most grains.

Orthopyroxene is a minor mineral in these microxenoliths and is again interstitial to olivine (Plate 4.17). It occurs as very pale brownish-pink, subhedral to anhedral grains that range from 0.4mm up to 1.8mm in size. Minor very fine, discontinuous, parallel exsolution lamellae of possible clinopyroxene are discernible in some of the grains. In general the grains appear to be strain free. Orthopyroxene is characterised by a distinctive reaction rim where in contact with the melilitite groundmass (Plates 4.17 and 4.24). This rim consists predominantly of clinopyroxene microlites and phlogopite set in an amorphous, isotropic base. The microlites are generally orientated parallel to one of the orthopyroxene cleavage traces. Surrounding this zone, at the interface with the groundmass, is a narrow rim containing abundant finely speckled opaque minerals. In many of the more altered samples and the smaller microxenoliths this reaction material is all that remains of the original orthopyroxene grain (Plate 4.18).

Spinel occurs as translucent brick-red or orange-brown grains that are either interstitial to the other xenolith minerals

(Plate 4.18) or are, more rarely, enclosed within olivine. They occur as euhedral to anhedral grains that range from 0.02mm up to 0.4mm in size. Where in contact with the melilitite matrix they are rimmed by a corona of titano-magnetite and minor perovskite (Plates 4.24 and 4.26).

4.8.2 DUNITES

The most prominent of the other microxenoliths are coarse, tabular textured dunites. These are generally elongate or irregular in shape and are commonly the largest microxenoliths present (Plate 4.19). They are, on average, 8mm long by 4mm wide but range from 13.5mm to 1.4mm in longest dimension.

These xenoliths are characterised by the presence of abundant generally coarse-grained, tabular olivines. The olivines range from 0.4mm up to 10mm but average 3mm in size. Deformation is slight and the olivines show vague undulous extinction or, rare, parallel, subgrain strain lamellae. As for the lherzolites these lamellae are broad bands and again only one or two subgrain boundaries are present in a single grain. Olivines are corroded where in contact with the melilitite matrix but not as extensively as those in the lherzolite xenoliths. Within the dunite fragments the olivines are often characterised by straight grain boundaries and a distinctive internal, blocky fracture pattern. A characteristic feature of these microxenoliths is that many of the olivines are partially altered to and disrupted by a

yellowish alteration material. This alteration is concentrated along irregular internal fractures and grain boundaries.

Clinopyroxene is present as a minor mineral in these microxenoliths and occurs as anhedral, rounded to elongate grains that range from 0.23mm up to 1.8mm in size. It is pale greenish or brownish in colour and again trails of minute blebs are evident in the grains. The mineral is interstitial to olivine.

Phlogopite is a conspicuous constituent in these xenoliths. It occurs as subhedral to anhedral laths and basal plates that range from 0.11mm up to 1mm in length. The phlogopite is interstitial to the minerals described above and invades, along fractures, into some of the olivine grains (Plate 4.19). In a few of the dunites it is most conspicuous near the margins but some 'veins' do penetrate into the fragment centres. The mica is similar in colour and appearance to the discrete phlogopite macrocrysts. It varies from orange- or pale yellowish-brown to very pale brown or almost colourless and is generally weakly pleochroic. A slight turbid, corroded alteration zone occurs where the mica is in contact with the melilite matrix and groundmass phlogopite rims these laths.

Spinel has only been observed in one of the dunite micro-xenoliths (Plate 4.19). The grain is anhedral, almost oval in shape, 1.4mm in longest dimension and is opaque. A small

clover leaf shaped opaque spinel extends off the main grain. The grain is located within a phlogopite 'vein' in the microxenolith and appears to poikilitically enclose a small mica lath.

4.8.3 OTHERS

Two clinopyroxene rich microxenoliths were observed in the Emtilombo thin sections. These consist of coarse granular intergrowths of abundant pale greenish to colourless clinopyroxene. The largest microxenolith is 7mm long by 5.6mm wide and is irregular oval in shape (Plate 4.20). Rare euhedral olivine (0.5mm) and anhedral orthopyroxene occurs in the latter microxenolith. The clinopyroxene ranges from 0.3mm to 3mm and is on average about 3mm in size. At the contact with the melilitite matrix the microxenolith is characterised by a distinctive spongy textured alteration rim and a narrow outer zone of clear colourless clinopyroxene. The latter may represent a late stage overgrowth by groundmass clinopyroxene.

One microxenolith consists of an intergrowth of clinopyroxene and phlogopite and is 2.3mm long by 0.7mm wide (Plate 4.21). The clinopyroxene occurs as pale green euhedral to subhedral grains that range from 0.4mm up to 1mm in size. These grains are slightly darker greenish in colour but have a similar size range to those observed in the peridotite microxenoliths and trails of minute blebs are again present.

Phlogopite occurs as an intergrowth of relatively coarse and fine grained laths and ranges from about 0.03mm up to 2mm in length. The laths are pale orange-brown, exhibit weak pleochroism and are again similar in appearance to the discrete phlogopite macrocrysts. The larger laths are kinked and show strained extinction. Rare small rounded opaque minerals that range from about 0.01mm up to 0.09mm in diameter are present within the microxenolith (Plate 4.21). They occur within the mica intergrowth but are commonly adjacent to the clinopyroxene grains.

4.8.4 XENOCRYSTS

4.8.4.1 OLIVINE

Olivine xenocrysts are characterised by anhedral grain shapes, extensive corrosion, mosaic re-crystallisation textures and subgrain strain lamellae (Plate 4.22). Some grains show a combination of extensive subgrain deformation lamellae with a narrow margin or partial margin of recrystallised neoblasts. Xenocrysts occur as rounded to oval, colourless to turbid grains. The latter is due to alteration and resultant development of abundant granules of secondary opaque spinels along internal grain fractures or to the presence of numerous trails of minute blebs. These blebs may represent zones along which previously deformed grains have annealed, trapping fluids (Moore 1979). Inclusions of small opaque spinels are present in some of the olivine xenocrysts. Xenocrysts have an average grain size of 1mm but range from 2.3mm down to 0.4mm

in longest dimension. Discrete xenocrysts are difficult to recognise and are really only positively identified by the presence of distinctive deformation textures.

4.8.4.2 CLINOPYROXENE

One clinopyroxene xenocryst was positively identified as such on the basis that abundant ilmenite lamellae are present within the grain (Plate 4.23). The clinopyroxene is an elongate, anhedral grain that is 3.6mm in longest dimension. There is a vague suggestion of a relict euhedral morphology despite the extensive corrosion that has affected grain boundaries. It is unlike the discrete clinopyroxene macrocrysts and the xenocrysts in microxenoliths in that it does not show the classic reaction relationship with the groundmass of the melilitite, ie. no turbid spongy zone is present at the rim. The grain has a very pale brownish tint and it shows no evidence of strain as extinction is uniform throughout.

The ilmenite lamellae occur as translucent orange to opaque, very narrow elongate lenses (Plate 4.23). They are orientated parallel to each other and to the relict dome face of the grain and at 26° to the extinction angle of the clinopyroxene. Rare small, oval to rounded blebs of opaque ilmenite are also present in the clinopyroxene. The lamellae are about 2μ in width and 0.9mm in length while the blebs are less than and equal to 5μ.

4.8.4.3 ORTHOPYROXENE

Orthopyroxene occurs as rare, discrete, anhedral, very pale brownish-pink grains that range in size from 0.68mm up to 1.35mm. The grains are elongate oval to wedge shaped and are rimmed by the characteristic reaction corona described above (Plate 4.24). In some cases, discrete grains with a similar size and shape to the orthopyroxene grains consist entirely of reaction material (Plate 4.25). These grains are believed to be completely altered orthopyroxene xenocrysts. One xenocryst occurs as a bi-mineralic aggregate with translucent orange-brown spinel (Plate 4.24). The spinel has a clear sharp contact with the orthopyroxene and is translucent at the contact. No orthopyroxene reaction rim is present at this interface. A corona of opaque titanomagnetite rims the spinel where it is in contact with the melilitite groundmass and the characteristic reaction rim occurs on the orthopyroxene where it is not protected by the spinel.

4.8.4.4 TRANSLUCENT SPINEL

Translucent spinels are again rare but are, with the possible exception of olivine, the most abundant xenocryst minerals present in the Emtilombo melilitite. One to four grains of translucent spinel are conspicuous in most of the Emtilombo thin sections. They are characterised by a range of colours: green (one grain), orange-brown (relatively abundant), brown (rare) and red (rare). They occur as euhedral to subhedral grains and rare fragments. In most cases they are

characterised by a rim of opaque spinel. This occurs as an overgrowth of small groundmass opaques that have nucleated against the xenocrystic mineral (Plates 4.24, 4.26 and 4.27). Towards the outer edge of the rim small perovskite grains are enclosed by the opaque spinel aggregates. The translucent cores range from 0.01mm up to 0.4mm and are on average about 0.2mm in size. The opaque rims consist predominantly of titanomagnetite and in general are between 0.03mm and 0.1mm wide.

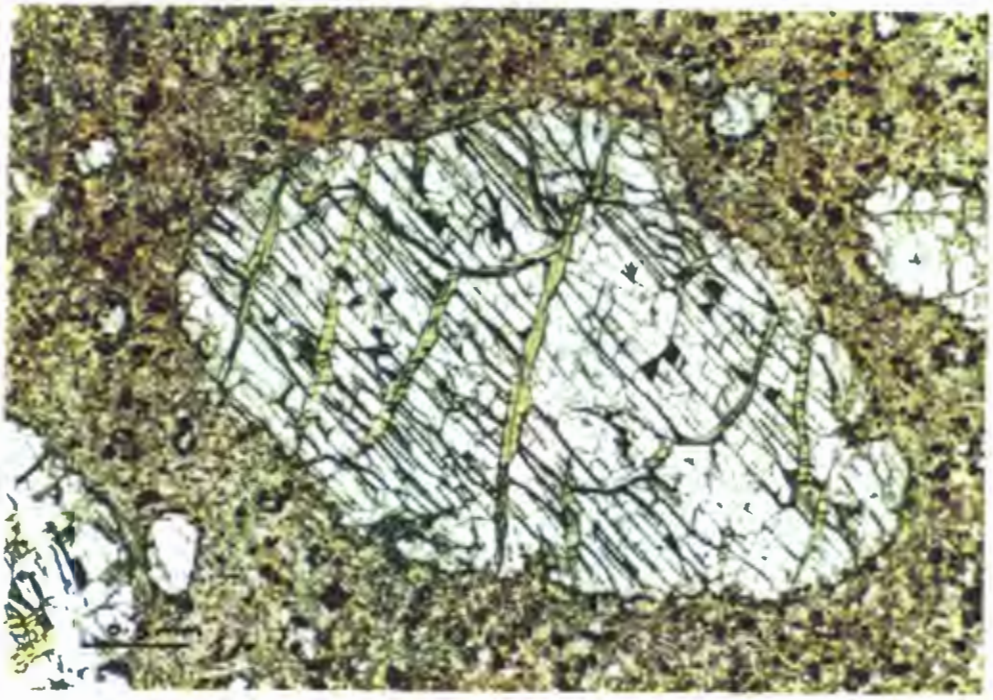

PLATE 4.1
EMTILOMBO - OLIVINE MACROCRYST

Large anhedral, tabular grain with pseudo-subhedral grain boundaries. Extensively fractured. A yellowish alteration product occurs along some of the fractures (PK003/59B OLI/3).

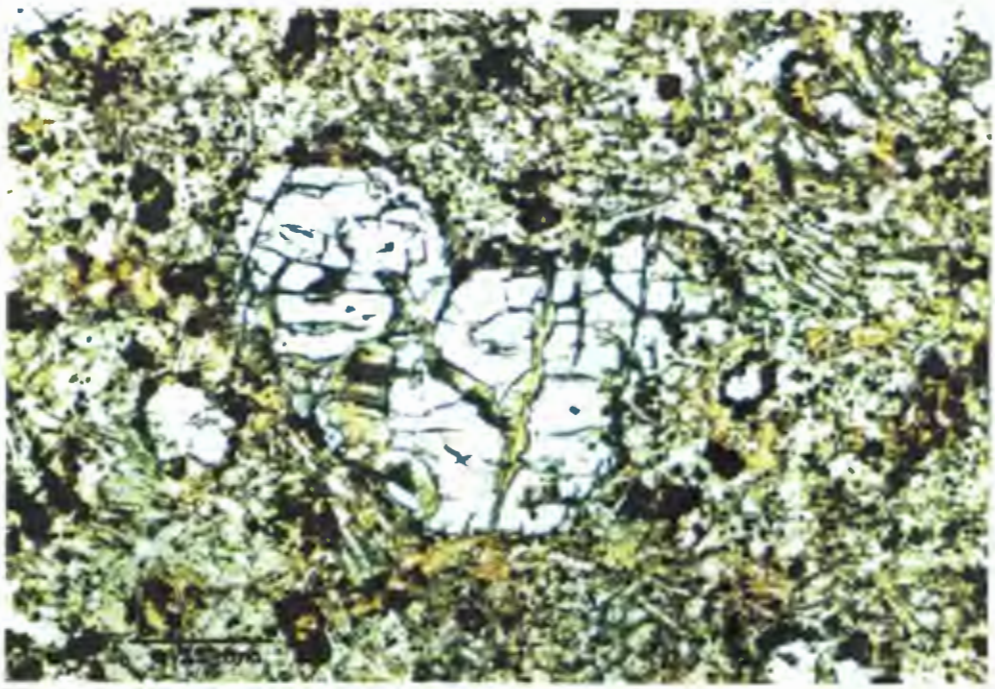

PLATE 4.2
EMTILOMBO - OLIVINE COMPLEX PHENOCRYST

Subhedral knee-shaped phenocryst. Fairly fractured and showing evidence of corrosion by residual potassic-rich liquids. A yellowish alteration product occurs along some fractures. The grain is rimmed by opaque minerals and perovskite (PK003/59B OLI/18).

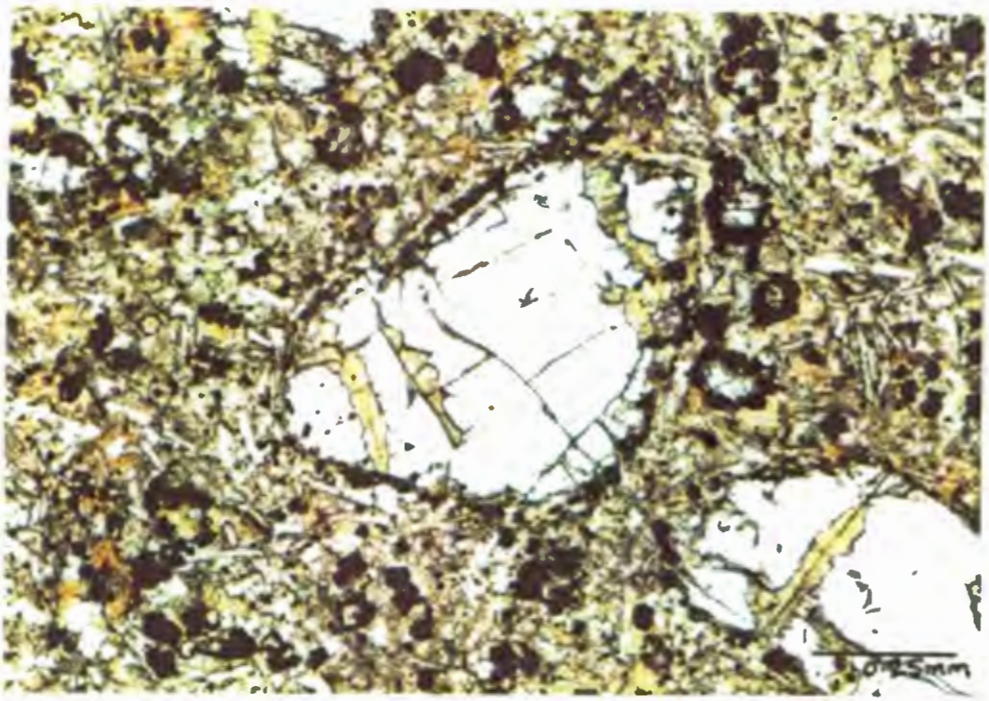

PLATE 4.3
EMTILOMBO - OLIVINE PHENOCRYST

Euhedral olivine phenocryst with a rim of opaque minerals (black) and minor perovskite. A yellow alteration product occurs along internal grain fractures (PK003/59B OLI/7).

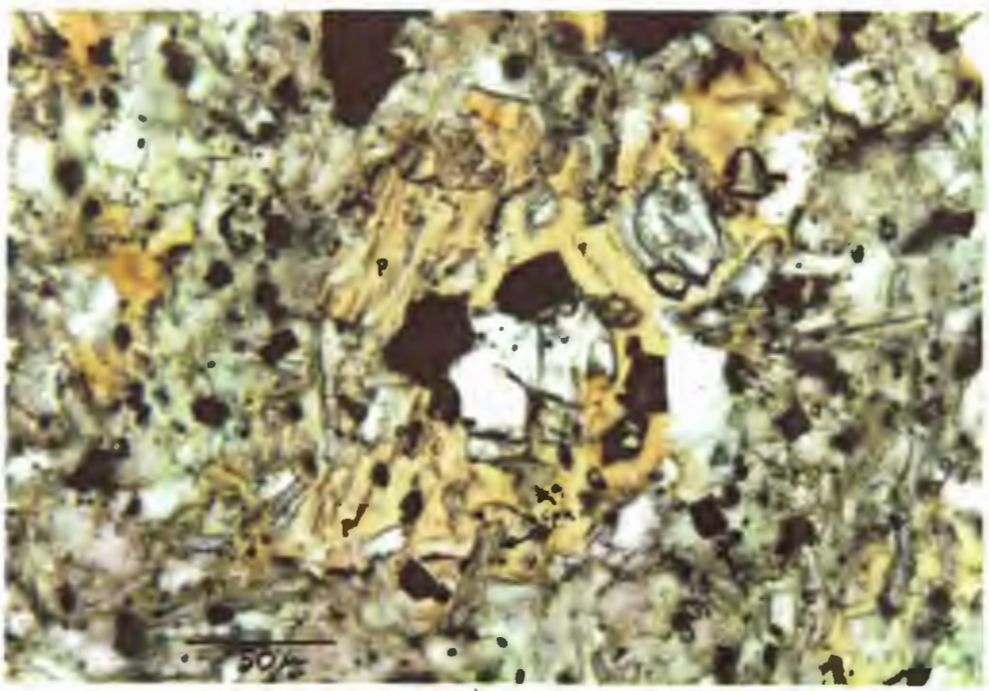

PLATE 4.4
EMTILOMBO - OLIVINE MICROPHENOCRYST

Anhedral olivine microphenocryst partially enclosing opaque minerals. The olivine is rimmed by and shows a strong reaction relationship with phlogopite (p). Clinopyroxene (cpx) is associated with this reaction (PK003/59B OLI/9).

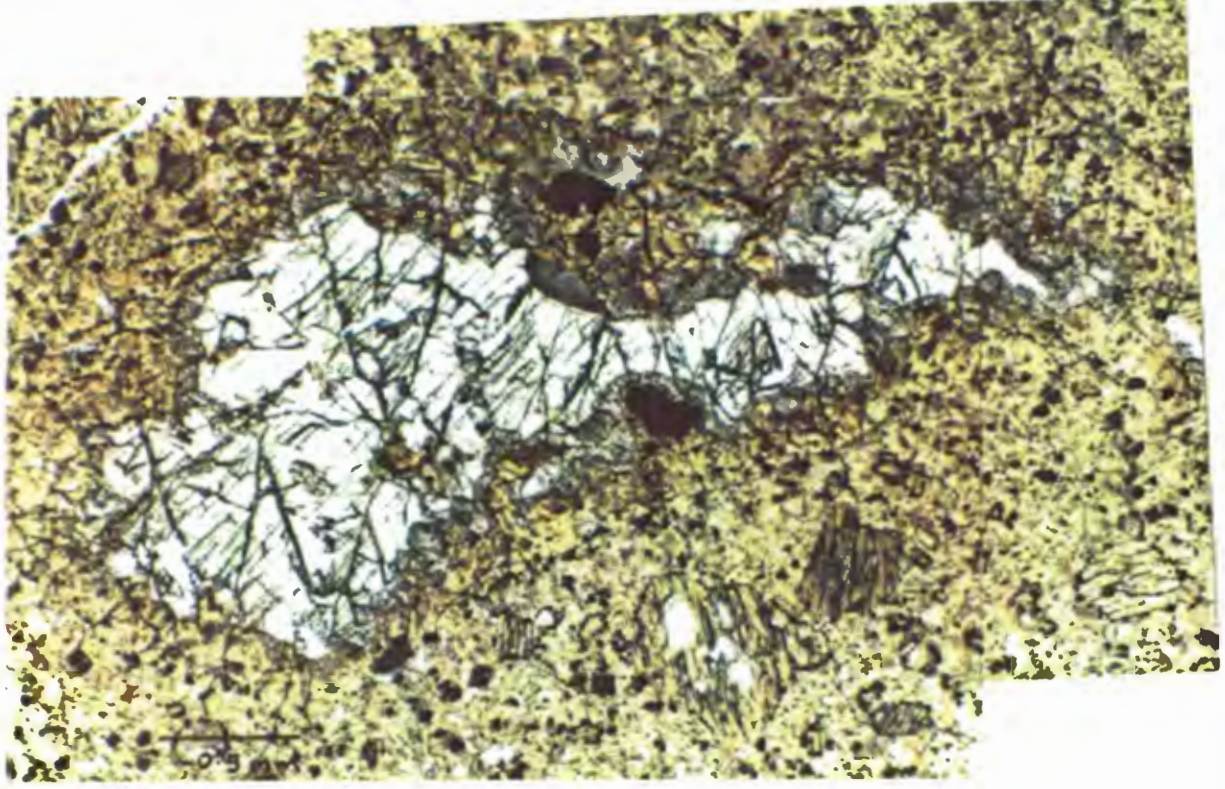

PLATE 4.5
EMTILOMBO - CLINOPYROXENE MACROCRYST

Extremely corroded, anhedral clinopyroxene macrocryst with a clear pale green core and turbid, spongy reaction rim. The clinopyroxene partially encloses an anhedral opaque mineral (PK003/36C CPX/1).

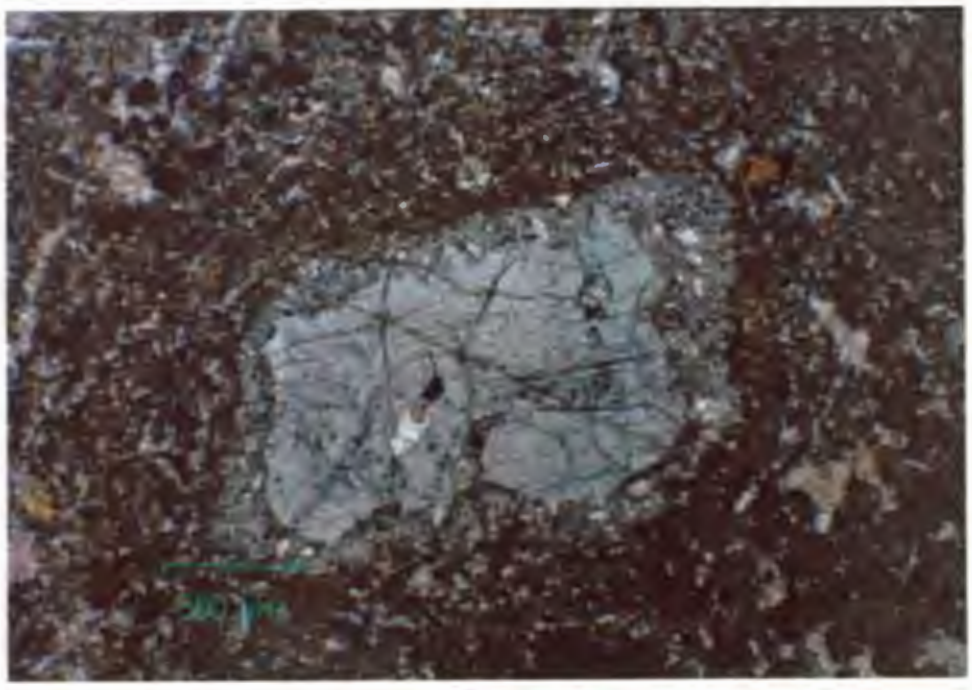

PLATE 4.6
TEMBANI RANCH - CLINOPYROXENE PHENOCRYST

Clinopyroxene phenocryst with a clear green core and spongy textured rim. The core shows extensive corrosion but a relict subhedral morphology is preserved by the rim.

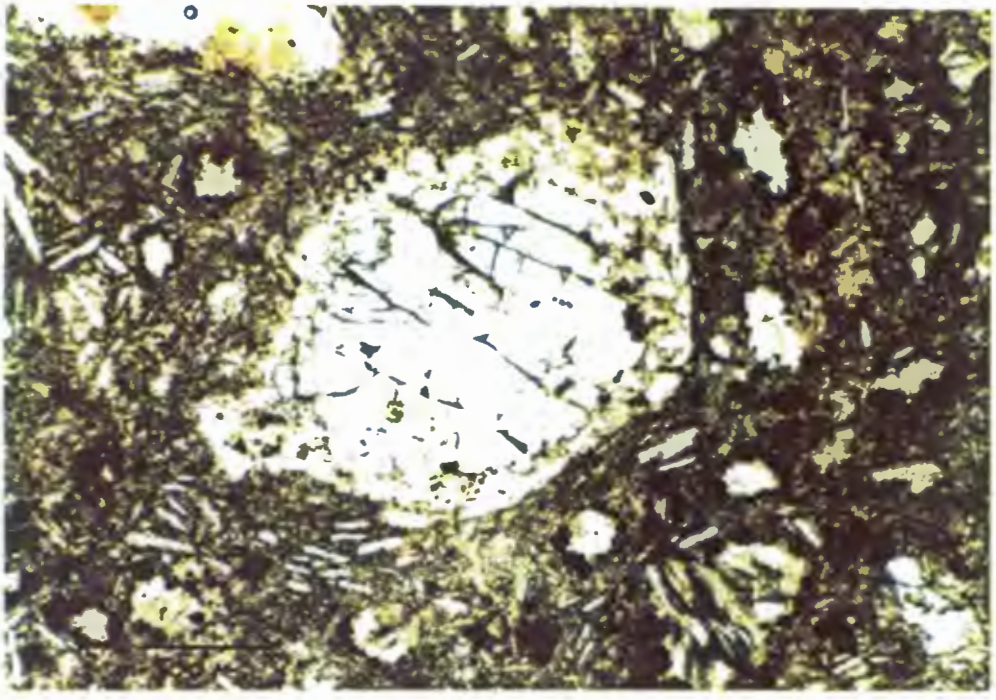

PLATE 4.7
EMTILOMBO - CLINOPYROXENE PHENOCRYST

Anhedral very pale brownish clinopyroxene. The original euhedral grain shape is preserved by the orientation of altered melilite laths. No turbid reaction rim is present (PK003/64C CPX/2).

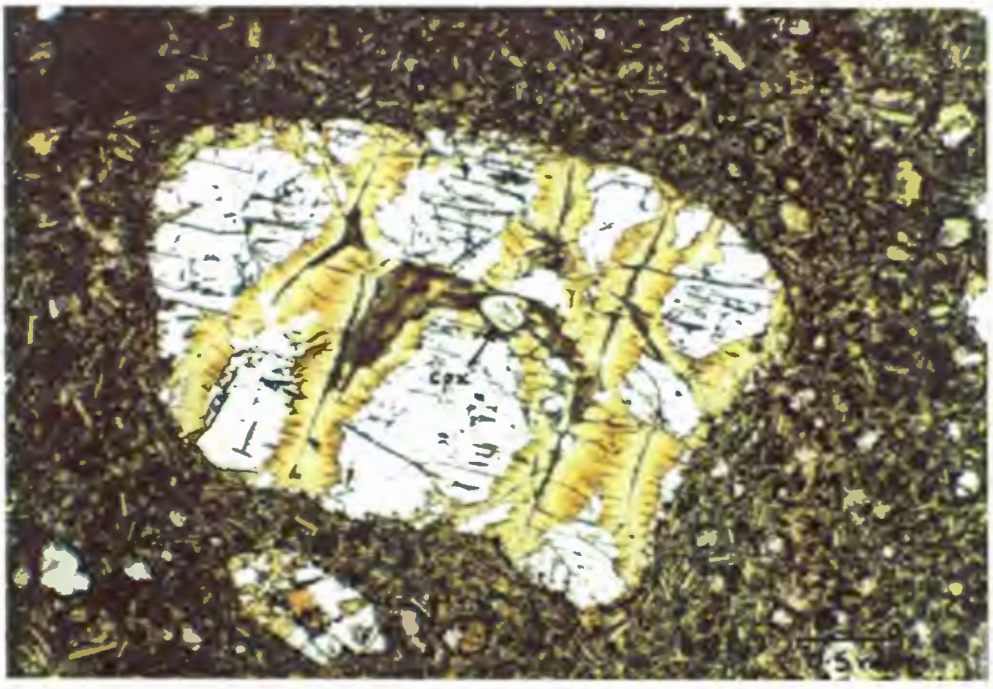

PLATE 4.8
EMTILOMBO - CLINOPYROXENE INCLUSION

Small, rounded, very pale brownish clinopyroxene inclusion (cpx) in a tabular, pseudo-subhedral olivine macrocryst (PK003/64C CPX/1).

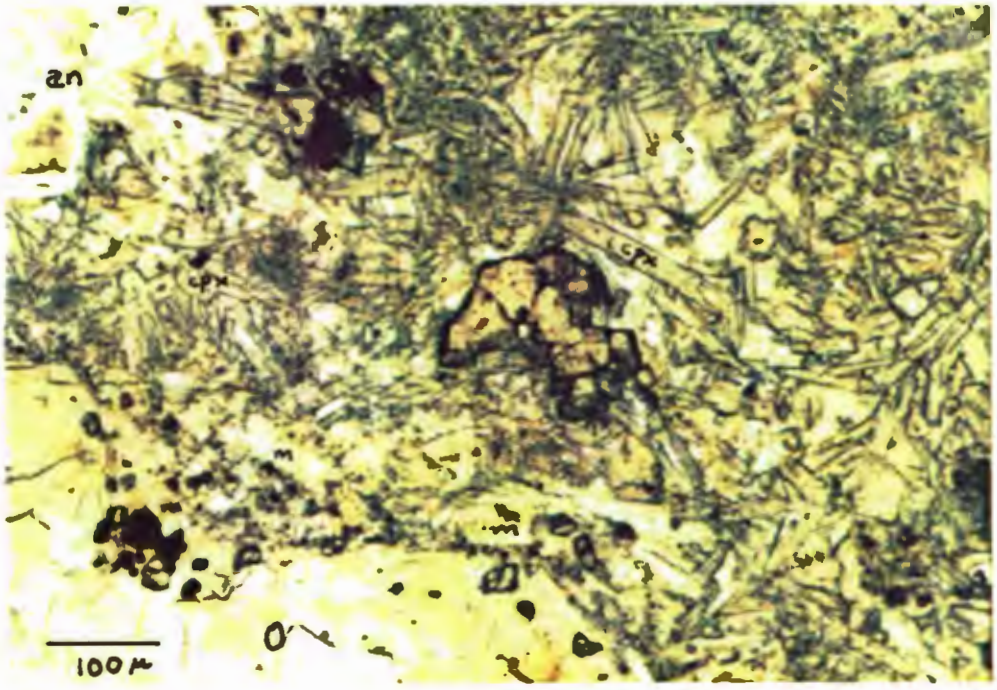

PLATE 4.9
EMTILOMBO - GROUNDMASS CLINOPYROXENE

A felty mesh of pale olive-green clinopyroxene laths (cpx) in a pool of analcite (an). A coarse, anhedral perovskite (pale purplish) grain is present in the groundmass. Altered melilite (m), altered olivine macrocryst (O).

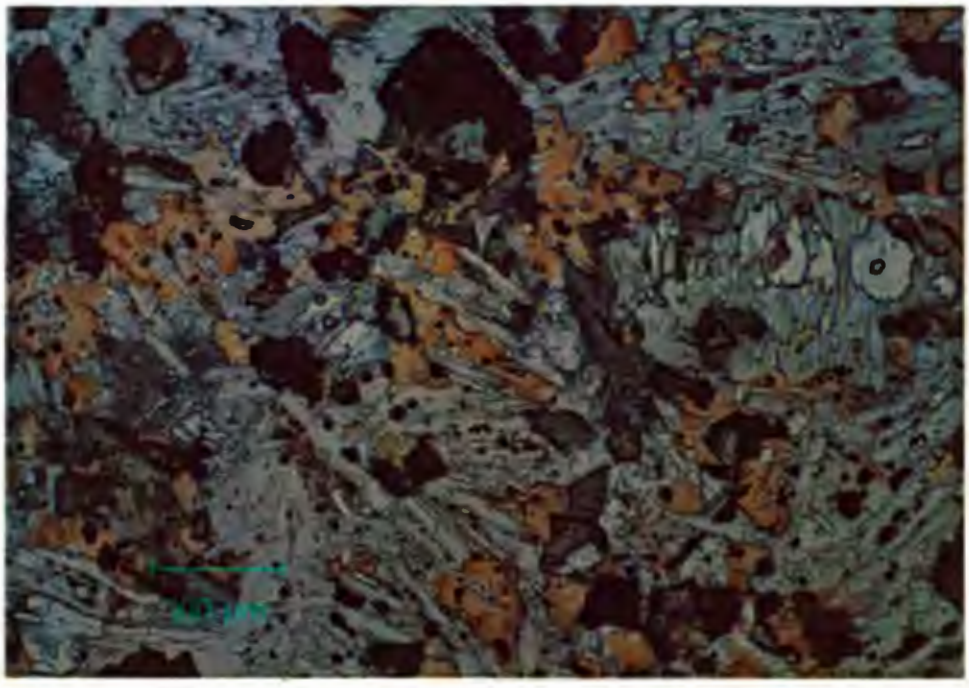

PLATE 4.10
EMTILOMBO - GROUNDMASS CLINOPYROXENE

Emerald green clinopyroxene associated with phlogopite (p) and melilite (m) in the micaceous melilitite. Olivine microphenocryst (o).

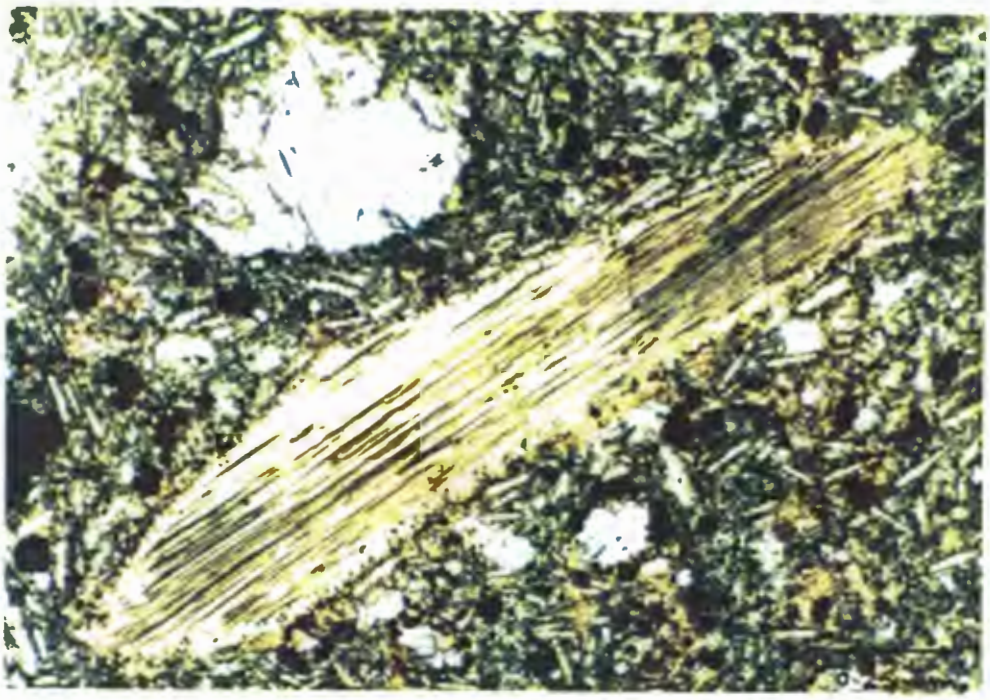

PLATE 4.11
EMTILOMBO - PHLOGOPITE MACROCRYST .

Pale brown, subhedral phlogopite macrocryst with rounded terminations. A narrow overgrowth of orange-brown groundmass phlogopite with a fine speckling of opaque minerals is present around most of the macrocryst.

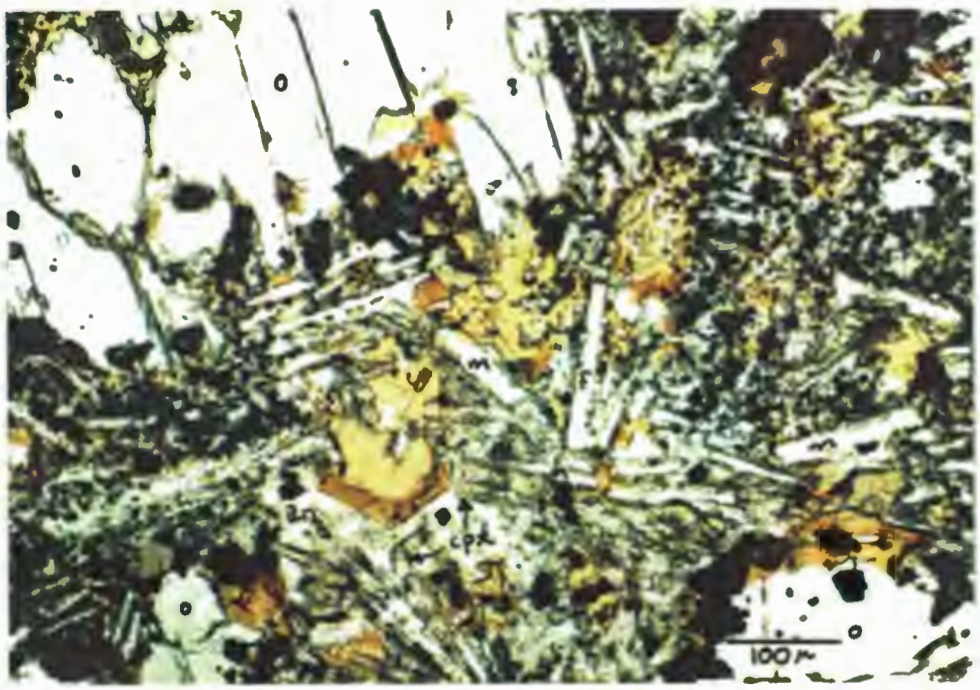

PLATE 4.12
EMTILOMBO - GROUNDMASS PHLOGOPITE

Pale orange-brown groundmass phlogopite with deeper reddish-brown tetra-ferriphlogopite rims. Phlogopite is a late stage interstitial mineral that sub-ophitically and poikilitically encloses melilite (m), opaque minerals (black) and clinopyroxene (cpx). Analcite (an). Olivine (o).

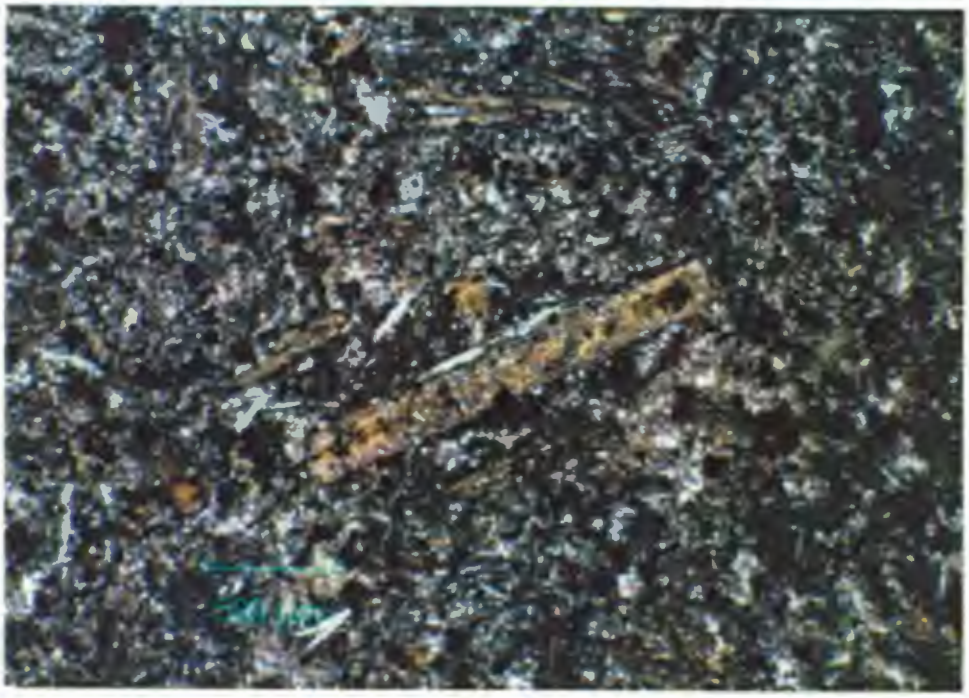

PLATE 4.13
TEMBANI RANCH - MELILITE PHENOCRYST

Elongate, euhedral altered melilite phenocryst (yellow). Small apatite (colourless laths) grains occur as inclusions and parallel to grain rims. Some possible clinopyroxene microlites (turbid grey) are present in the melilite lath

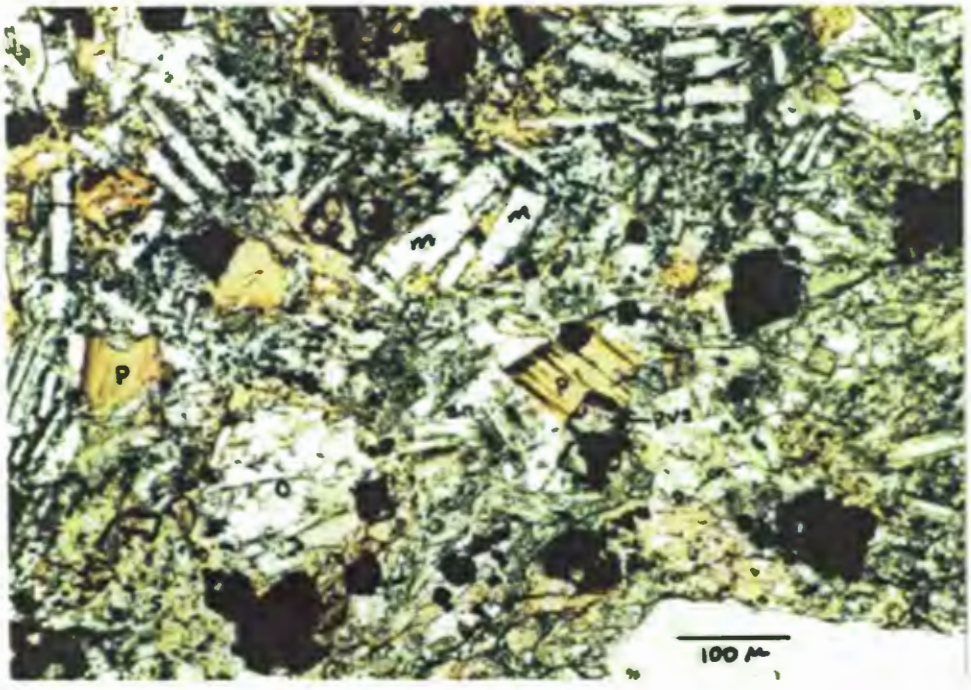

PLATE 4.14
EMTILOMBO - GROUNDMASS MELILITE

Small colourless melilite laths (m) associated with phlogopite (p), opaque minerals (black), perovskite (pvs) and granular clusters of sodalite (s) in the melilititite groundmass. Olivine microphenocryst (o), analcite (an).

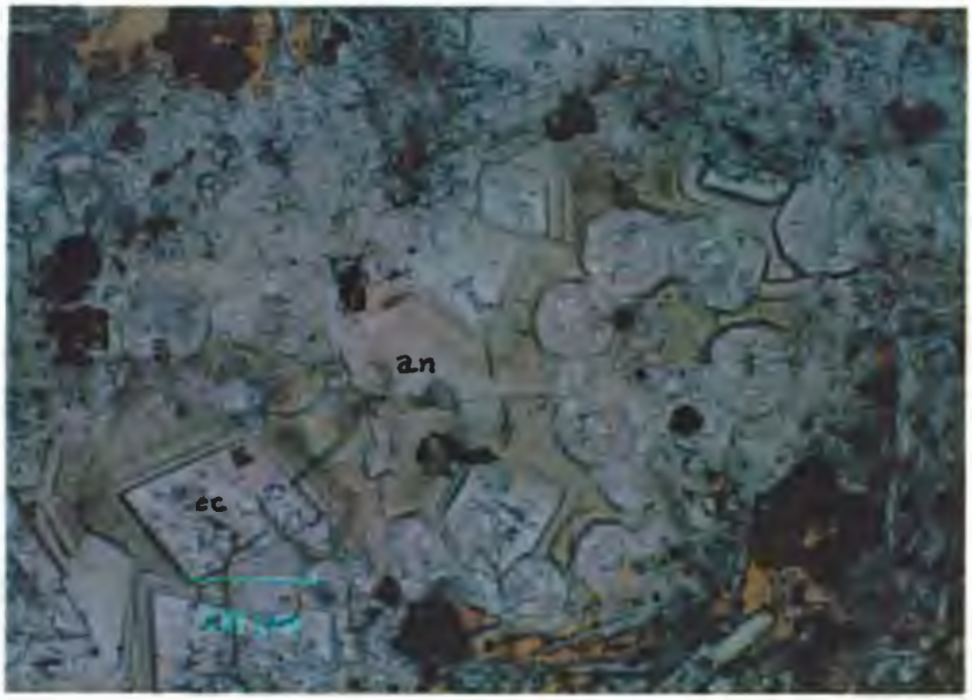

PLATE 4.15
EMTILOMBO - CARBONATE AND ZEOLITE VEINLET

A small veinlet containing distinct, euhedral sodalite (s), rhombs of carbonate (cc) and analcite (an).

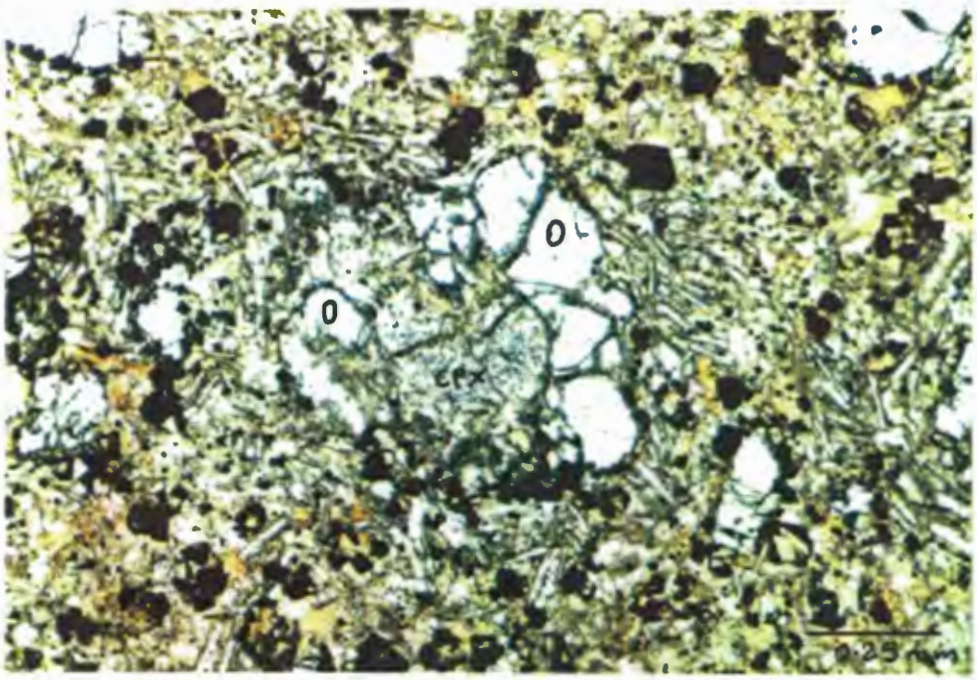

PLATE 4.16
EMTILOMBO - OLIVINE CLINOPYROXENE MICROXENOLITH

A small extremely corroded microxenolith consisting of olivine (O) and clinopyroxene (CPX). Probably part of the lherzolite suite.

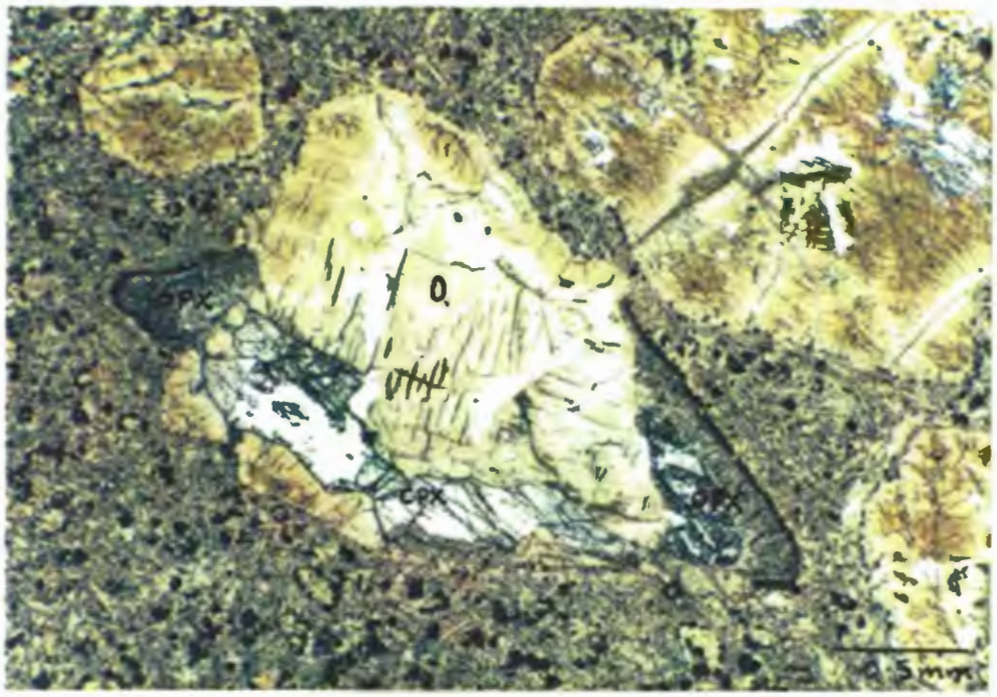

PLATE 4.17
EMTILOMBO - ALTERED LHERZOLITE MICROXENOLITH

An aggregate of altered olivine (O) and fresh clinopyroxene (CPX) and orthopyroxene (OPX). A reaction rim is present around the orthopyroxenes and a spongy textured zone around the clinopyroxene where the grains are in contact with the melilite matrix.

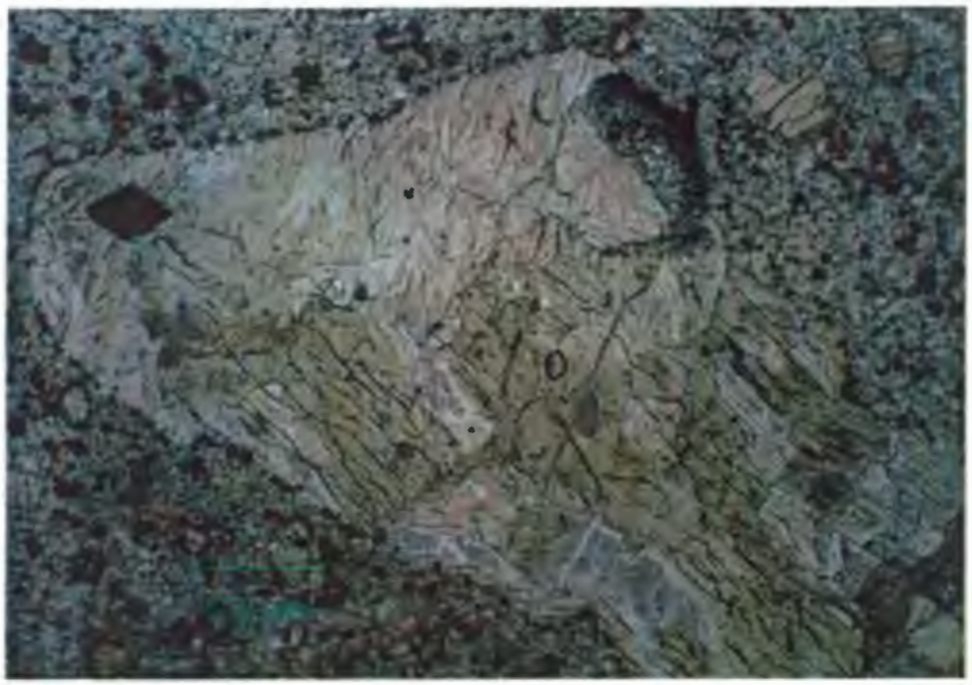

PLATE 4.18
EMTILOMBO - ALTERED SPINEL LHERZOLITE MICROXENOLITH

An aggregate of altered olivine (O) and orthopyroxene (OPX) and a euhedral, translucent, brick-red spinel. The orthopyroxene is completely altered to 'reaction rim' material.

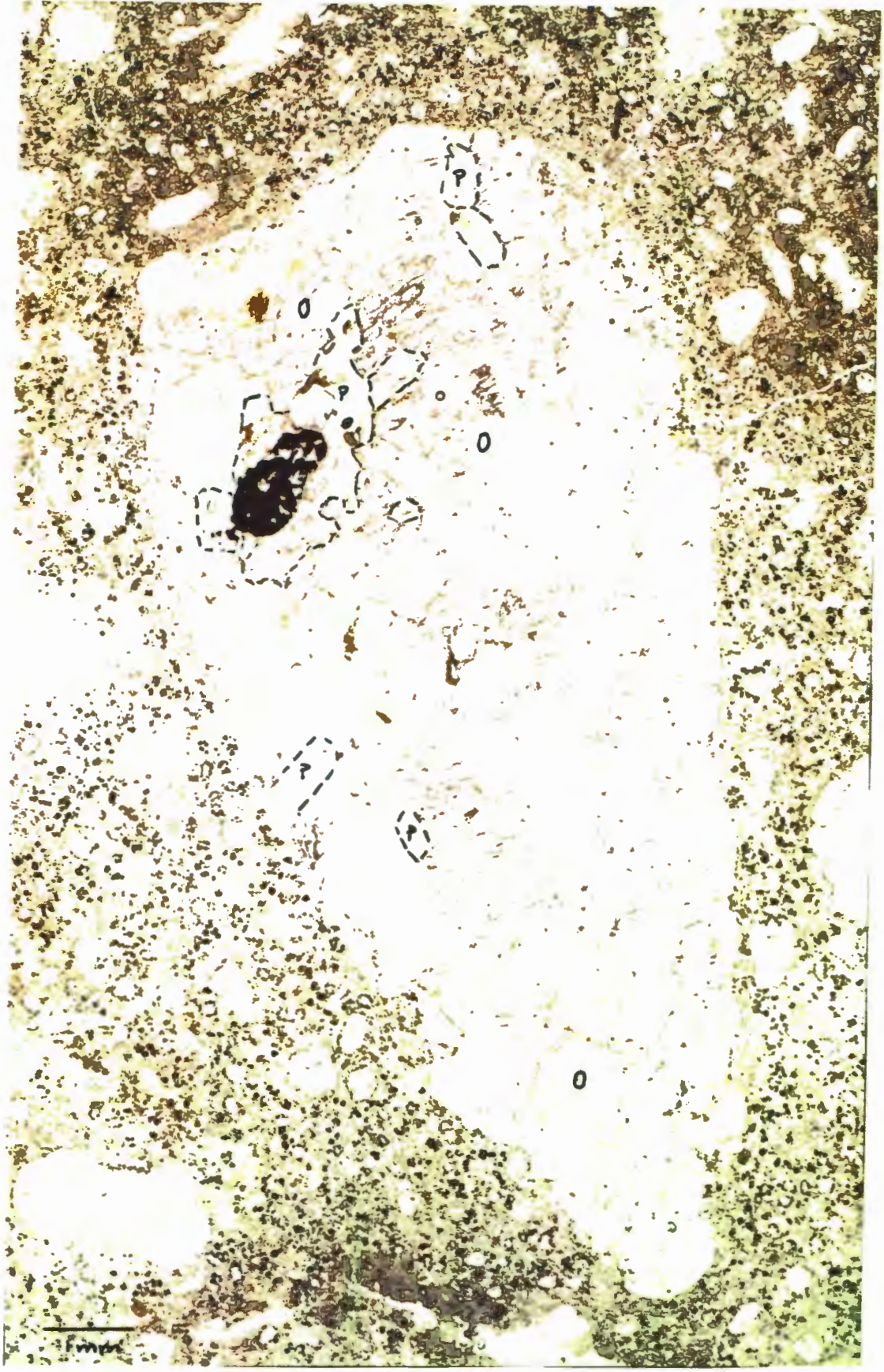

PLATE 4.19
EMTILOMBO - DUNITE MICROXENOLITH

An elongate aggregate of extensively fractured, tabular olivines (O), one chromite (black) and phlogopite (P). Olivines are extensively altered along internal fractures.

PLATE 4.20
EMTILOMBO - PYROXENITE MICROXENOLITH

An aggregate of anhedral irregular shaped clinopyroxene (CPX), orthopyroxene (OPX) and rare olivine (O). Some of the minerals have been plucked out during polishing of the section (white areas).

PLATE 4.21
EMTILOMBO - PHLOGOPITE/CLINOPYROXENE MICROXENOLITH

An intergrowth of phlogopite (P), clinopyroxene (CPX) and aluminous chromite (black). Some of the minerals have been plucked out during polishing of the section (white areas).

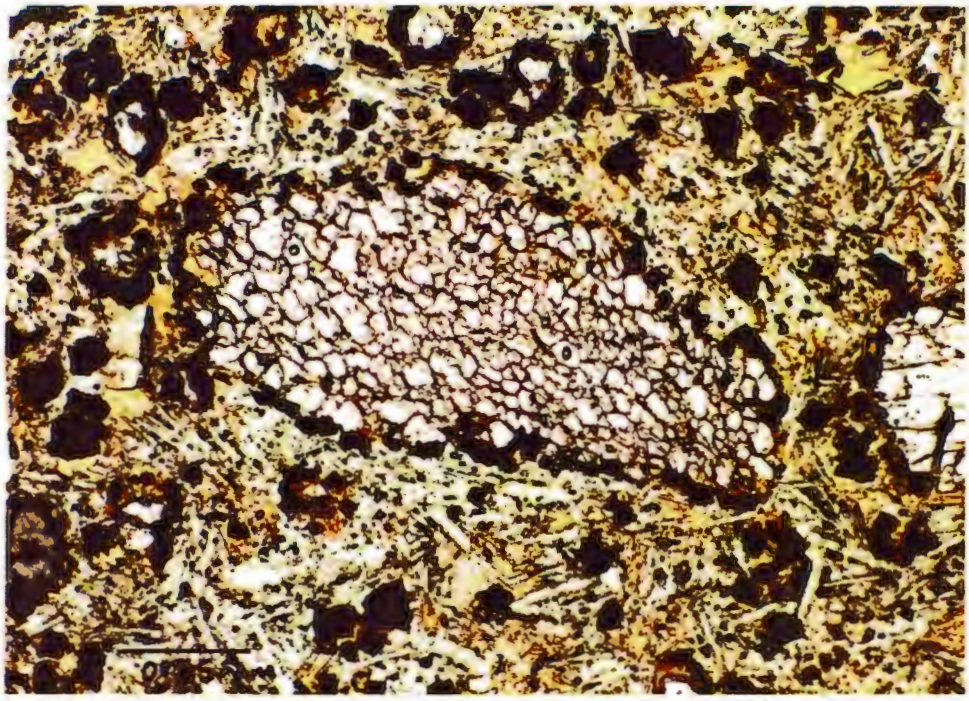

PLATE 4.22
EMTILOMBO - OLIVINE XENOCRYST

An anhedral mosaic textured olivine. The grain consists of abundant recrystallised olivine neoblasts (o). Extensive corrosion by phlogopite is evident at the grain margin and alteration occurs between neoblasts.

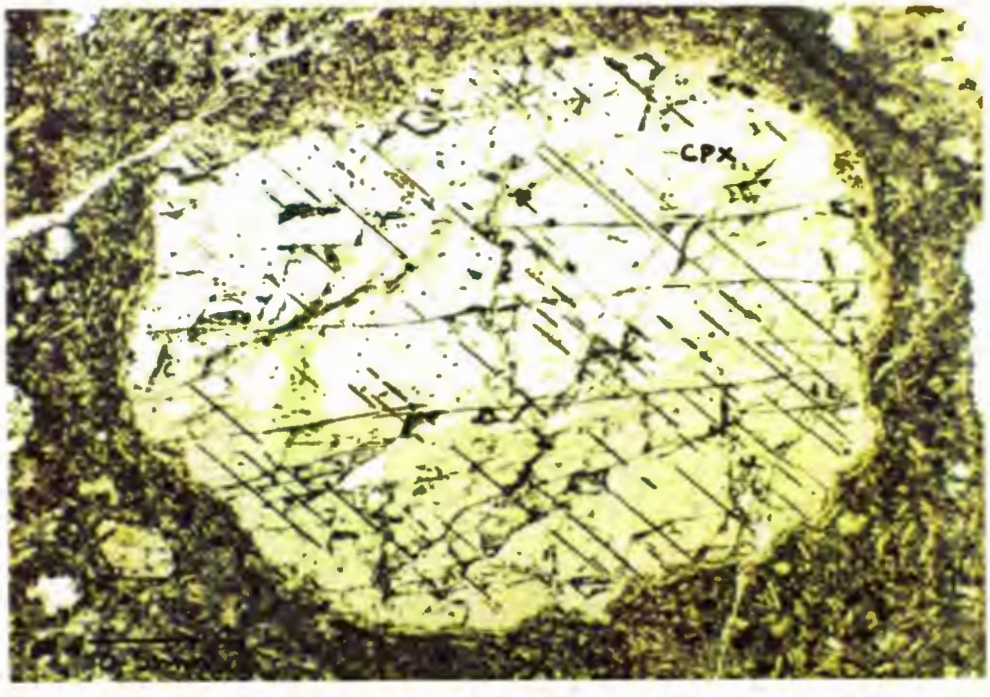

PLATE 4.23
EMTILOMBO - CLINOPYROXENE XENOCRYST

A large anhedral, very pale brownish clinopyroxene (CPX) with abundant translucent, orange-brown ilmenite lamellae and rare opaque blebs of ilmenite.

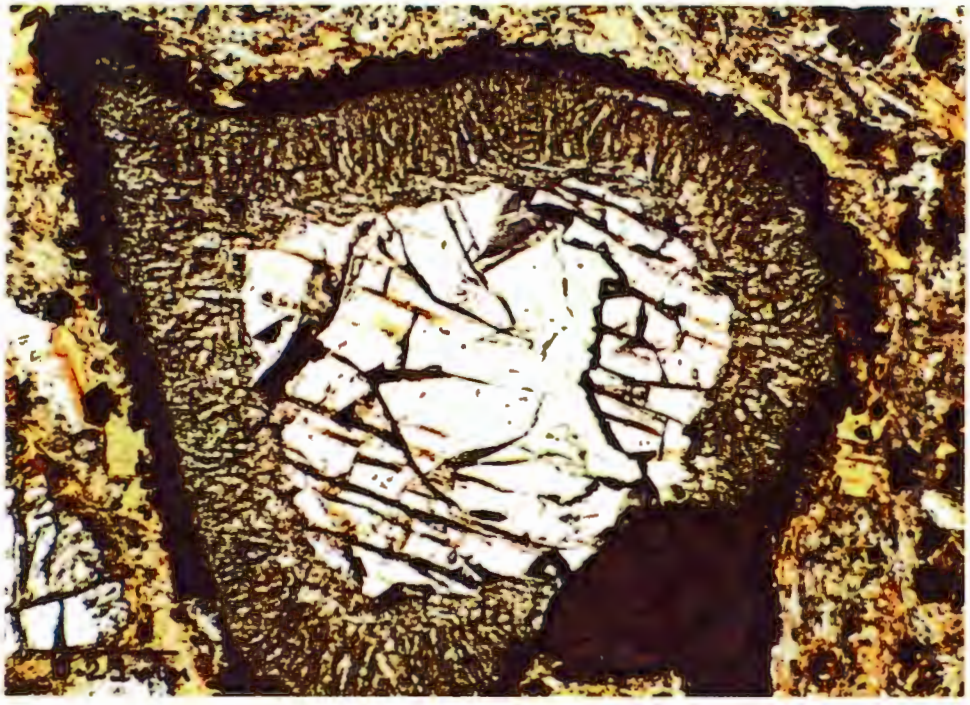

PLATE 4.24
EMTILOMBO - ORTHOPYROXENE/SPINEL MICROXENOLITH

A bi-mineralic aggregate of a very pale pinkish-brown orthopyroxene and a translucent brick-red spinel. A reaction rim surrounds the pyroxene and opaque titanomagnetite rims the spinel.

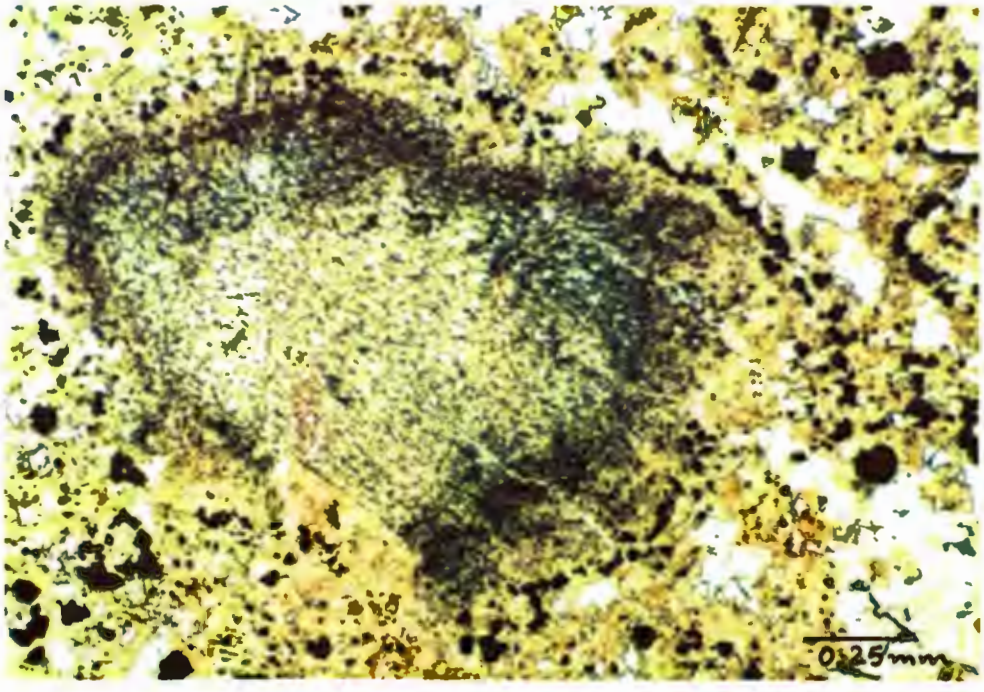

PLATE 4.25
EMTILOMBO - ALTERED ORTHOPYROXENE

A completely altered orthopyroxene consisting entirely of 'reaction rim' material. The latter consists of microlites of clinopyroxene in an amorphous, pale buff coloured base and is rimmed by a zone of abundant fine opaque mineral specks.

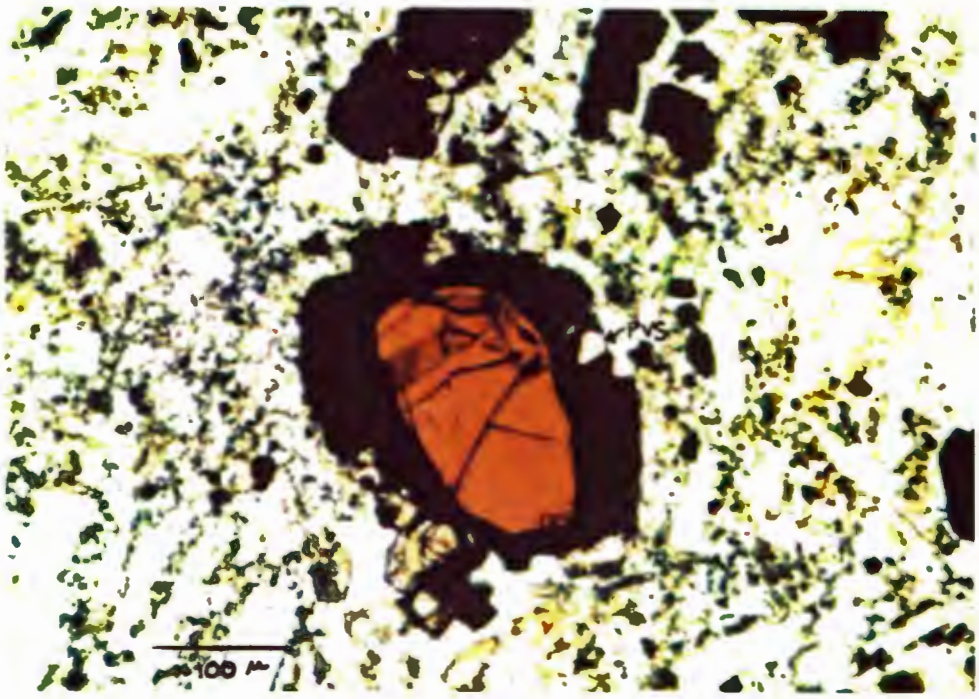

PLATE 4.26
EMTILOMBO - TRANSLUCENT ORANGE-BROWN SPINEL

An anhedral, elongate oval, translucent orange-brown spinel with an overgrowth of opaque titanomagnetite and minor perovskite (pvs).

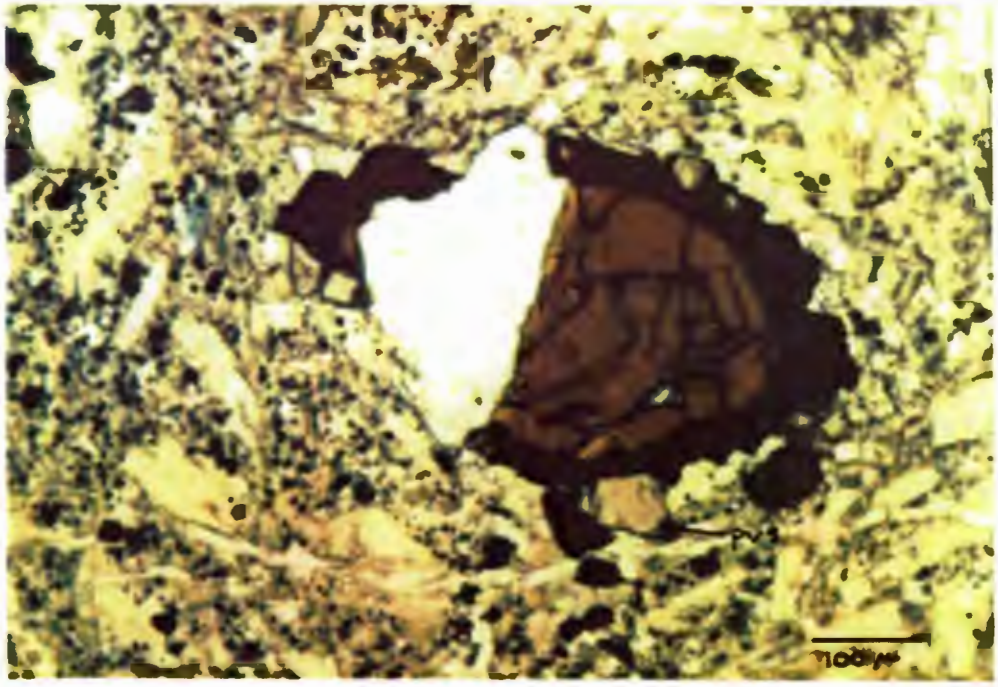

PLATE 4.27
EMTILOMBO - TRANSLUCENT BROWN SPINEL

An anhedral, oval, translucent brown spinel with an overgrowth of opaque titanomagnetite and minor perovskite (pvs). Part of the grain has been plucked out during polishing (white area).

CHAPTER FIVE

MINERAL CHEMISTRY

5.1 GENERAL INTRODUCTION

Microprobe analyses were undertaken on selected matrix and xenolithic minerals in the Emtilombo thin sections. The chemical compositions and zonation trends of the olivines and spinels are described in this Chapter as these minerals have important implications with respect to paragenesis of the Emtilombo melilitite. The paragenetic significance of these minerals is discussed in Chapter 7 in conjunction with comments on chemistries of other minerals. The chemistry of spinels from concentrate derived from a variety of the Eshowe melilitites is described and compared to the xenolith and groundmass mineral chemistries. No attempt has been made to calculate the Fe_2O_3 contents of the silicates and FeO refers to total iron in these minerals. The proportion of ferrous and ferric iron are calculated, based on stoichiometry, for the oxides.

Analytical conditions are described in Appendix 1 and the mineral chemistry data is stored on the disk in the back pocket. Printouts of the analyses of all minerals are

included in Appendix 2. A listing of files on the disk and the format of the data is included in Appendix 3.

5.2 OLIVINE

The olivine populations (all grains: cores and rims) show a range of forsterite contents of from 91 to 79 but the bulk of the grains occur between Fo 83 to 86. The most conspicuous variation is shown by NiO which ranges from 0.40 down to 0.05 wt%. The overall chemical trend is one of decreasing NiO and MgO associated with increasing FeO (Figure 5.1).

Olivine compositions, in the various morphological groups, show a considerable degree of overlap (Figure 5.1). Differences between the groups are apparent as variations in the range of spread of forsterite, NiO and CaO contents and in the nature of the core to rim zonation patterns. Manganese does not show any significant differences between the groups.

Rim compositions of all olivine morphological groups show a total overlap and a much more restricted spread of forsterite and, in general, lower nickel compared to core compositions (Figure 5.2). At low NiO contents there is a small but distinctive dogleg slant to slightly increasing MgO associated with a continued decrease of NiO and decreasing FeO. This trend is generally a feature of the phenocrysts and microphenocrysts core to rim analyses.

Several zonation trends from core to rim and with respect to forsterite and NiO have been observed in olivines from the different morphological groups. These are as follows:

1) Decreasing forsterite and NiO;
2) Increasing forsterite with decreasing NiO;
3) Unchanged forsterite with decreasing NiO;
4) Increasing forsterite and NiO;
5) Unchanged forsterite with increasing NiO;
6) Decreasing forsterite and increasing NiO;
7) Increasing forsterite unchanged NiO.

A histogram of the frequency of occurrence of the various trends, per olivine group, is shown in Figure 5.3.

5.2.1 OLIVINE XENOCRYSTS

Discrete xenocrysts and olivines in microxenoliths are, in general, characterised by high forsterite and NiO and low MnO and CaO contents when compared to the remainder of the olivine groups (Figure 5.1). Forsterite, MnO and CaO show a fairly wide compositional spread while NiO is relatively restricted. Xenocrysts compositions overlap slightly with the more magnesian olivine macrocrysts and microphenocrysts (Figure 5.4). They are distinguished from the latter by their lower calcium contents.

Olivines with the highest forsterite, 88.60 to 91.06, and NiO, 0.33 to 0.43 wt% occur in the lherzolite group of micro-xenoliths (Figure 5.4). These olivines have the lowest MnO

and CaO of all the olivine morphological groups. Olivines in a dunite microxenolith have lower forsterite and NiO and higher MnO and CaO than the former and are compositionally similar to the more magnesian macrocrysts. A discrete olivine xenocryst with a mosaic texture plots amongst the bulk of the macrocrysts (Figure 5.4). An olivine within the pyroxenite microxenolith is compositionally distinct from any of the other olivine groups. It is distinguished by having a relatively high NiO (0.31 wt%) with a relatively low forsterite content (83.7). The olivines define a continuous trend of decreasing forsterite and NiO from the most magnesian lherzolites to the more iron rich macrocryst compositions (Figure 5.4).

5.2.2 MACROCRYST CORE COMPOSITIONS

Macrocrysts are uniform in composition across almost the entire width of the grain and chemical zonation, where detected, is confined to a narrow, approximately 0.02mm rim at the grain boundary. The cores have relatively restricted compositions (Figure 5.1) particularly with respect to forsterite which ranges between 81.71 and 87.39 (mean 84.11). Two populations of macrocrysts are present (Figure 5.4): 1) a high forsterite and nickel population; and 2) a lower forsterite and nickel population. In the former group forsterite in the bulk of the macrocrysts varies from 84.2 to 85.4 and NiO between 0.25 and 0.3 wt%. The latter population is typified by forsterite contents of from 82.5 to 84.2 and

NiO of 0.15 to 0.21 wt%. No other chemical differences are apparent between these two populations, manganese ranges from 0.15 to 0.25 wt% (mean 0.19 wt%) and CaO from 0.10 to 0.17 wt% (mean 0.13 wt%).

5.2.3 PHENOCRYST CORE COMPOSITIONS

5.2.3.1 COMPLEX PHENOCRYSTS

Core compositions for the complex phenocrysts overlap the range of macrocryst core compositions but show a slightly wider spread of forsterite, MnO, CaO and NiO (Figure 5.1). Forsterite varies from 79.6 up to 87. Mean forsterite, 83.52, is slightly lower than that of the macrocrysts but the bulk of the grains fall between Fo 83.8 and 85.6. The complex phenocrysts appear to bridge the gap between the two macrocryst populations. Two distinctive populations of complex phenocrysts are evident (Figure 5.1): a high iron low nickel population (rare grains) and a more magnesian and higher NiO group (most abundant population).

5.2.3.2 PHENOCRYSTS

Phenocryst cores completely overlap the extent of macrocryst and complex phenocryst compositions with respect to forsterite NiO, CaO and MnO but tend to have slightly lower forsterite at similar concentrations of NiO (Figure 5.1). Some phenocrysts do show similar compositional features to the main microphenocryst population but these are in the minority (see

below). When compared to all the above olivine groups phenocrysts generally have a relatively more restricted range of forsterite, NiO and CaO contents. Rare grains do contain higher CaO, up to 0.29 wt%. The spread of MnO contents is similar to that of the macrocrysts and complex phenocrysts.

5.2.3.3 MICROPHENOCRYSTS

Microphenocryst cores are characterised by a much wider spread of forsterite, NiO, CaO and MnO contents, than the macrocryst, complex phenocryst, and phenocryst core chemistries (Figure 5.1). They completely overlap the extent of all the latter morphological groups and some of the xenocrysts with respect to forsterite and NiO. In general they have slightly higher forsterite at similar concentrations of NiO and trend to much higher and, at the other extreme, lower NiO contents. CaO contents of the microphenocrysts are generally relatively higher than in all of the other morphological groups. One small population of microphenocrysts shows closer compositional similarities to the bulk of the phenocrysts than to the predominant microphenocryst population (Figure 5.1).

5.2.4 RIM COMPOSITIONS AND ZONATION PATTERNS

As mentioned above rim compositions of all the olivines show a more restricted spread of forsterite when compared to cores. They also have a wider range of calcium contents compared to core compositions and there is, almost without exception, a

distinctive increase in CaO at grain rims. MnO variably increases, remains unchanged or decreases in rims but, in general, the trend is towards higher manganese. Nickel contents show a wider range and trend to higher and/or lower amounts in rims of macrocrysts and complex phenocrysts than in their cores. In the rims of phenocrysts and microphenocrysts NiO generally has a more restricted spread and is lower than in their respective core compositions.

Olivine macrocryst rims usually contain higher forsterite, MnO and CaO relative to their cores. CaO ranges from 0.10 to 0.52 wt% with a mean of 0.25 wt%. A more detailed look at core to rim chemistries, with respect to forsterite and NiO, shows a wide variety of differing zonation trends are present. As mentioned above this is restricted to a narrow margin at grain rims and only one or two patterns are apparent on a single grain, ie. zonation is simple. Six different trends, from core to rim, have been observed on a variety of grains. These are zonation trends 1 to 6, as defined above. The dominant trend is to increasing forsterite and NiO, pattern 4 (Figure 5.3) and olivine macrocrysts with lower forsterite values tend to show the strongest rim zonation patterns.

In general, forsterite contents of the complex phenocryst rims are similar to those of the cores but the range is slightly more restricted. Calcium ranges from 0.12 up to 1.04 wt% with a mean of 0.35 wt%. A characteristic feature of these olivines is that they display unusual and complex zonation

patterns, with respect to forsterite and NiO, ie. they show a pattern of two or more trends from core to rim as opposed to the relatively simple patterns shown by the macrocrysts. This zonation occurs over a relatively broad grain margin which can be up to 0.2mm in width. All chemical zonation trends observed on macrocrysts are found on the complex phenocrysts but in addition pattern 7 is also present. The most frequent trend from core to rim is that of increasing forsterite and NiO, pattern 4, followed by either decreasing or increasing forsterite and decreasing NiO, patterns 1 and 2 (Figure 5.3).

Phenocryst rims generally have similar levels of forsterite to those in the cores but the range is much more restricted. CaO ranges from 0.12 to 1.04 wt% (mean 0.35 wt%). Core to rim zonation patterns of phenocrysts, with respect to forsterite and NiO, are simple. Fewer zonation trends are evident in these grains than are present in the macrocrysts and complex phenocrysts. Four patterns have been recognised, patterns 1 to 4 (Figure 5.3) and the predominant trends are those of decreasing NiO and either decreasing or increasing forsterite, patterns 1 and 2.

In general, forsterite in the microphenocryst rims is lower and has a more restricted range than in the cores. Core to rim zonation patterns of microphenocrysts, with respect to forsterite and NiO, are again simple and the variety is even more restricted than for the phenocrysts (Figure 5.3). Three patterns have been recognised, patterns 1 to 3. The

predominant trend is of decreasing forsterite and NiO, pattern 1, but in all cases NiO decreases and it is the forsterite trend that varies.

5.3 SPINELS

5.3.1 GROUNDMASS SPINELS

The groundmass spinels are essentially titanomagnetite solid solutions that incorporate chromium, aluminium and magnesium (Figure 5.5). Cr_2O_3 contents range from 0.05 up to 5.34 wt% with the cores of the larger grains having the highest chromium. Aluminium contents are generally between about 3 and 4 wt%, but can be as low as 0.23 wt%, and titanium is between 11 and 22 wt%. The grains contain FeO ranging from 29.31 to 36.72 wt% and Fe_2O_3 from 24.31 up to 52.42 wt%.

The titanomagnetites$_{ss}$ are characterised by a distinct decrease in Cr_2O_3 and TiO_2 from core to rim and from large to small grains. Similarly Al_2O_3 and FeO show a variable decrease, increase or no change while Fe_2O_3 shows a consistent increase.

Initially the grains show a normal magmatic trend of increasing titanium and ferric iron. At concentrations of 37.5 and 16 wt% (Fe_2O_3 and TiO_2 respectively) this trend shows a distinct change to one of increasing ferric iron associated with decreasing titanium.

5.3.2 XENOCRYST AND CONCENTRATE SPINELS

Two populations of concentrate spinels are present (Figure 5.6): a titanium-poor magnesian, aluminous chromite population and a titanium magnesium aluminium chromite that shows a trend towards magnesian ulvospinel compositions. The xenocrysts analysed show a similar division into the two populations. Two "xenocrysts" were optically identified as such but are large groundmass titanomagnetites$_{ss}$ that have nucleated on the corroded rim of a clinopyroxene macrocryst. These grains are excluded from this discussion.

The titanium-poor grains contain less than 1 wt% TiO_2, chromium contents range from 21.21 up to 42.2 wt% and aluminium is between 12.74 and 38.82. Ferrous and ferric iron contents generally fall between 6 and 14 wt% and 3 and 9 wt%, respectively.

These grains plot along the base of the prism (Figure 5.6). They show a strong negative correlation of chromium and aluminium but no other trends are apparent.

The titanium chromites$_{ss}$ contain up to 14.93 wt% TiO_2, between 14 and 46 wt% chromium and aluminium ranges from 4 to 26 wt%. Ferrous iron contents are between 8.81 and 33.64 wt% and ferric iron is from 5.86 to 35.38 wt%.

The grains show a distinct trend of increasing ferrous iron and titanium associated with increasing ferric iron. There is

also a strong negative trend of increasing titanium with decreasing chromium. These features suggest that this population shows a normal magmatic trend from more chromium rich compositions to more iron and titanium rich compositions.

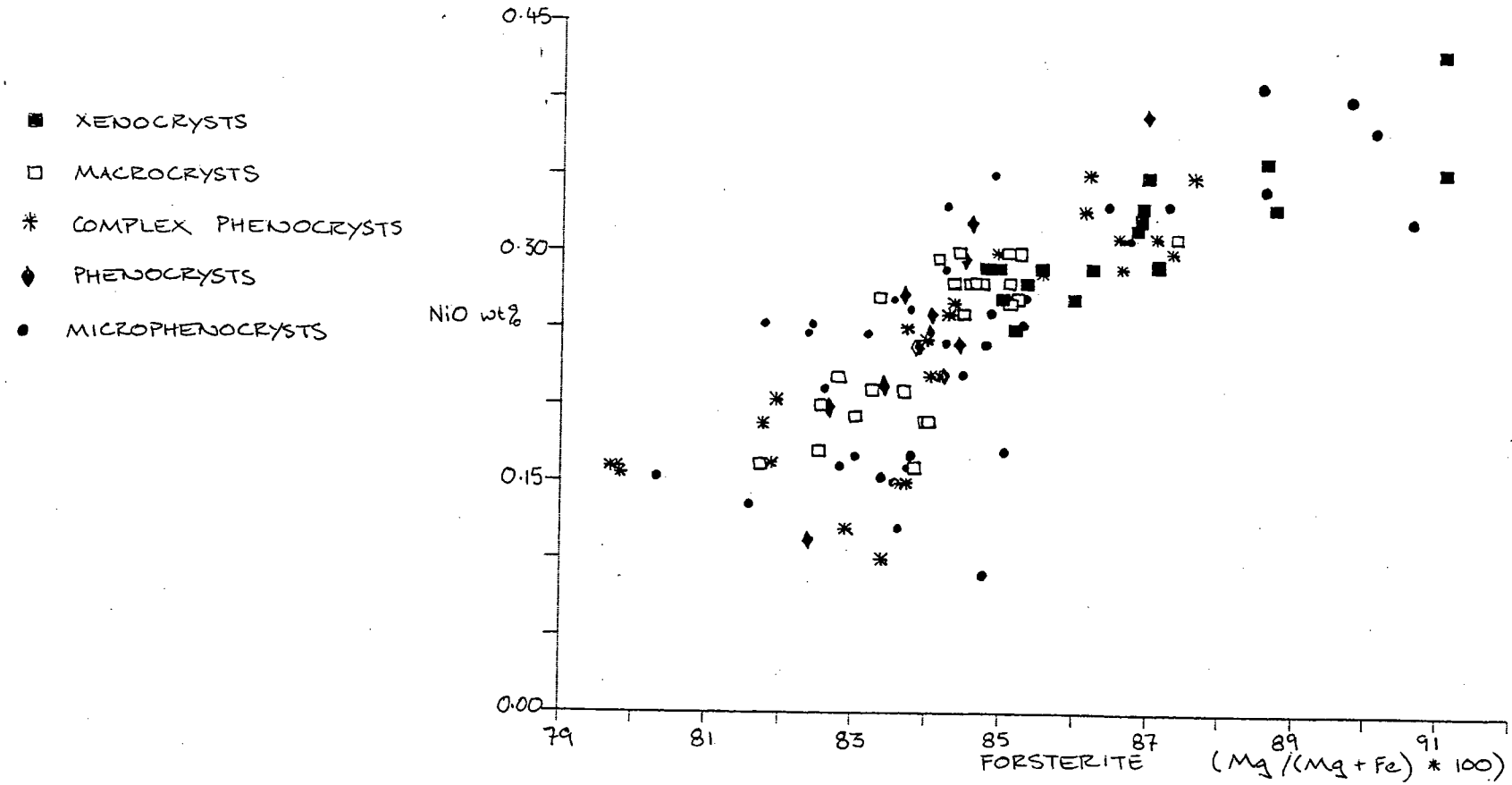

FIGURE 5.1

TOTAL OLIVINE POPULATION - CORES

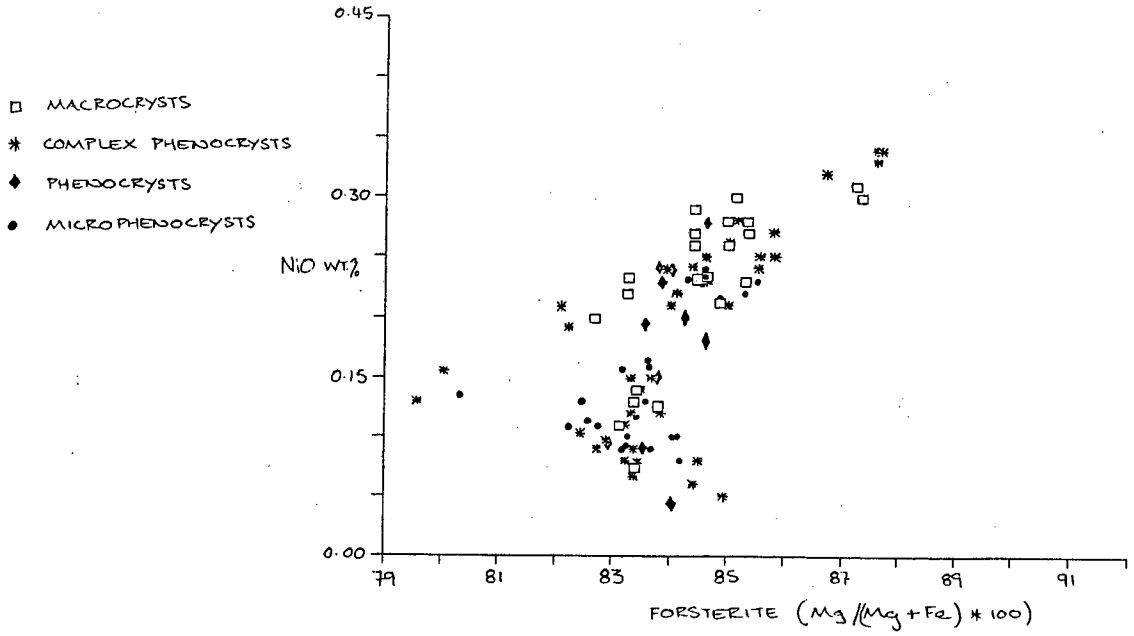

FIGURE 5.2

TOTAL OLIVINE POPULATION - RIMS

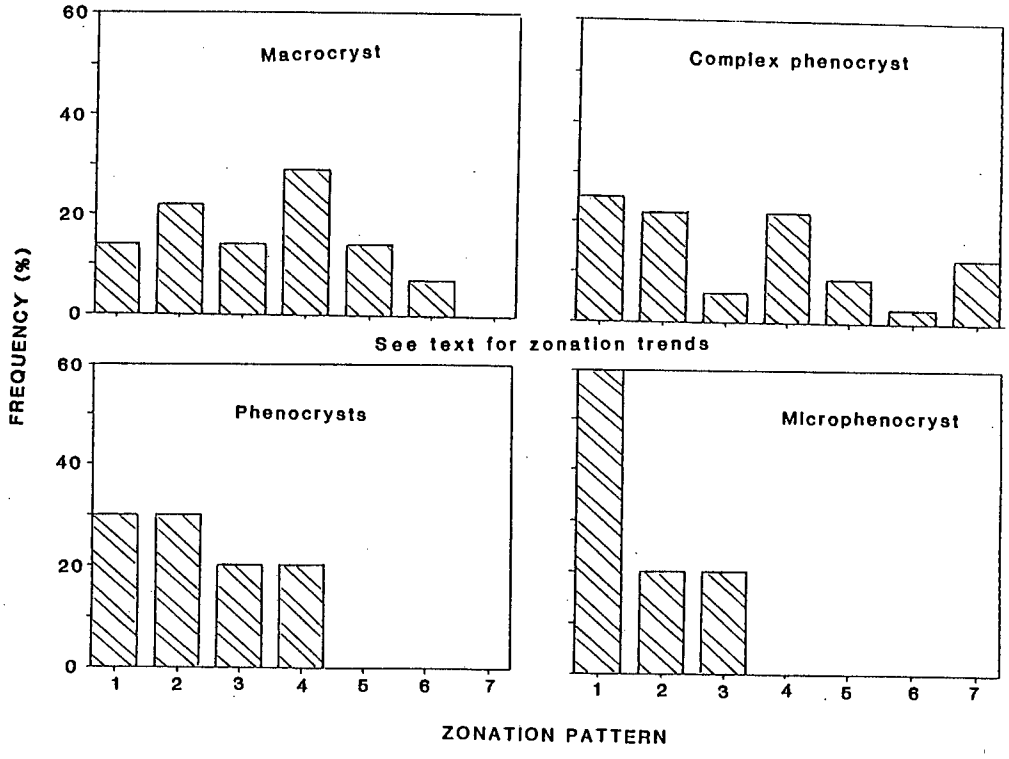

FIGURE 5.3

FREQUENCY OF OLIVINE CORE TO RIM ZONATION PATTERNS

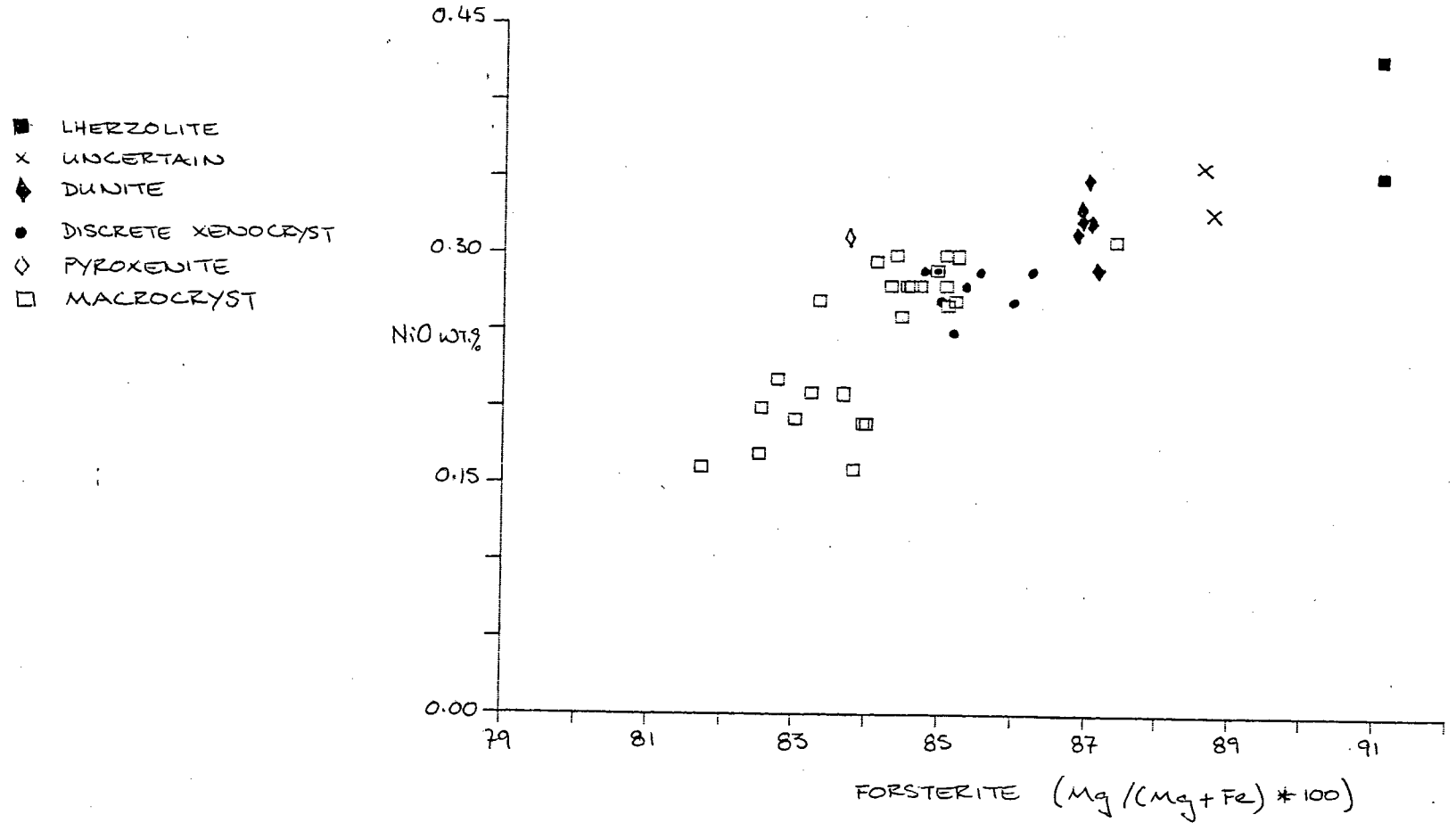

FIGURE 5.4

XENOCRYST TO MACROCRYST TREND

OXIDISED SPINEL PRISM

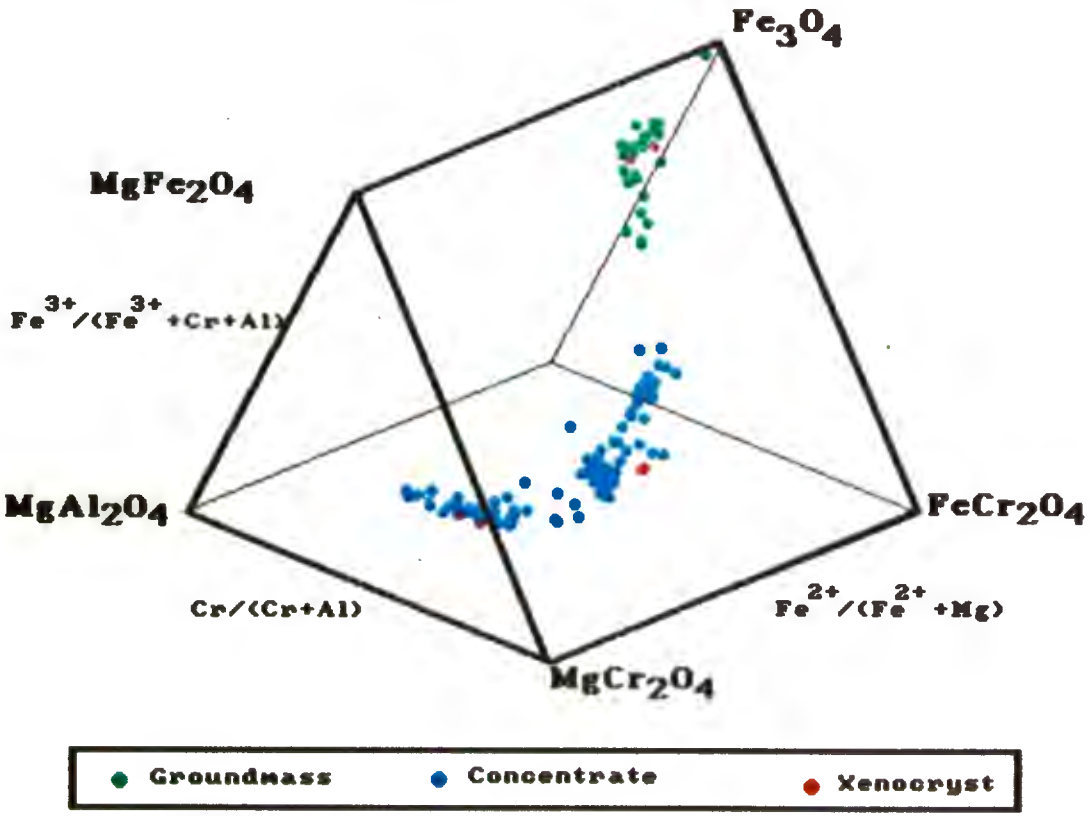

FIGURE 5.5

REDUCED SPINEL PRISM

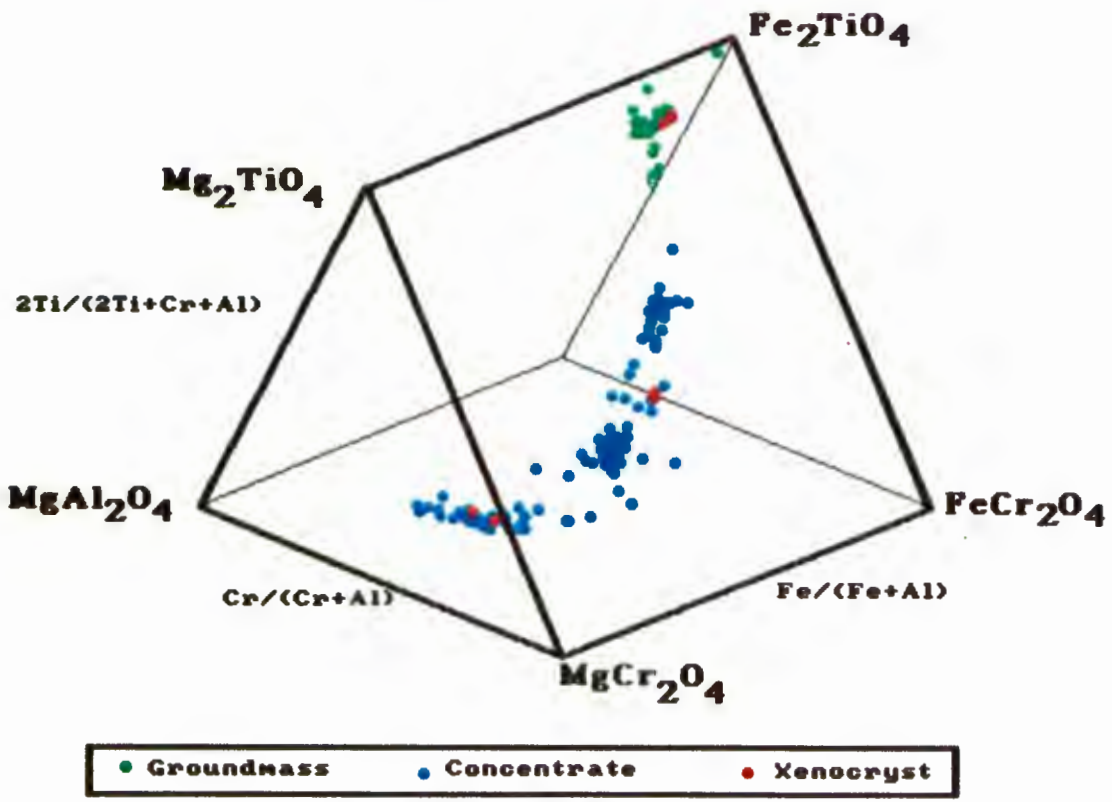

FIGURE 5.6

CHAPTER SIX

WHOLE ROCK GEOCHEMISTRY

6.1 GENERAL INTRODUCTION

Two samples of Tembani Ranch melilitite and of each of the main rock types in Emtilombo dyke were selected for whole rock major and trace element chemical investigations. Samples from the latter locality include the uniform melilitite, the micaceous variety of the uniform melilitite and the clino-pyroxene-rich melilitite breccia. A variety of samples from Emtilombo were also analysed by T. Clark of the BPI for Rb-Sr isotopes.

The Emtilombo samples were selected for a variety of reasons;

1) They are the freshest samples available and therefore warrented more detailed investigation than the Tembani Ranch samples.
2) The uniform melilitite is the predominant rock type in the Emtilombo dyke and on a petrographic basis is considered to be the most "primitive" representative of the intrusive magma.
3) The micaceous variety is thought to represent a more volatile rich later stage varient of the uniform melilitite (on petrographic grounds). It was thought that this rock type may show an evolutionary

trend from the "primitive" samples.

4) The clinopyroxene-rich rock type was believed to show extensive country rock contamination. The nature of the contamination was therefore investigated.

The Tembani Ranch samples show extensive alteration. However, much of this alteration is considered to be a product of the intrusive process and it was considered worthwhile to examine the geochemical characteristics of the rock type. Late stage secondary alteration does complicate the interpretation.

Analytical conditions and sample details are described in Appendix 1 and the data is stored on the disk in the back pocket. A printout of the data is included in Appendix 2 and a listing of the format of the data on the disk is included in Appendix 3. Fe_2O_3 refers to total iron throughout the text. The major and trace element contents and possible fractionation trends are described in this Chapter. The petrogenetic significance of the analyses is discussed in Chapter 7.

6.2 MAJOR ELEMENT CHEMISTRY

6.2.1 TEMBANI RANCH DYKE

The rock type from Tembani Ranch dyke is characterised by distinctly low MgO, 9.5 wt%, and SiO_2, 24.01 wt%, and variable Fe_2O_3, 11.82 and 16.1 wt%. CaO and P_2O_5 contents are high,

being 20.17 and 3.13 wt%, respectively. Na_2O contents are low, 0.33 and 0.51 wt% (Figure 6.1).

6.2.2 EMTILOMBO DYKE

The Emtilombo melilitites are all strongly undersaturated with MgO contents ranging from 17 to 22 wt% but individual rock types show some distinctive chemistries.

The uniform melilitite is characterised by high MgO contents of 20.73 and 22.00 wt%, Fe_2O_3 of 14.5 wt% and SiO_2 contents of 30.84 wt%. The rocks have fairly high CaO, Na_2O and P_2O_5 contents of 10.56, 1.24 and 1.75 wt%, respectively. MnO contents are identical to those in the Tembani Ranch rocks and Al_2O_3, K_2O TiO_2 similar but slightly higher than in the latter locality. The most significant differences between Tembani Ranch and the Emtilombo uniform melilitite are that the rock type at the former locality is depleted in SiO_2, MgO and Na_2O and enriched in CaO and P_2O_5 relative to the latter (Figure 6.1).

The micaceous variety of the uniform melilitite has similar MgO, TiO_2, Na_2O (one sample, PK003/56) and Fe_2O_3 (one sample, PK003/56) contents to those in the uniform melilitite. The most significant differences between the two rock types are that SiO_2, Al_2O_3, MnO, K_2O and P_2O_5 are relatively enriched and CaO is relatively depleted in the micaceous variety. One sample of the latter melilitite (PK003/55) has lower Na_2O and

higher Fe_2O_3 than the uniform melilitite (Figure 6.1).

The clinopyroxene-rich melilitite is characterised by distinctly higher SiO_2 and CaO and lower Fe_2O_3 and MgO than the other Emtilombo melilitites. Minor differences are shown by TiO_2 and K_2O which are depleted relative to the other rock types within the dyke. Al_2O_3 contents are intermediate between the uniform melilitite and the micaceous variety and MnO, Na_2O and P_2O_5 contents are similar to those in the former melilitite.

6.3 TRACE ELEMENT CHEMISTRY

6.3.1 TEMBANI RANCH DYKE

Tembani Ranch melilitite is enriched in both combatible and incompatible trace elements. Abundances of the various elements are shown in variation diagrams of trace elements versus MgO contents in Figure 6.2. The most conspicuous enrichment relative to the Emtilombo rock types is shown by Sr, La, Th, Ce, Nd, Zn and Y. Ba is extremely enriched in one sample, PK001/4, at 6641 ppm. The Tembani Ranch rocks are depleted in Cr, Ni, Co and Rb relative to those from Emtilombo. Zirconium in samples from Tembani Ranch shows an enrichment trend from the uniform and the clinopyroxene-rich melilitites while niobium contents are similar to contents of these rock types. Vanadium and barium are extremely variable in the Tembani Ranch samples. They differ by 87 ppm in the case of vanadium and 4850 ppm for barium.

6.3.2 EMTILOMBO DYKE

The Emtilombo dyke samples are also enriched in compatible and incompatible trace elements (Figure 6.2). As mentioned above the Emtilombo uniform melilitite has similar Nb contents to the Tembani Ranch rock type but Cr, Ni, Co and Rb are relatively higher. La, Nd, Sr, Zn, Zr and Y are depleted relative to Tembani Ranch.

The most significant differences between the uniform melilitite and the micaceous variety is in the enrichment of Ba, Rb, Sc, Nb, V, Zn, Zr and Y in the latter. Ce and Nd are slightly depleted relative to the uniform melilitite. One sample (PK003/55) contains high proportions of Cr and Ni (Figure 6.2). This is believed to be due to the presence of spinel peridotite microxenoliths in the sample.

The clinopyroxene-rich melilitite contains high Ba and Sr relative to the uniform and micaceous melilitites. Cr, La, Nb, Ni, Rb and Zn are all low compared to contents in the other Emtilombo rock types (Figure 6.2). Zirconium and vanadium are enriched to slightly enriched in the clinopyroxene-rich rock type relative to the uniform melilitite but strongly depleted relative to the micaceous variety.

6.4 Rb-Sr ISOTOPES

6.4.1 WHOLE ROCK ANALYSES

Whole rock Rb-Sr isotope determinations were undertaken on samples from the uniform melilitite (altered and fresh samples), the micaceous variety and the clinopyroxene-rich melilitite. A copy of the isotopic data is included in Appendix 2 (T. Clark, unpublished).

Whole rock $^{87}Rb/^{86}Sr$ and $^{87}Sr/^{86}Sr$ ratios show a wide scatter of data (Figure 6.4) and there do not appear to be any distinct differences in isotope concentrations between the various rock types. The $^{87}Sr/^{86}Sr$ ratio of sample PK003/59 is considered to be statistically poor and this was not improved by repeat analysis (Clark, unpublished). The data from samples PK003/23, 56, 58, 66 and 67 appears to define a general linear trend along a 100 Ma isochron (Clark, unpublished) and with an approximate initial ratio of 0.708. These samples comprise all three varieties of the rock types analysed.

6.4.2 GEOCHRONOLOGY

Based on geological evidence the Eshowe melilitites would appear to be, at maximum, lower Triassic in age. Tembani Ranch and the two pipes intrude lower Beaufort sediments which were probably deposited in early Triassic (Dingle et al. 1983). No crater tuff ring deposits, which would have been associated with the pipes, remain. This suggests that several hundreds of metres erosion has occurred and, therefore, a

younger age of emplacement.

Rb-Sr isotope analyses undertaken on phlogopite separates from Emtilombo (Allsopp unpublished data) and Tembani Ranch (Smith unpublished data) indicate an age of approximately 80 my.
A best fit regression line (York 1966) on data for Emtilombo was inferred to be an isochron with an age of 81 ± 11my. The initial ratio calculated from these data was 0.70467 ± 0.0019 (Allsopp unpublished data).

Model ages of 65, 80 and 92 my were obtained, for Tembani Ranch, using assumed initial ratios of 0.706, 0.705 and 0.704, respectively (Smith unpublished data). There is a remarkably close agreement between the age of 80 my and initial ratio of 0.705 for Tembani Ranch with the age and initial ratio calculated for Emtilombo. These data are, therefore, considered to be reliable although error limits are large (±11 my). Whole rock Sr initial ratios, calculated for 80my, show a considerable range from 0.706 to 0.722. As discussed above a possible isochron of 100my and an approximate initial ratio of 0.708 is indicated for the whole rock data. The variability of the whole rock data may suggest that crustal contamination has occurred. Alternatively Rb has been lost from the system due to a redistribution of the isotopes (Clark unpublished). The age data based on whole rock analyses is therefore considered to be unreliable while data from the phlogopite separates, though somewhat sparse, are considered to be reliable.

FIGURE 6.1

MAJOR ELEMENT VARIATION DIAGRAMS
(VS MgO WT.%)

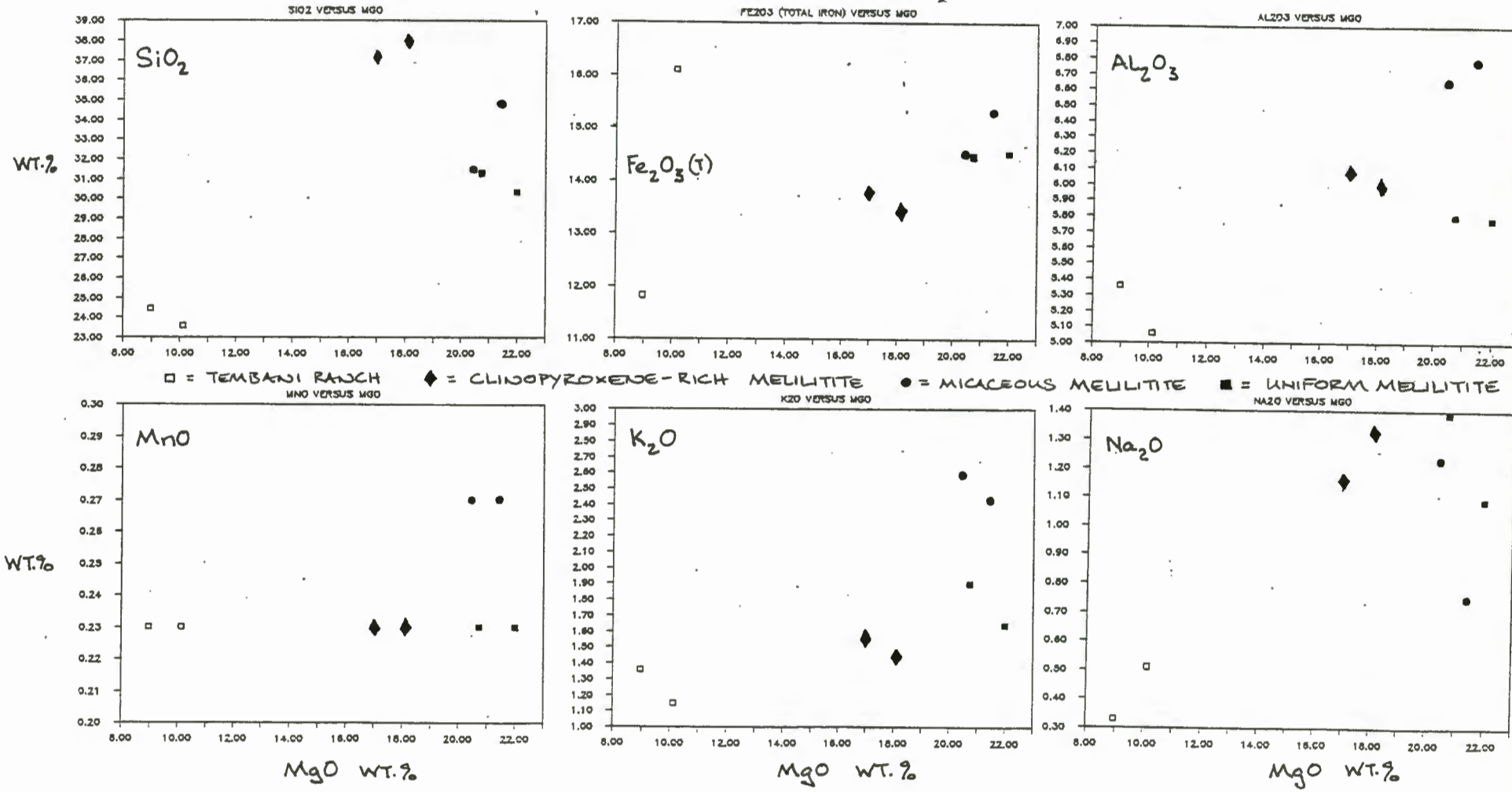

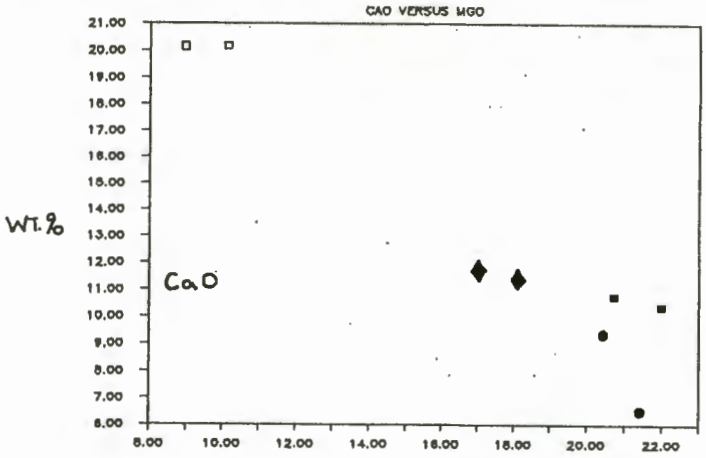
CAO VERSUS MGO
WT.%
CaO
21.00
20.00
19.00
18.00
17.00
16.00
15.00
14.00
13.00
12.00
11.00
10.00
9.00
8.00
7.00
6.00
6.00
10.00
12.00
14.00
16.00
18.00
20.00
22.00

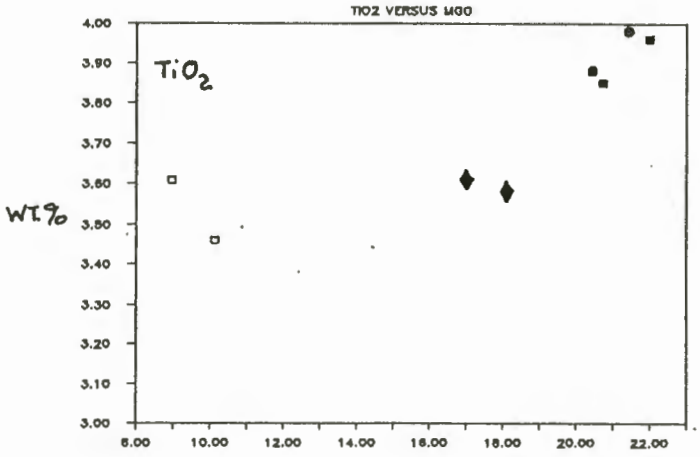
TIO2 VERSUS MGO
WT.%
TiO2
4.00
3.90
3.80
3.70
3.60
3.50
3.40
3.30
3.20
3.10
3.00
6.00
10.00
12.00
14.00
16.00
18.00
20.00
22.00

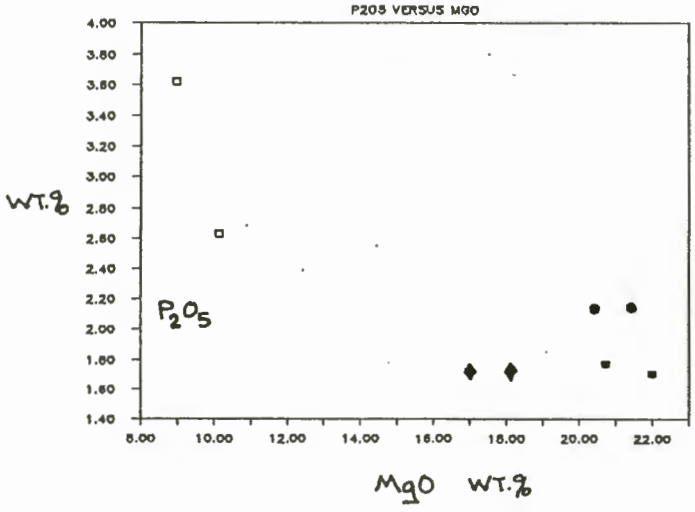
P2O5 VERSUS MGO
WT.%
P2O5
4.00
3.80
3.60
3.40
3.20
3.00
2.80
2.60
2.40
2.20
2.00
1.80
1.60
1.40
6.00
10.00
12.00
14.00
16.00
18.00
20.00
22.00
MgO WT.%

FIGURE 6·2
TRACE ELEMENT VARIATION DIAGRAMS
(VS MGO WT%)

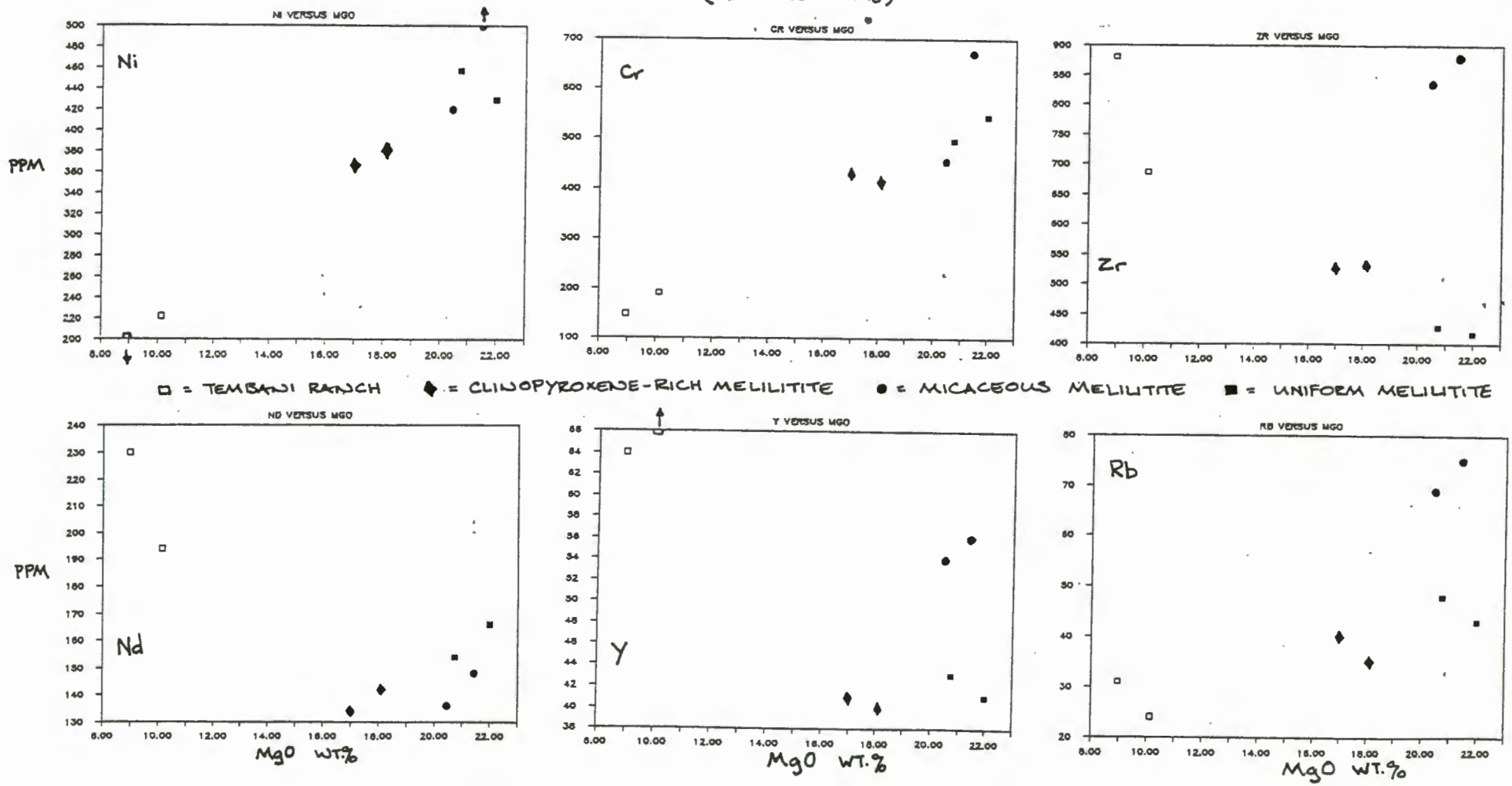

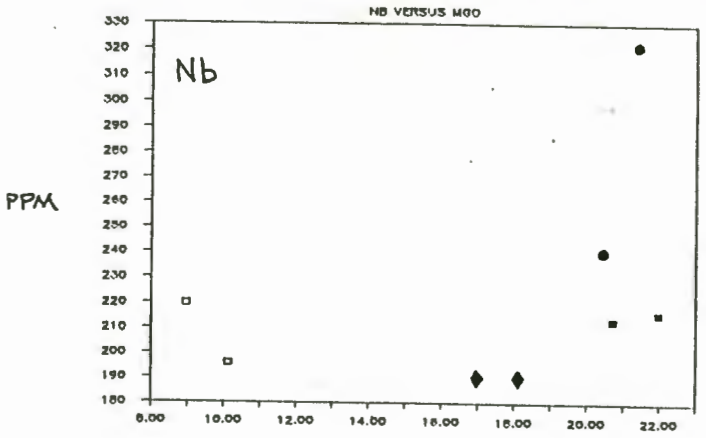
NB VERSUS MGO
Nb
PPM
330
320
310
300
290
280
270
260
250
240
230
220
210
200
190
180
8.00
10.00
12.00
14.00
16.00
18.00
20.00
22.00

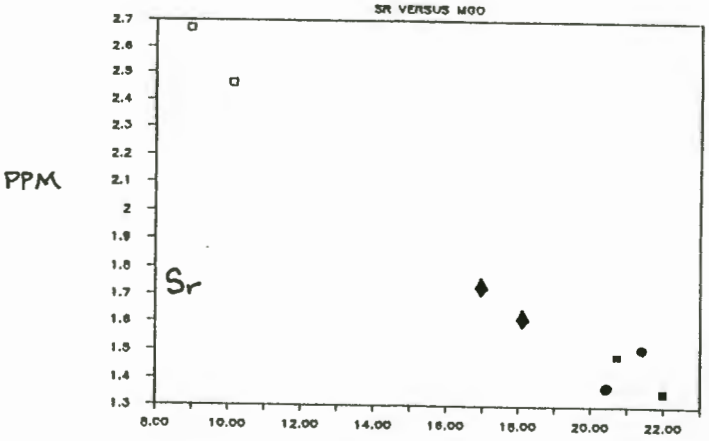
SR VERSUS MGO
Sr
PPM
2.7
2.6
2.5
2.4
2.3
2.2
2.1
2
1.9
1.8
1.7
1.6
1.5
1.4
1.3
8.00
10.00
12.00
14.00
16.00
18.00
20.00
22.00

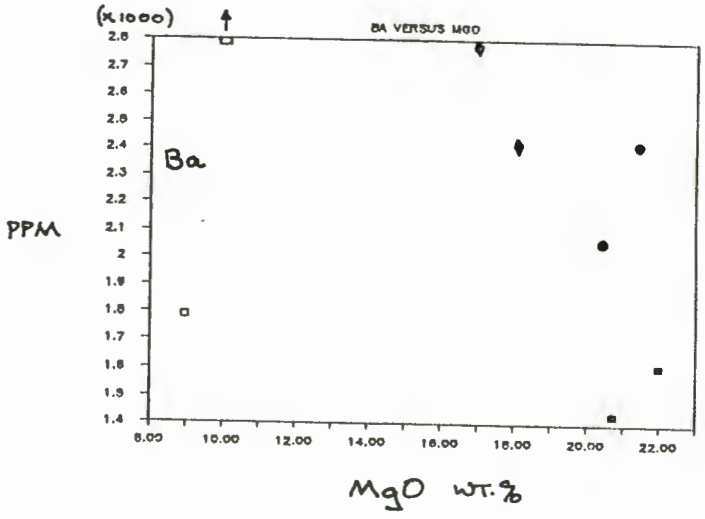
(X1000)
BA VERSUS MGO
Ba
PPM
2.8
2.7
2.6
2.5
2.4
2.3
2.2
2.1
2
1.9
1.8
1.7
1.6
1.5
1.4
8.00
10.00
12.00
14.00
16.00
18.00
20.00
22.00
MgO WT.%

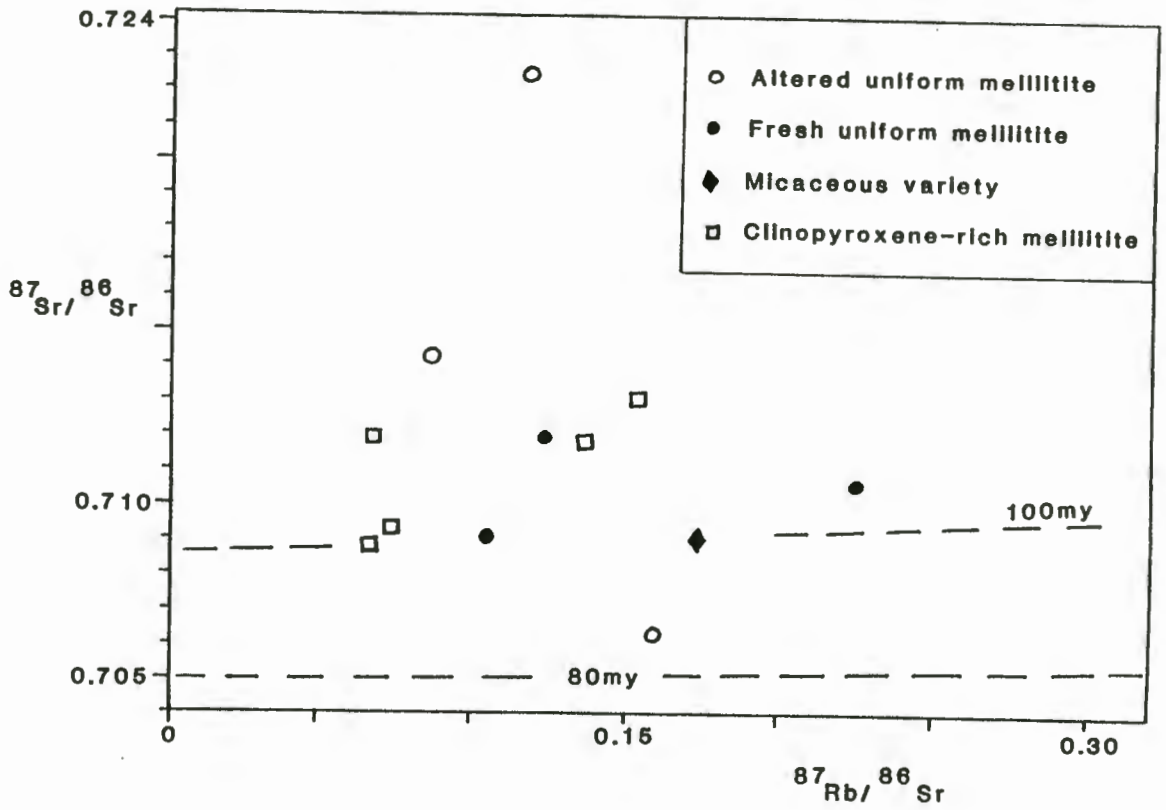

FIGURE 6.3

EMTILOMBO Rb-Sr ISOTOPES

CHAPTER SEVEN

PETROGENESIS OF THE ESHOWE MELILITITES

7.1 GENERAL INTRODUCTION

The geological, petrological and geochemical characteristics of the Eshowe melilitites described in the earlier Chapters are discussed together in this Chapter. The aim of this is to deduce the petrogenetic evolution of the melilitites from magma genesis to emplacement. As the geological setting has influenced the nature of the intrusives this is also included.

7.2 MELT GENERATION AND INTRUSION OF THE ESHOWE MELILITITES

7.2.1 MAGMA SOURCE AREA

The presence of high nickel, chromium and magnesium contents suggest that the Emtilombo intrusion was derived from a primary "primitive" mantle source. The initial strontium ratio (0.705) of the Eshowe melilitites, based on phlogopite data from Emtilombo and Tembani Ranch dykes, is similar to that of bulk earth. This indicates an asthenospheric source area. Enrichment of the magmas in incompatible elements such as potassium, rubidium, neodymium and barium suggests either the source area was enriched or there was interaction between magma and metasomatised lithosphere. A large body of evidence

exists for the latter process (Wilson 1989, Menzies et al. 1987, Harte et al 1987, Viljoen 1988) and this is the process that is favoured for the formation of the Eshowe melilitite magmas.

7.2.2 MAGMATISM

Two major types of peridotite microxenoliths are present in the Emtilombo dyke: a lherzolite suite and a dunitic suite.

The lherzolite suite microxenoliths are associated with magnesian aluminium chromites that are characterised by low titanium contents. A large population of chromites$_{ss}$ from concentrate show similar chemical characteristics (Figure 5.6) and define a trend of increasing aluminium with decreasing chromium. Olivine grains associated with the lherzolites are characterised by high forsterite and nickel and have similar compositions to olivines in mantle derived spinel lherzolites (Shee 1985). The petrographic and chemical characteristics of these microxenoliths and concentrate grains therefore indicates that they are mantle derived and are probably from a range of depths. They are compositionally similar to a variety of nodules from Ngopetsoeu and Lipelaneng kimberlites in Lesotho (Carswell et al. 1984).

The dunite suite microxenoliths comprise olivines with lower forsterite and nickel contents than the spinel lherzolites and are associated with chromite$_{ss}$ characterised by high titanium.

Similar chromites$_{ss}$ are present in the concentrate and help to define compositional trends. These grains show the distinctive trend from magnesian aluminium chromite to ulvospinel compositions (Figure 5.6). The more magnesian macrocryst olivines are compositionally similar to olivines in the dunites. In addition olivines in the microxenoliths are petrographically similar, in size and shape, to the discrete macrocrysts and together they define a continuous compositional trend of decreasing forsterite and nickel (Figure 5.4). The macrocrysts are therefore thought to represent xenocrysts from disaggregated dunites. Many of the complex phenocrysts (characterised by unusual morphologies developed through resorption) are chemically similar to the 'macrocryst' olivines and define a trend towards even more iron rich and nickel poor compositions. These grains are also believed to be related to the dunite suite.

The relatively high magnesium and nickel contents of some of the dunites and presence of clinopyroxene suggests that this suite of rocks represents cumulates from a magma source rather than depleted mantle residue. The compositional trend shown by the 'complex phenocrysts' and macrocryst (xenocryst populations) and microxenolith olivines indicates fractionation towards relatively iron rich compositions and is suggestive of a magmatic trend. Jackson (1980) describes a suite of similar rock types from Lipelaneng kimberlite in Lesotho. He believes the original magma to these rock types was picritic and may have been associated with the Karoo

volcanism.

Olivines in the dunite suite (discrete xenocryst grains and microxenoliths) show close compositional similarities to the microphenocryst population of the Emtilombo melilitite. In addition the dunites are associated with chromites that show a magmatic trend towards increasing titanium and iron contents. It is therefore suggested that these rock types represent high pressure cumulates from earlier, failed, intrusions of alkaline magmas that crystallized at depth. Intrusion of these magmas was probably associated with the introduction of incompatible trace elements, H_2O and CO_2 into spinel peridotite lithosphere. The dunite microxenoliths show extensive evidence of modal metasomatism characterised by the introduction of phlogopite laths. In view of the close chemical similarities this deep seated magmatism was probably closely related to the genesis of the Eshowe melilitites.

7.2.3 MAGMA GENESIS

The process of magmatic intrusion from asthenospheric depths is uncertain. Two possibilities exist: diapiric upwelling (Wilson 1989) or hot spot related activity (Le Roex 1986). Magma generated in the asthenosphere intersected and interacted with the metasomatised lithosphere resulting in the formation of the incompatible element enriched parental magmas to the Eshowe melilitites. Evidence from the olivine phenocryst population and some of the complex phenocrysts

decrease of nickel suggests titanomagnetite$_{ss}$ was competing for iron. The olivine zonation patterns were established by this stage. Titanomagnetite$_{ss}$ shows a brief period of crystallisation towards increasing ferric iron and titanium contents. This was soon followed by a change in the trend to decreasing titanium and increasing ferric iron. It is at this point that perovskite started crystallising and competed strongly for titanium (Haggerty 1976). Perovskite crystallisation is controlled by low silica activities at relatively low oxygen fugacities (Haggerty 1976, Mitchell 1986) and by availability of calcium (Hatton pers com). This could suggest that the loss of a CO_2-rich volatile phase increased the calcium activity in the magma. This event followed after the formation of the complex reverse zonation patterns on the olivine xenocrysts. Magma mixing is therefore the favoured process.

The 'parental magma' to the Eshowe melilitites formed through a combination of magma mixing and interaction with metasomatised lithosphere. It was a complex mixture of mantle components and primary magma at the initiation of eruption to surface. It entrained fragments of spinel lherzolite host rock, earlier cumulates of alkaline magmatism and phenocrysts and complex phenocrysts from a variety of magma mixes.

The olivine microphenocrysts are believed to represent the only olivine population to crystallise from the 'parental magma' to the Eshowe melilitites. They are the most abundant

single population of olivines present that are characterised by primary morphological shapes. They show the most consistent olivine magmatic trend from high forsterite and nickel to more iron rich, low nickel contents. They are also characterised by a normal, simple, magmatic core to rim zonation pattern. The small size and abundance of these grains suggests they crystallised over a fairly short interval and from a small batch of magma. It is suggested that the microphenocrysts formed at the initiation of the eruption to surface.

7.3 MODE OF EMPLACEMENT

7.3.1 DYKES

7.3.1.1 TEMBANI RANCH

Tembani Ranch dyke consists of a fine-grained, porphyritic, rock type that shows no significant mineralogical or textural variation and no evidence for violent disruptive emplacement. The presence of rounded segregations in an essentially uniform groundmass is thought to indicate that minor turbulent flow did occur during emplacement. Rotation of aggregated clusters of crystals in a partially consolidated magma could result in rounding and concentric orientation of elongate minerals. The dyke has a narrow, anastomosing shape and apparently restricted aerial extent. All of these features suggest that Tembani Ranch dyke formed in a single, low energy intrusive event. It is unlikely that the magma reached the surface, it probably died out in the Beaufort sediments in which the

locality is exposed at present.

7.3.1.2 EMTILOMBO

The Emtilombo occurrence is unusual in that is shows features characteristic of quiescent magma emplacement (uniform melilitite) and more violent emplacement (melilitite breccia).

Clement (1982) describes in detail the process of fluidised intrusion and believes that this is the mechanism responsible for the formation of the extensive diatreme zone in kimberlites. It occurs essentially at near surface levels as a result of depressurisation vaporisation of volatiles included within the magma. This results in rapid cooling, adiabatic expansion and explosive breakthrough to surface. The release of pressure affects progressively deeper levels and results in downward migration of the diatreme along the path of the precursor intrusion. The process continues until the partial pressure of the volatiles is too low to maintain the system. This results in the formation of tuffisitic kimberlite breccia (TKB) which is considered to be the typical rock type formed by violent, explosive, gas/solid, emplacement. TKB is characterised by a disrupted, close-packed, fragmental texture and consists of pelletal lapilli (juvenile lapilli) and incorporated country rock xenoliths and xenocrysts all set in a cryptocrystalline base of serpentine and clinopyroxene microlites. The latter minerals represent phases that have condensed from gases. No thermal effects on

or reaction between xenoliths and magma are evident in TKB indicating relatively cool intrusion. No primary carbonate is present as CO_2-rich volatiles are lost to the atmosphere on emplacement.

Clement (1982) believes that the source of volatiles, in kimberlites, responsible for the fluidisation process, is primary ie. kimberlite magma is essentially volatile-rich (largely CO_2).

The presence of well developed, globular-segregationary to segregationary textural varieties within the Emtilombo uniform melilitite indicates that volatiles were an important constituent of the magma. Calcite is a common and ubiquitous mineral associated with late-stage segregationary 'pools' and veinlets suggesting that the volatile phase was CO_2-rich. Very few country rock xenoliths or disaggregated xenocrysts occur within the 'globular-segregations' of the melilitite breccia suggesting that segregation of volatiles from the partially consolidated silicate magma occurred prior to formation of the rock type and incorporation of country rock fragments. The dissociation of volatiles from the silicate melt must have occurred at deeper levels than the present level of exposure.

The melilitite breccia has a fragmental texture and an abundance of xenolithic splinters which suggest that relatively violent emplacement occurred. 'Globular-segregations' are similar to pelletal (juvenile) lapilli,

larger constituents are set in a cryptocrystalline base of altered serpentine(?) and no thermal reaction between xenoliths and magma is evident suggesting the melilitite breccia was a relatively cool intrusion. Several differences to TKB are apparent. These include features such as: the well developed rounded nature of the 'segregations' and absence of fragmental olivine grains in the 'inter-segregationary' matrix which suggest less disruption of magma has taken place than is commonly observed in TKB (or the melilitite equivalent: TMB - tuffisitic melilitite breccia); the complete lack of clinopyroxene microlites, although this may be due to the masking effect of alteration, and; presence of possible primary carbonate which suggests some CO_2-rich volatiles were trapped within the intrusion on consolidation.

Geological and petrographic features suggest that primary volatiles may not have been the driving force in the formation of the melilitite breccia. Water may have played an important part in its development. Emtilombo intrudes Natal Group sediments and a dolerite dyke (Figure 3.4). Country rock in the vicinity of the dolerite is a very hard, reddish quartzite in which some pyrite mineralisation is evident. Away from the dolerite it is a paler coloured, pink, indurated, but porous sandstone. Emtilombo intrudes both quartzite and sandstone. This, in addition to the presence of pyrite in the quartzite, suggests that dolerite intrusion was responsible for baking the sediments prior to intrusion of the melilitite and that the latter had little apparent effect on the country rock.

The melilitite breccia is confined to the ends of the dyke where the sandstone country rock is not baked. It is suggested that the production of steam and incorporation of additional volatiles (water) from country rock into the magma, in association with the primary magmatic volatiles already present, initiated or enhanced more vigorous emplacement.

The relatively cool nature of the melilitite breccia may provide evidence for fluidised emplacement. The incomplete disruption of semi-consolidated magma and presence of probable primary carbonate suggests that this fluidisation was incomplete. The Emtilombo magma was probably partially consolidated, polymerised and relatively viscous at the time of emplacement at the current level of exposure. Addition of water into this crystal/liquid system could have decreased the viscosity, by depolymerisation of the melt (Mysen 1988, Fisher and Schmincke 1984), resulting in more turbulent, 'fluidised' flow. Adiabatic expansion associated with this process could have been controlled by jointing in the country rock. Water, and steam, in association with the expansion would have cooled the magma. The absence of extensive disruption of the magma argues against violent, phreatomagmatic volcanism.

There is no conclusive evidence to show that Emtilombo broke through to surface as a pipe. A considerable amount of erosion has occurred so it is possible that the present level of exposure represents the deep root zone of a diatreme that has subsequently been removed. The confining pressures of the

country rock at depth would perhaps restrict expansion of the intrusion, particularly as it appears to preferentially follow a zone of weakness. The distinct dyke like shape of the occurrence and absence of brecciation in the surrounding country rock does suggest that the intrusion was a sub-surface phenomenon at this level of exposure.

It is envisaged that a single volatile-rich magma pulse was associated with simultaneous, but short lived, fluidisation. This was restricted to the areas of waterlogged sandstone and occurred mainly at the dyke contacts. It was probably triggered by the generation of steam and incorporation of water from the country rock into the magma. This could have led to widening of the dyke and rapid upward expansion of the melilitite breccia into the uniform melilitite. Volatiles (steam and CO_2) could have escaped upwards along joints which would have lowered the fluidisation potential of the intrusion and perhaps "frozen" the dyke at depth. Alternatively continued upwelling of magma, of the same pulse, followed fluidisation and cut irregularly through the breccia zone.

It is considered unlikely that two phases of magmatic activity occurred as there is no clear evidence for multiple intrusion. Mineralogical and textural variation within the dyke was probably controlled by varying degrees of crustal contamination, resorbed water content, localised magmatic volatile concentrations and differences in thermal regimes between contact zones and the centre of the dyke.

7.3.2 PIPES

Both the pipes share features in common with kimberlite diatreme zones. The latter are characterised by simple geology, regular pipe shapes and the presence of TKB. Both Cowards Bush and Nqoleni have fairly regular, roughly elliptical to rounded pipe shapes and they each consist of clast-rich, fragmental rock types. There are, however, several important differences. There is strong evidence for bedding, accretionary lapilli occur in both pipes, glass fragments are present in Nqoleni and there is an abundance of finely comminuted material thought to be ash particles. These features are all typical products of phreatomagmatic processes (Fisher and Schmincke 1984, Lorenz 1985). Further evidence for this comes from the nature of the bedded units. Thin zones of fine-grained material containing rounded juvenile lapilli could represent base-surge deposits. The occasional massive, boulder-rich zones (conspicuous in Cowards Bush) could represent later debris flow material or infill from collapsing wall rocks (Lorenz 1985).

It is uncertain whether primary volatiles played a part in the development of the volcaniclastic breccias. Juvenile lapilli are similar to the 'globular segregations' in the Emtilombo melilitite breccia which could suggest segregation of the magma and volatiles took place prior to emplacement. However a much higher proportion of small country rock fragments and mineral fragments are present within the lapilli, 15 vol.% as opposed to 2 vol.% in Emtilombo segregations (Table 3.3B). It

is therefore probable that a large proportion of the lapilli formed by frictional rotation of semi-consolidated magma blobs during phreatomagmatic explosions and xenolithic inclusions were incorporated during this process. A second consideration is that magmatic volatiles would probably lead to large explosive events, as proposed for kimberlites (Clement 1982), and it would be difficult to reconcile this with the bedded sequence present in the Cowards Bush diatreme. Primary volatiles probably did play a part, evidence from all of the Eshowe melilitites suggests H_2O- and CO_2-rich volatiles are present in the magma, but it seems unlikely that they were the driving force in the formation of the volcaniclastic sequences.

The pipes are located in the Nkwaleni graben. This was very likely a river valley at the time of emplacement as the structure would have influence the drainage system. They also intrude sediments of the Karoo Sequence which, in view of the setting, were probably water saturated. Water was therefore an abundant phase in the vicinity of the pipes and the potential for phreatomagmatic volcanism high.

7.3.2.1 COWARDS BUSH

Cowards Bush consists of at least 160m of volcaniclastic sediments. The mineralogy of the juvenile lapilli appears to be similar throughout this depth suggesting derivation from a single magma pulse. The bedding features and variety of textural types is, however, more indicative of complex

multiple explosion events. It seems possible that fairly long lived reaction between continuously upwelling magma and water was responsible for the formation of the Cowards Bush diatreme zone. This suggests that the pipe formed from a larger volume of magma than the melilitites in the dykes.

7.3.2.2 Nqoleni

Nqoleni pipe is thought to represent a deeper level of exposure than that at Cowards Bush. It is smaller than at the latter locality, which could indicate more erosion has occurred, but the most convincing evidence is in the nature of the rock type. Cowards Bush volcaniclastic breccia has a relatively open textured matrix while that at Nqoleni has a cemented base comprising predominantly analcite and carbonate. It is suggested that the cement formed by hot, vapour phase crystallisation. The latter involves the growth of minerals, in open pore spaces, as a result of precipitation from volatiles (Cas and Wright 1987). This process was probably responsible for masking much of the original texture of the Nqoleni rock and the formation of an indurated rock type.

The nature of the glass spherulites in Nqoleni provides further evidence for vapour phase crystallisation. Glasses either devitrify during formation of tuffs or are altered because of their metastable state under diagenetic to low grade metamorphic conditions. Vapour phase crystallisation occurs contemporaneously with or after devitrification. The

devitrification process results in the development of spherulitic and bow-tie textured glass which distorts the original shard like nature of the fragments (Cas and Wright 1987). Four stages based on experiments on rhyolitic obsidian have been identified: an initial hydration stage, a glassy stage, a spherulitic stage and a granophyric stage. Nqoleni glass shows features typical of the glassy stage in which the morphology of spherulites varies according to the temperature to which they have been exposed during devitrification. Bow-tie shaped aggregates are predominant between 400° to 600° C while lath like fibres or open framework circular clusters of spaced fibres develop at 700° C. Bow-tie shaped aggregates with lath-like fibres are conspicuous in the Nqoleni volcaniclastic breccia which may perhaps suggest temperatures of formation of between 600° and 700° C. It is, however, possible that the fibres present in glass spherulites represent quench induced crystallisation (Cas and Wright 1987).

The source of the volatiles in Nqoleni is believed to be a combination of primary magmatic, CO_2-rich gases fluxing from the nearby cooling magma column and steam derived from the water-rich country rocks. These volatiles precipitated calcite, analcite, zeolites, and amphibole in the open pore spaces and the devitrification of the glass shards was associated with this process. Cowards Bush volcaniclastic does not show any influence of vapour phase crystallisation. This suggests the current level of exposure was further away

from the hot volatile flux zone and the magma column and is therefore believed to show a higher level of the melilitite diatreme.

7.4 GEOCHEMICAL EVOLUTION OF THE ESHOWE MELILITITES

Petrographic and geochemical features of the Tembani Ranch dyke suggest that this rock type formed by crystallisation of a fractionated melt. Olivine phenocrysts are present in relatively low proportions (average 7 vol.%) in Tembani Ranch dyke, phenocrysts are relatively small and macrocrysts are absent. Melilite phenocrysts are conspicuous in Tembani Ranch dyke. This in addition to the presence of relatively abundant clinopyroxene phenocrysts and apatite suggest there are some distinct chemical differences between Tembani Ranch and Emtilombo dykes.

Whole rock geochemistry shows some influence by secondary alteration processes. This is particularly evident in the amount and distribution of magnesium, iron and the alkalis. The high P_2O_5 contents are primary and are associated with the presence of relatively coarse apatite. The high calcium contents are also believed, to some extent, to be primary. Calcium was probably introduced during late stage volatile exhalation from the trapped cooling magma. Some calcium may be associated with interaction between country rock and the dyke either as a result of secondary processes or during emplacement. The high enrichment in Ba and Sr may indicate

interaction with crustal rocks occurred. This is shown particularly by the variable, high and low, Sr initial ratios of the whole rock data.

The presence of P_2O_5 could result in a more polymerised melt (Mysen 1988) and hence a more viscous and slower rate of intrusion. The presence of melilite phenocrysts in Tembani Ranch could also suggest that it is chemically different to the Emtilombo magma. Velde and Yoder (1976) found rocks with relatively high alkali contents contained melilite phenocrysts whereas rocks with lower alkalis and higher MgO contained groundmass melilite. Lower abundance of olivine phenocrysts could suggest a lower MgO content. These features in addition to the enrichment in P_2O_5, Zr and Y relative to the Emtilombo rock types suggest Tembani Ranch crystallised from a fractionated residual magma and that the dyke represents a small volume, low energy intrusion.

Whole rock geochemistry of the Emtilombo uniform melilititе confirms the relatively primitive nature of the intrusion (high MgO, NiO and Cr_2O_3 contents). The micaceous varient shows some chemical similarities to the former rock type and is also relatively primitive. There are however some chemical trends that suggest some fractionation occurred. This corroborates the petrographic evidence. The rock type is enriched in SiO_2, Al_2O_3, K_2O and P_2O_5. This is reflected by the presence of abundant phlogopite, lesser clinopyroxene and conspicuous apatite in the groundmass. The presence of higher

contents of Zr, Y and Rb in the micaceous variety compared to the uniform melilitite also suggest the former is relatively more fractionated than the latter magma. The close chemical similarities in some of the major and trace element compositions suggest that these rock types could have formed from a single intrusive event. Differential cooling rates and magma flow regimes may have influenced the development of the relatively more fractionated micaceous melilitite.

The clinopyroxene-rich melilitite shows distinctive contamination by crustal rocks both petrographically and chemically. SiO_2, CaO, Ba and Sr are enriched and FeO and MgO depleted relative to the uniform melilitite. All the Emtilombo rock types show some evidence for crustal contamination. This contamination is largely reflected in the high Sr contents.

7.5 TECTONO-THERMAL HISTORY ALONG THE EAST COAST

On the basis of age data, intrusion of the Eshowe melilitites post-dated rift tectonics, alkaline intrusive events and voluminous basaltic and lesser acidic magmatism of the Lebombo volcanics (Figure 7.1). Earlier recurrent tectonism along the east African coast resulted in progressive attenuation of continental crust through time. Evidence for this is provided by the progressive northward extension and westward widening of the Natal Basin from Devonian to Permian and from resultant continental fragmentation along this zone of weakness.

Further evidence for crustal thinning comes from the ocean basement. Seismic data suggests the northern Natal Valley and Mozambique Ridge consist of thinned continental crust, approximately 15km and 20km thick, respectively (Dingle et al. 1983) and Eales et al. (1984) suggest the Lebombo volcanics delineate the margin between attenuated crust and craton.

Crustal attenuation was associated with changes in the mantle thermal regime and probable lithospheric thinning. This is reflected by a change in nature of the Lebombo volcanism. The major part of the magmatism was basaltic but this was followed by late stage acidic and finally transitional alkaline basalt magmatism (Bristow 1980). This suggests progressively increasing heat flow, melt volume and shallower levels of melting followed by a decrease in mantle temperatures which resulted in smaller melt volumes being generated at deeper mantle sources. The change in nature and volume of volcanism to the south of the Lebombo could reflect differences in the style of fragmentation and mantle processes between the two areas (Bristow 1976, 1980).

The closest known alkaline intrusives to the Eshowe melilitites occur to the north and southwest and are represented by Dokolwayo kimberlite (Hawthorne et al. 1979, Daniels 1989) and the Griqualand East kimberlites (Nixon et al. 1983). Intrusion of Dokolwayo preceded the Lebombo volcanics (Figure 7.1). Intrusion of the Griqualand East localities preceded and post-dated intrusion of the

Drakensberg basalts. The timing and spatial association of the intrusive events and rift tectonics along the east coast suggests that magmatism in the area was strongly controlled by mantle processes related to the breakup of Gondwanaland.

The Eshowe melilitites intruded an area of attenuated crust and thinned lithosphere, an essentially rift valley environment. The nature of the rock types, ie. melilitites as opposed to kimberlites, in a marginal cratonic setting suggests a relatively shallower, upper mantle, source area.

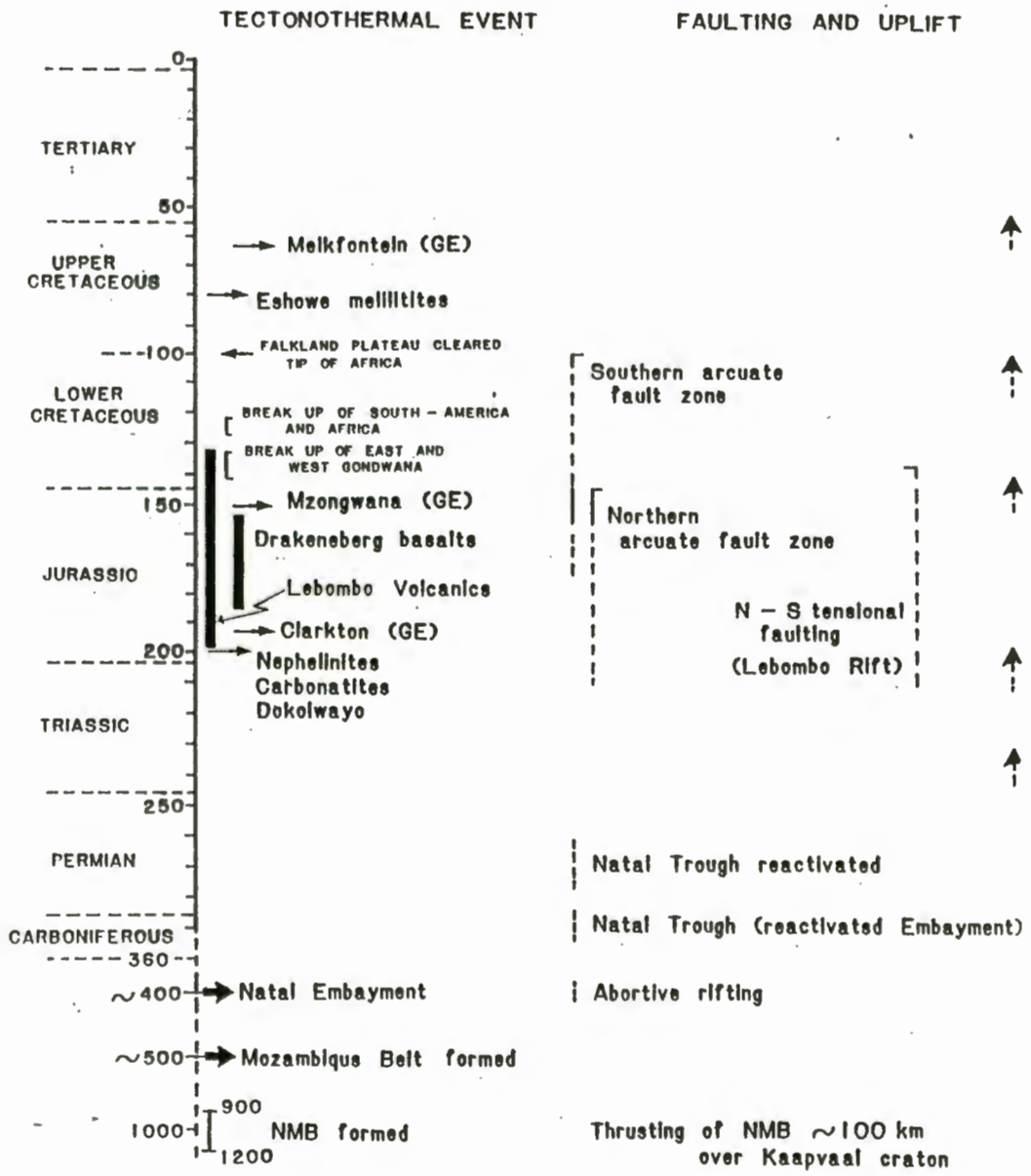

FIGURE 7.1

TECTONO-THERMAL HISTORY OF THE EAST COAST

GE = GRIQUALAND EAST

NMB = NATAL MOBILE BELT

(from Colgan et al 1989)

BIBLIOGRAPHY

Armstrong R.A., Bristow J.W. and Cox K.G. (1984). The Rooi Rand dyke swarm, southern Lebombo. *In*: Erlank A.J., Ed., *Petrogenesis of the volcanic rocks of the Karoo Province*. Geol. Soc. S.Afr. Spec. Publ. 13, 77-86.

Beater B.E. and Maud R.R. (1960). The occurrence of an extensive fault system in SE Zululand and its possible relationship to the evolution of a part of the coastline of Southern Africa. *Trans. Geol. Soc. S.Afr.*, 63, 51-61.

Bristow J.W. (1976). *The geology and geochemistry of the southern Lebombo*. M.Sc. thesis (unpubl.), Univ. Natal, Durban, 331 pp.

------- (1980). *The geochronology and geochemistry of Karoo volcanics in the Lebombo and adjacent areas*. Ph.D. thesis (unpubl.), Univ. Cape Town, 257 pp.

Cadle A.B. and Hobday D.K. (1977). A subsurface investigation of the middle Ecca and lower Beaufort in northern Natal and the south eastern Transvaal. *Trans. Geol. Soc. S.Afr.*, 80(2), 111-115.

Carswell D.A., Griffin W.L. and Kresten P. (1984). Peridotite nodules from the Ngopetsoeu and Lipelaneng kimberlites, Lesotho: a crustal or mantle origin. *In:* Kornprobst J., Ed., *Kimberlites II: the mantle and crust-mantle relationships*. Third International Kimberlite Conference. Elsevier (publ.), Amsterdam. 229-243.

Cas R.A.F. and Wright J.V. (1987). *Volcanic successions. Modern and ancient. A geological approach to processes, products and successions*. Allen and Unwin (Publ.), London, 528 pp.

Charlesworth E.G. (1981). *Tectonics and metamorphism of the northern margin of the Namaqua-Natal mobile belt, near Eshowe, Natal*. Ph.D. thesis (unpubl.), Univ. Natal, Durban.

------- and Matthews P.E. (1981). Archaean granulites along the southern margin of the Kaapvaal craton in eastern South Africa. *Geol. Soc. S.Afr., Geocongress 81 Abstracts*.

Clement C.R. (1982). *A comparative geological study of some major kimberlite pipes in the northern Cape and Orange Free States*. Ph.D. thesis (unpubl.), Univ. Cape Town.

------- and Skinner E.M.W. (1985). A textural-genetic classification of kimberlites. *Trans. Geol. Soc. S.Afr.*, 88, 403-409.

Christie A.D.M. and Tavener-Smith R. (1979). Middle Ecca sedimentary associations on the Natal coast north of Durban. *Geol. Soc. S.Afr., Geocongress 79 Abstracts.*, 69-70.

Colgan E.A. (1982). The petrology of olivine melilitites from Natal, South Africa. *Third International Kimberlite Conference Abstracts. Terra Cognita.*, 2(3), 205.

-------, Clark T.C., Bristow J.W. and Allsop H.L. (1989). Geological setting, petrography and petrogenesis of olivine melilitites of the Natal Coast, South Africa. *In: Kimberlites and related rocks. Their composition, occurrence, origin and emplacement. Vol. 1.* Fourth International Kimberlite Conference. GSA Special Publication 14. Blackwell (Publ.), Carlton. 417-435.

Daniels L.R.M. and Gurney J.J. (1989). The chemistry of the garnets, chromites and diamond inclusions of the Dokolwayo kimberlite, Kingdom of Swaziland. *In: Kimberlites and related rocks. Their mantle/crust setting, diamonds and diamond exploration. Vol. 2.* Fourth International Kimberlite Conference. GSA Special Publication 14. Blackwell (Publ.), Carlton. 1012-1021.

Deer W.A., Howie R.A and Zussman J. (1982). *Rock forming minerals. Orthosilicates.* Vol. 1A. 2nd Ed. Longmans (Publ.), London. 1-336.

De Swardt A.M.J. and Bennet G. (1974). Structural and physiographic development of Natal since the late Jurassic. *Trans. Geol. Soc. S.Afr.*, 77(3), 309-322.

Dingle R.V., Siesser W.G. and Newton A.R. (1983). *Mesozoic and Tertiary geology of Southern Africa.* A.A. Balkema (Publ.), Rotterdam.

Eales H.V., Marsh J.S. and Cox K.G. (1984). The Karoo Igneous Province: An introduction. *In*: Erlank A.J., Ed., *Petrogenesis of the volcanic rocks of the Karoo Province.* Geol. Soc. S.Afr. Spec. Publ. 13, 1-26.

Eastell J. (1986). *A low dilution fusion technique for the determination of major, minor and trace elements in lamproite and kimberlite samples by X-Ray fluorescence spectrometry.* M.Sc. thesis (unpubl.), Univ., Cape Town. 204 pp.

Fisher R.V. and Schmincke H.-U. (1984). *Pyroclastic rocks.* Springer-Verlag (Publ.), Berlin, 472 pp.

Frankel J.J. (1960). The geology along the Umfolosi River South of Mtubatuba, Zululand. *Trans. Geol. Soc. S.Afr.*, 63, 231-252.

Groenewald P.B., Grantham G.H. and Moyes A.B. (1988). Kibaran and Pan African Orogeny in Dronning Maud Land, Antarctica, and south eastern Africa: Relations in a Gondwana context. *Geol. Soc. S.Afr., Geocongress 88 Abstracts.*, 203-206

Geological Series 1:50000 (1975). *Maps: 2831DA to 2831DC.* Dept. Mines, Geol Surv. Pretoria S.Afr.

Haggerty S.E. (1976). Opaque mineral oxides in terrestrial igneous rocks. *In:* Rumble D., Ed., *Oxide minerals. Reviews of mineralogy, vol. 3.* Min. Soc. Am., Washington, DC., Hg101-Hg300.

Harmer R.E. (1981). A critical evaluation of possible oceanic-type rocks within the frontal sector of the Natal mobile belt. *Geol. Soc. S.Afr., Geocongress 81 Abstracts.*, 101-102.

Harte B. (1977). Rock nomenclature with particular relation to deformation and recrystallisation textures in olivine-bearing xenoliths. *J. Geol.*, 85, 279-288.

Harte B., Winterburn P.A. and Gurney J.J. (1987). Metasomatic and enrichment phenomena in garnet peridotite facies mantle xenoliths from the Matsoku kimberlite pipe, Lesotho. *In:* Menzies M.A. and Hawkesworth C.J., Eds., *Mantle metasomatism.* Academic Press (Publ.), London. 145-220.

Hawthorne J.B., Carrington A.J., Clement C.R. and Skinner E.M.W. (1979). Geology of the Dokolwayo kimberlite and associated palaeo-alluvial diamond deposits. *In*: Boyd F.R. and Meyer H.O.A., Eds, *Kimberlites, diatremes and diamonds: their geology, petrology and geochemistry. Vol. 1.* Second International Kimberlite Conference, AGU, Washington. 59-70.

Hobday D.K. (1973). Middle Ecca deltaic deposits in the Muden-Tugela Ferry area of Natal. *Trans. Geol. Soc. S.Afr.*, 76(3), 309-318.

------- and Mathew D. (1974). Depositional environment of the Cape Supergroup in the Transkei. *Trans. Geol. Soc. S.Afr.*, 77(3), 223-227.

-------, Tavener-Smith R. and Mathew D. (1975). Markov analysis and the recognition of palaeoenvironments in the Ecca Group near Vryheid, Natal. *Trans. Geol. Soc. S.Afr.*, 78(1), 75-82.

Jackson P.M. (1980). *Petrology of some nodules from kimberlites in northern Lesotho.* Ph.D. thesis (unpubl.), Univ. Edinburgh.

Kingsley C.S. (1975). A new stratigraphic classification implying a lithofacies change in the Table Mountain sandstone in Southern Natal. *Trans. Geol. Soc. S.Afr.*, 78(1), 43-55.

Lawless P.J. (1978). *Some aspects of the mineral chemistry of peridotitic xenoliths from the Bultfontein mine.* Ph.D. thesis (unpubl.), Univ. Cape Town.

Le Roux A.P. (1986). Geochemical correlation between southern African kimberlites and South Atlantic hotspots. *Nature*, 324 (6094), 243-245.

Lorenz V. (1985). Maars and diatremes of phreatomagmatic origin: A review. *Trans. Geol. Soc. S.Afr.*, 88(2), 459-470.

Mason T.R. and Tavener-Smith R. (1978). A fluvio-deltaic middle Ecca succession west of Empangeni, Zululand. *Trans. Geol. Soc. S.Afr.*, 81(1), 13-22.

Matthews P.E. (1961). Slump structures in the Table Mountain Series of Natal. *Trans. Geol. Soc. S.Afr.*, 64, 55-69.

------- (1970). Palaeorelief and the Dwyka glaciation in the eastern region of South Africa. *Second International Gondwana Symposium. Proceedings and Papers*, 491-499.

------- (1972). Possible Precambrian obduction and plate tectonics in southeastern Africa. *Nature*, 240, 37-39.

------- (1981a). Eastern or Natal sector of the Namaqua-Natal mobile belt in Southern Africa. *In*: Hunter D.R., Ed., *Precambrian of the Southern Hemisphere*. Elsevier (Publ.), Amsterdam. 705-715.

------- (1981b). A new tectonic model for the northern region of the Namaqua-Natal belt in Natal. *Geol. Soc. S.Afr. Geocongress 81 Abstracts. S.Afr.*, 150-151.

------- and Charlesworth E.G. (1981). *A geological review of the northern margin of the proterozoic Namaqua-Natal mobile belt in Natal. Guide book to the post Congress excursion to Natal, Geocongress 81.* Geol. Soc. S.Afr.

Maud R.R. (1961). A preliminary review of the structure of coastal Natal. *Trans. Geol. Soc. S.Afr.*, 64, 247-256.

McCarthy M.J. (1988). Late Gondwana to recent geology of the Natal coast. *Geol. Soc. S.Afr., Geocongress 88 Abstracts.*, 405a-405e.

Menzies M.A., Rodgers N., Tindle A. and Hawkesworth C.J. (1987). Metasomatic and enrichment processes in lithospheric peridotites, an effect of asthenosphere-lithosphere interaction. *In:* Menzies M.A. and Hawkesworth C.J., Eds., *Mantle metasomatism*. Academic Press (Publ.), London. 313-361.

Mitchell R.H. (1986). *Kimberlites. Mineralogy, geochemistry and petrology.* Plenum Press (Publ.), London. 442 pp.

Moore A.E. (1979). *The geochemistry of the olivine melilitites and related rocks of Namaqualand-Bushmanland, South Africa.* Ph.D. thesis (unpubl.), Univ. Cape Town, 383 pp.

Moore A.E. and Erlank A.J. (1979). Unusual olivine zoning - evidence for complex physico-chemical changes during the evolution of olivine melilitite and kimberlite magmas. *Contrib. Mineral. Petrol.* 70, 391-405.

Mysen B.O. (1988). *Structure and properties of silicate melts.* Elsevier (Publ.), Amsterdam, 354 pp.

Nixon P.H., Boyd J.V. and Boctor N.Z. (1983). East Griqualand kimberlites. *Trans. Geol. Soc. S.Afr.*, 86(3), 221-235.

SACS (South African Committee for Stratigraphy). (1980). *Stratigraphy of South Africa. Part 1* (Comp. Kent L.E.). *Lithostratigraphy of the Republic of South Africa, South West Africa/Namibia, and the Republics of Bophuthatswana, Transkei and Venda:* Handb. Geol. Surv. S.Afr., 8, 690 pp.

Shee S.R. (1985). *The petrogenesis of the Wesselton mine kimberlites, Kimberley, Cape Province, R.S.A.* Ph.D. thesis (unpubl.), Univ. Cape Town.

Skinner E.M.W. and Clement C.R. (1979). Mineralogical classification of southern African kimberlites. *In*: Boyd F.R. and Meyer H.O.A., Eds, *Kimberlites, diatremes and diamonds: their geology, petrology and geochemistry. Vol. 1.* Second International Kimberlite Conference, AGU, Washington. 129-139.

Stratten T. (1970). Tectonic framework of sedimentation during the Dwyka period in South Africa. *Second International Gondwana Symposium. Proceedings and Papers*, 483-490

Tankard A.J., Jackson M.P.A., Eriksson K.A., Hobday D.K., Hunter D.R. and Minter W.E.L. (1982). *Crustal evolution of Southern Africa: 3.8 billion years of earth history.* Springer-Verlag (Publ.), New York.

Tavener-Smith R. (1979). Prograding middle Ecca coastal associations from the Effingham Quarries near Durban. *Geol. Soc. S.Afr., Geocongress 79 Abstracts*, 61-68.

Truswell J.F. and Ryan P.J. (1969). A flysch facies in the lower Ecca Group of the southern Karroo and a portion of the Transkei. *Trans. Geol. Soc. S.Afr.* 72(3), 151-158.

Velde D. and Yoder H.S. Jr. (1976). The chemical composition of melilite-bearing eruptive rocks. *Carnegie Institute Yearbook 1975-1976,* 574-580.

Viljoen K.S. (1988). *Petrology of the Sutherland Commonage melilitite intrusives*. M.Sc. thesis (unpubl.), Univ. Cape Town.

Von Brunn V. (1977). A furrowed intratillite pavement in the Dwyka Group of northern Natal. *Trans. Geol. Soc. S.Afr.*, 80(2), 125-130.

------- and Gravenor C.P. (1983). A model for late Dwyka glaciomarine sedimentation in the eastern Karoo basin. *Trans. Geol. Soc. S.Afr.*, 86(3), 199-209.

Whateley M.K.G. (1980). Deltaic and fluvial deposits of the Ecca group, Nongoma Graben, northern Zululand. *Trans. Geol. Soc. S.Afr. Special Issue.*, 83(3), 345-351.

Wilson M. (1989). *Igneous Petrogenesis*. Unwin Hyman (Publ.), London, 466 pp.

York D. (1966). Least squares fitting of a straight line. *Can. J. Phys.*, 44, 1079-1086.

ACKNOWLEDGEMENTS

I am indebted to a number of people for their help advice and encouragement whilst writing this thesis.

I would like to thank J.B Hawthorne, C.R. Clement, E.M.W. Skinner and J.W. Bristow for permitting me to work on this project.

J. Eastell and T. Clark are thanked for undertaking XRF analyses and Rb, Sr isotope analyses, respectively, and helpful comments on analytical techniques.

H. Horsch, C. Hatton, M. Field and K.S. Viljoen are thanked for proof reading bits of this work, helpful advise and many discussions. H. Horsch and B. Lowry are also thanked for their time and patience in teaching me to use the electron microprobe. John Gurney is thanked for his advise and comments on this work and for a great deal of patience in waiting for its completion.

Tony and Ann Robertson are thanked for their hospitality during numerous field trips to Eshowe.

My father and sister are thanked for their never ending support and encouragement. This thesis is dedicated to the memory of my mother who taught me a lot about patience and endurance.

APPENDIX 1

1.1 SAMPLE DETAILS

1.1.1 PETROGRAPHY - MODAL ANALYSES

In modal abundance analyses recognisable pseudomorphs were counted as the original primary minerals while unrecognisable constituents were counted as the secondary alteration product. Carbonate in modal analyses includes both crystalline and cryptocrystalline calcite and lesser dolomite.

1.1.2 TEMBANI RANCH

All samples are from borehole core. They are magmatic (hypabyssal facies) porphyritic melilitite. The groundmass has a generally uniform distribution but occassional globular structures are present. The 'globules' comprise essentially the same groundmass minerals but melilite laths are orientated tangentially. The samples are all carbonatised opaque mineral-rich olivine-clinopyroxene phlogopite-melilite melilititites. Some varieties are apatite rich. The relative abundances of the various minerals differs between thin sections.

1.1.3 COWARDS BUSH

All samples are from borehole core. They comprise volcaniclastic breccias in which pelletal lapilli are present. The samples are all extremely altered. The abundance and size of the various constituents differs from sample to sample.

1.1.4 EMTILOMBO

PK003/1 and 2 (samples from pit) - Globular segregationary melilitite breccia.

PK003/7 - 14 (core samples) - With the exception of PK003/8 and 12 the samples are all altered macrocrystic uniform melilitite. PK003/8 is a globular segregationary melilitite (segregationary varient of the uniform melilitite). PK003/12 is a globular segregationary melilitite breccia.

PK003/23 (sample from pit) - Fresh macrocrystic uniform melilitite.

PK003/36, 40, 47, 48, 49 (core samples) - Altered macrocrystic uniform melilitite.

PK003/55, 56 (core samples) - Fresh macrocrystic micaceous melilitite.

PK003/58, 59, 60, 61 (core samples) - Fresh macrocrystic uniform melilitite.

PK003/64, 66, 67 (core samples) - Fresh clinopyroxene-rich melilitite (contaminated melilitite).

1.1.5 NQOLENI

PK003/6 (core) - Two thin sections were examined: a relatively coarse grained and a fine grained variety. All core from the borehole looked similar so 'representative' sample of the borehole was examined. The rock type is a volcaniclastic breccia. PK005/6A is a coarse textured variety. PK005/6B is a fine grained variety.

1.2 SAMPLE TREATMENT

SAMPLE NUMBER	PETROGRAPHY	MIN. CHEMISTRY	WHOLE ROCK	ISOTOPES
TEMBANI RANCH				
PK001/3, 4	X		X	
PK001/5 - 8	X			
COWARDS BUSH				
PK002/3, 5 - 13	X			
EMTILOMBO				
PK003/1, 2, 7 - 14, 49	X			
PK003/36	X	X		
PK003/23, 40, 47, 48, 60, 61, 67	X			X
PK003/55	X		X	
PK003/56, 58, 59, 64, 66	X	X	X	X
NQOLENI				
PK005/6A, 6B	X			

1.3 ANALYTICAL TECHNIQUES

1.3.1 MINERAL CHEMISTRY

1.3.1.1 ARL-SEMQ

The procedures, operating parameters, standards, error and detection limits are as outlined by Lawless (1978) and Shee (1985). Analyses from the ARL-SEMQ are recorded to two decimal places.

1.3.1.2 CAMECA SX-50

The CAMECA SX-50 is a fully automated microprobe with 5 spectrometers (WDS) and an EDS system linked to it. Analyses from the SX-50 are recorded to three decimal places.

OPERATING PARAMETERS:

ACCELERATING VOLTAGE: 20 KV (Accelerating potential)

BEAM CURRENT: 20 nA

COUNTING TIMES: 20 sec on peak

10 sec on background

PAP correction procedures are used.

STANDARDS:

Pure Oxides	for	Mg, Al, Cr, Fe, Ni
$MnTiO_3$	for	Mn, Ti
Wollastonite	for	Si, Ca
Albite	for	Na
Orthoclase	for	K
V_2O_5	for	V

1.3.2 WHOLE ROCK GEOCHEMISTRY

Six samples from Emtilombo dyke and two from Tembani Ranch were selected for analysis. The samples were initially crushed to approximately 0.5cm in diameter. As conspicuous large, upto 1cm, dunite microxenoliths and macrocrysts are present in Emtilombo rock chips from these samples were examined, using a binocular microscope, and chips carefully selected to avoid inclusion of obvious large olivines, mica and ilmenite macrocrysts. In the case of samples from the globular segregationary clinopyroxene-rich melilitite chips with obvious country rock inclusions were selectively excluded. Approximately 80 to 100 grams of material was collected for analysis. Tembani Ranch melilitite is a relatively 'clean' looking porphyritic rock type so the whole sample (in both cases) was used for XRF analysis. Approximately 500 grams of sample was used. Rock chips were reduced to powder in a tungsten-carbide sieb mill.

The powders were prepared for XRF analysis using a low dilution fusion technique (2:1, flux:sample). The technique is described by Eastell (1986). XRF analyses were undertaken by J. Eastell (AARL). Elemental intensities of eleven major and 21 trace elements are determined using a Phillips PW1404 sequential X-ray spectrometer. Major element intensities are corrected for background and spectral line overlap using the computer program TRACE and inter element (matrix) effects using the computer program NBSGSC. Trace element concentrations are calculated using the computer program

TRACE.

The average absolute errors for the calibration standards are detailed below:-

	Ave. Abs. Error	Concentration Range %
SiO2	0.45	8 - 75
TiO2	0.03	0.1 - 4
Al2O3	0.09	0.3 - 27
Fe2O3	0.14	1.8 - 45
MnO	0.03	0.1 - 9
MgO	0.42	0.5 - 48
Na2O	0.06	0.1 - 4
CaO	0.09	0.1 - 48
K2O	0.03	0.1 - 15
P2O5	0.03	0.1 - 15

Negative trace element values indicate that the calculated concentration is below the lower limit of detection.

1.4 RESULTS

All analytical results are recorded on the disk in the pocket on the back cover. Details of the samples analysed are recorded above and file names and format of the data on disk are included in Appendix 3.

APPENDIX 2

1.1 KEY TO ABBREVIATIONS

1.1.1 TITLES

OCCNUM	-	Locality and sample number.
MIN	-	Mineral analysed.
GR	-	Grain number.
A	-	Analysis number.
PO	-	Analytical position in grain.
PA	-	Paragenesis.
NA2O (etc)	-	List of elements analysed (wt%).
TOTAL	-	Total concentration of elements (wt%).
CORRTOT	-	Corrected total concentration of elements (wt%) after recalculation of FeO and Fe_2O_3 (spinels only).
FO	-	Forsterite content

1.1.2 LOCALITY NUMBER

PK001 - Tembani Ranch

PK003 - Emtilombo

PK004 - Ndundulu

PK005 - Nqoleni

1.1.3 MINERAL

OLI - Olivine

SPI - Spinel

1.1.4 POSITION

C - Core of grain.

CI - Intermediate between core and 'IC'.

IC - Intermediate between 'CI' and 'I'.

I - Intermediate between core and rim.

IR - Intermediate between 'I' and 'RI'.

RI - Intermediate between rim and 'IR'.

R - Rim of grain.

1.1.5 PARAGENESIS

C - Concentrate.

X - Xenocryst.

M - Macrocryst.

CP - Complex Phenocryst (olivine).

P - Phenocryst.

MP - Microphenocryst.

G - Groundmass.

1.1.6 GENERAL

'.' = Not determined.

Major elements are recorded in wt%.

Trace elements are recorded in ppm.

OLIVINE ANALYSES

OCCNUM	MIN	GR	A	PO	PA	NA2O	SIO2	FEO	K2O	CR2O3	AL2O3	MGO	MNO	TIO2	CAO	NIO	V2O5	TOTAL	FO
PK003/58B	OLI	29	1	C	X	0.022	41.004	8.661	0.000	0.046	0.011	49.515	0.097	0.004	0.038	0.354	0.005	99.757	91.062
PK003/58B	OLI	29	2	C	X	0.014	40.871	8.729	0.000	0.006	0.011	49.749	0.087	0.003	0.052	0.431	0.001	99.954	91.036
PK003/59A	OLI	24	1	R	X	0.00	39.11	14.13	0.00	0.31	0.11	45.52	0.19	0.12	0.23	0.25	.	99.97	85.165
PK003/59A	OLI	24	2	IR	X	0.02	39.20	13.49	0.00	0.03	0.03	46.30	0.19	0.04	0.21	0.27	.	99.78	85.947
PK003/59A	OLI	24	3	C	X	0.00	39.30	14.54	0.00	0.02	0.04	45.96	0.16	0.04	0.14	0.29	.	100.49	84.923
PK003/59A	OLI	24	5	R	X	0.00	39.21	14.50	0.00	0.02	0.02	46.06	0.16	0.03	0.14	0.27	.	100.41	84.986
PK003/59A	OLI	24	6	C	X	0.01	39.24	13.88	0.00	0.02	0.04	45.21	0.14	0.03	0.17	0.28	.	99.02	85.303
PK003/59A	OLI	24	7	C	X	0.01	39.41	13.10	0.00	0.02	0.02	45.89	0.13	0.03	0.18	0.29	.	99.08	86.192
PK003/59A	OLI	24	8	C	X	0.02	39.09	14.52	0.00	0.01	0.02	45.32	0.17	0.02	0.15	0.29	.	99.61	84.761
PK003/59A	OLI	24	9	C	X	0.01	39.55	13.84	0.00	0.02	0.03	45.84	0.15	0.03	0.14	0.29	.	99.90	85.512
PK003/59B	OLI	32	1	C	X	.	39.90	11.10	.	0.00	0.02	48.41	0.16	0.04	0.09	0.36	.	100.08	88.600
PK003/59B	OLI	32	2	C	X	.	40.10	11.01	.	0.00	0.02	48.62	0.15	0.02	0.08	0.33	.	100.33	88.725
PK003/61B	OLI	1	1	C	X	0.024	39.455	15.298	0.000	0.010	0.055	43.490	0.111	0.027	0.141	0.294	0.023	98.927	83.515
PK003/61B	OLI	1	2	C	X	0.022	39.502	15.139	0.012	0.018	0.064	43.732	0.161	0.032	0.155	0.307	0.000	99.143	83.734
PK003/64	OLI	1	1	C	X	0.002	39.910	12.504	0.006	0.000	0.003	46.265	0.210	0.023	0.107	0.315	0.000	99.346	86.831
PK003/64	OLI	2	1	C	X	0.003	40.202	12.467	0.010	0.011	0.000	46.233	0.185	0.032	0.111	0.322	0.000	99.577	86.857
PK003/64B	OLI	1	1		X1	0.000	40.242	12.360	0.001	0.007	0.000	45.626	0.176	0.031	0.123	0.316	0.021	98.904	86.804
PK003/64B	OLI	2	1		X1	0.003	39.993	12.342	0.006	0.021	0.001	46.181	0.213	0.024	0.123	0.350	0.013	99.272	86.958
PK003/64B	OLI	3	1		X1	0.002	40.305	12.209	0.006	0.003	0.011	46.340	0.263	0.030	0.122	0.292	0.000	99.584	87.119
PK003/64B	OLI	4	1		X1	0.010	40.168	12.424	0.000	0.005	0.000	46.198	0.208	0.026	0.120	0.330	0.012	99.501	86.887
PK003/58B	OLI	1	1	C	M	0.029	39.921	16.047	0.000	0.000	0.007	43.215	0.188	0.024	0.114	0.218	0.008	99.772	82.756
PK003/58B	OLI	1	2	I	M	0.000	39.606	15.875	0.000	0.006	0.007	43.629	0.178	0.011	0.135	0.259	0.000	99.706	83.043
PK003/58B	OLI	1	3	R	M	0.027	39.798	14.562	0.005	0.035	0.015	44.428	0.198	0.052	0.290	0.232	0.005	99.646	84.464
PK003/58B	OLI	3	1	C	M	0.015	40.520	14.929	0.000	0.005	0.038	44.337	0.154	0.037	0.109	0.295	0.000	99.969	84.107
PK003/58B	OLI	3	2	R	M	0.015	39.959	15.070	0.000	0.031	0.026	43.732	0.316	0.055	0.560	0.126	0.011	99.901	83.796
PK003/58B	OLI	14	1	C	M	0.002	39.851	14.136	0.001	0.044	0.029	45.234	0.133	0.036	0.108	0.267	0.000	99.840	85.080
PK003/58B	OLI	14	1	C	M	0.033	39.828	14.041	0.019	0.033	0.033	45.357	0.150	0.023	0.102	0.299	0.000	99.919	85.199
PK003/58B	OLI	14	2	R	M	0.027	39.704	15.482	0.000	0.019	0.013	43.686	0.260	0.055	0.520	0.074	0.000	99.840	83.412
PK003/58B	OLI	16	1	C	M	0.000	39.419	15.710	0.006	0.029	0.012	44.085	0.146	0.025	0.124	0.270	0.000	99.825	83.335
PK003/58B	OLI	16	2	R	M	0.018	39.378	15.752	0.027	0.017	0.017	44.000	0.177	0.029	0.217	0.233	0.024	99.889	83.271
PK003/58B	OLI	22	1	C	M	0.012	39.699	15.944	0.001	0.024	0.030	43.688	0.148	0.021	0.127	0.193	0.000	99.887	83.001
PK003/58B	OLI	22	2	I	M	0.019	39.700	16.101	0.002	0.000	0.022	43.730	0.094	0.031	0.137	0.199	0.000	100.034	82.876
PK003/58B	OLI	36	1	C	M	0.025	38.103	15.670	0.000	0.000	0.025	45.081	0.155	0.032	0.146	0.209	0.011	99.457	83.678
PK003/58B	OLI	36	2	C	M	0.020	38.346	15.481	0.010	0.007	0.011	45.013	0.200	0.034	0.144	0.159	0.026	99.450	83.822
PK003/58B	OLI	36	3	R	M	0.007	38.033	14.753	0.001	0.019	0.021	46.431	0.164	0.034	0.186	0.212	0.000	99.862	84.868
PK003/58B	OLI	38	1	C	M	0.000	39.460	17.094	0.011	0.007	0.024	42.849	0.250	0.018	0.170	0.161	0.020	100.064	81.708
PK003/58B	OLI	38	2	R	M	0.006	39.989	14.540	0.000	0.047	0.002	44.995	0.189	0.021	0.222	0.234	0.000	100.247	84.650
PK003/59B	OLI	1	1	C	M	0.01	39.39	16.01	0.00	0.00	0.03	44.55	0.22	0.03	0.14	0.21	.	100.59	83.218
PK003/59B	OLI	1	3	IR	M	0.02	39.21	16.04	0.00	0.00	0.04	44.74	0.19	0.03	0.13	0.22	.	100.62	83.251
PK003/59B	OLI	2	1	C	M	0.00	39.59	14.24	0.00	0.00	0.04	45.96	0.17	0.03	0.12	0.27	.	100.42	85.188
PK003/59B	OLI	2	2	C	M	0.00	39.48	14.34	0.00	0.00	0.04	45.84	0.19	0.02	0.12	0.30	.	100.33	85.067
PK003/59B	OLI	2	3	I	M	0.00	39.58	14.28	0.00	0.00	0.03	45.77	0.18	0.03	0.12	0.26	.	100.25	85.100
PK003/59B	OLI	2	4	C	M	0.00	39.50	14.33	0.00	0.00	0.03	45.82	0.17	0.03	0.12	0.28	.	100.28	85.070
PK003/59B	OLI	2	5	R	M	0.00	39.75	14.12	0.00	0.00	0.03	46.07	0.19	0.03	0.13	0.28	.	100.60	85.325
PK003/59B	OLI	2	6	R	M	0.00	39.47	14.17	0.00	0.00	0.03	46.38	0.18	0.03	0.12	0.27	.	100.65	85.364
PK003/59B	OLI	2	7	R	M	0.00	39.64	14.38	0.00	0.00	0.04	45.65	0.18	0.04	0.14	0.28	.	100.35	84.978
PK003/59B	OLI	2	8	IR	M	0.02	39.71	14.39	0.00	0.01	0.03	46.21	0.18	0.04	0.13	0.30	.	101.02	85.124
PK003/59B	OLI	2	9	I	M	0.00	39.48	14.40	0.00	0.01	0.02	45.69	0.19	0.03	0.14	0.29	.	100.25	84.972
PK003/59B	OLI	2	10	C	M	0.00	39.58	14.42	0.00	0.00	0.02	45.61	0.16	0.03	0.15	0.29	.	100.26	84.932
PK003/59B	OLI	2	11	R	M	0.04	39.45	14.31	0.00	0.00	0.03	45.57	0.18	0.05	0.18	0.26	.	100.07	85.018
PK003/59B	OLI	3	1	I	M	0.00	39.72	14.65	0.00	0.00	0.02	45.78	0.18	0.03	0.12	0.28	.	100.78	84.776
PK003/59B	OLI	3	2	C	M	0.04	39.59	14.73	0.00	0.00	0.03	45.78	0.17	0.03	0.12	0.28	.	100.77	84.706
PK003/59B	OLI	3	3	C	M	0.00	39.74	14.88	0.00	0.01	0.03	45.86	0.19	0.03	0.13	0.28	.	101.15	84.597
PK003/59B	OLI	3	4	R	M	0.00	39.75	15.57	0.00	0.01	0.21	43.06	0.29	0.07	0.48	0.11	.	99.55	83.132
PK003/59B	OLI	3	5	C	M	0.02	39.77	14.86	0.00	0.01	0.03	45.08	0.18	0.04	0.13	0.30	.	100.42	84.389
PK003/59B	OLI	3	6	C	M	0.02	39.50	14.86	0.00	0.01	0.03	45.62	0.17	0.04	0.13	0.28	.	100.66	84.546
PK003/59B	OLI	3	7	R	M	0.01	39.41	15.75	0.00	0.00	0.03	44.32	0.26	0.05	0.37	0.13	.	100.33	83.373
PK003/59B	OLI	4	1	I	M	0.00	39.41	16.58	0.00	0.00	0.03	44.63	0.21	0.04	0.13	0.18	.	101.21	82.749
PK003/59B	OLI	4	2	C	M	0.00	39.30	16.88	0.00	0.00	0.02	44.70	0.21	0.03	0.14	0.17	.	101.45	82.514
PK003/59B	OLI	4	3	C	M	0.03	39.26	16.93	0.01	0.00	0.02	44.89	0.21	0.04	0.15	0.20	.	101.74	82.533
PK003/59B	OLI	4	4	R	M	0.01	39.64	16.03	0.00	0.00	0.03	45.29	0.24	0.05	0.31	0.14	.	101.74	83.429
PK003/59B	OLI	4	5	IR	M	0.02	39.05	16.73	0.00	0.00	0.01	44.79	0.21	0.04	0.17	0.20	.	101.22	82.671

OCCNUM	MIN	GR	A	PO	PA	NA2O	SIO2	FEO	K2O	CR2O3	AL2O3	MGO	MNO	TIO2	CAO	NIO	V2O5	TOTAL	FO
PK003/66A	OLI	1	1	R	M	0.000	39.470	15.190	0.000	0.000	0.000	46.180	0.200	0.050	0.140	0.290	.	101.520	84.418
PK003/66A	OLI	1	2	R	M	0.000	39.290	15.060	0.000	0.000	0.020	45.790	0.180	0.040	0.130	0.270	.	100.780	84.419
PK003/66A	OLI	1	3	IR	M	0.000	39.310	15.000	0.000	0.000	0.020	45.640	0.180	0.040	0.130	0.260	.	100.580	84.429
PK003/66A	OLI	1	4	IC	M	0.000	39.170	14.950	0.000	0.000	0.030	45.130	0.170	0.040	0.140	0.280	.	99.910	84.324
PK003/66A	OLI	1	5	C	M	0.000	39.120	14.930	0.000	0.000	0.030	45.510	0.170	0.030	0.120	0.260	.	100.170	84.453
PK003/66D	OLI	7	1	R	M	.	39.66	14.20	.	0.02	0.03	46.23	0.18	0.05	0.25	0.23	.	100.85	85.297
PK003/66D	OLI	7	2	IC	M	.	39.30	15.53	.	0.00	0.01	45.72	0.19	0.03	0.14	0.19	.	101.11	83.990
PK003/66D	OLI	7	3	C	M	.	39.10	15.43	.	0.00	0.02	45.32	0.18	0.02	0.15	0.19	.	100.41	83.959
PK003/66D	OLI	8	2	IR	M	.	39.79	12.42	.	0.00	0.01	47.69	0.19	0.02	0.10	0.31	.	100.53	87.249
PK003/66D	OLI	8	3	C	M	.	39.63	12.30	.	0.00	0.02	47.84	0.17	0.03	0.10	0.31	.	100.40	87.391
PK003/66D	OLI	8	4	R	M	.	39.72	12.42	.	0.00	0.02	48.06	0.19	0.03	0.10	0.30	.	100.84	87.335
PK003/58B	OLI	2	1	R	CP	0.022	39.272	14.157	0.021	0.000	0.013	44.756	0.356	0.036	1.043	0.050	0.006	99.732	84.925
PK003/58B	OLI	2	2	R	CP	0.005	39.484	14.613	0.001	0.000	0.003	44.459	0.310	0.048	0.719	0.059	0.000	99.702	84.428
PK003/58B	OLI	2	3	RI	CP	0.012	39.942	14.737	0.004	0.030	0.032	44.670	0.179	0.027	0.252	0.241	0.008	100.135	84.379
PK003/58B	OLI	2	4	IR	CP	0.020	39.328	16.808	0.021	0.000	0.040	43.206	0.205	0.028	0.132	0.209	0.033	100.031	82.081
PK003/58B	OLI	2	5	I	CP	0.005	39.373	17.051	0.004	0.000	0.023	43.029	0.176	0.030	0.138	0.244	0.021	100.094	81.808
PK003/58B	OLI	2	6	C	CP	0.023	39.496	16.788	0.000	0.015	0.011	42.759	0.181	0.018	0.138	0.203	0.000	99.631	81.945
PK003/58B	OLI	2	7	C	CP	0.019	39.384	16.817	0.002	0.006	0.014	42.667	0.176	0.022	0.139	0.162	0.007	99.416	81.888
PK003/58B	OLI	2	8	IC	CP	0.044	39.446	16.935	0.007	0.000	0.015	42.585	0.137	0.009	0.126	0.188	0.000	99.490	81.755
PK003/58B	OLI	2	9	I	CP	0.022	39.775	16.719	0.031	0.000	0.035	42.762	0.140	0.007	0.131	0.193	0.005	99.819	82.007
PK003/58B	OLI	2	10	R	CP	0.022	39.792	16.561	0.000	0.001	0.008	42.955	0.157	0.031	0.146	0.192	0.012	99.878	82.213
PK003/58B	OLI	23	1	C	CP	0.010	39.361	15.017	0.006	0.007	0.021	44.134	0.169	0.012	0.102	0.242	0.012	99.092	83.967
PK003/58B	OLI	23	2	R	CP	0.025	39.096	15.367	0.012	0.015	0.012	43.481	0.293	0.056	0.564	0.078	0.014	99.014	83.450
PK003/58B	OLI	23	3	R	CP	0.000	39.649	15.422	0.000	0.000	0.032	43.403	0.269	0.055	0.506	0.067	0.017	99.420	83.375
PK003/58B	OLI	28	1	C	CP	0.008	39.754	15.416	0.005	0.025	0.007	44.515	0.172	0.043	0.116	0.250	0.010	100.322	83.728
PK003/58B	OLI	28	2	R	CP	0.000	39.719	15.188	0.004	0.046	0.018	44.600	0.171	0.019	0.138	0.239	0.007	100.150	83.956
PK003/58B	OLI	34	1	C	CP	0.032	39.493	14.839	0.001	0.015	0.013	44.844	0.186	0.019	0.129	0.267	0.007	99.847	84.339
PK003/58B	OLI	34	2	R	CP	0.028	39.941	14.548	0.011	0.044	0.022	45.042	0.158	0.037	0.180	0.231	0.001	100.242	84.656
PK003/58B	OLI	34	3	C	I	0.04	39.65	15.41	0.00	0.00	0.00	45.01	0.20	0.02	0.19	0.21	.	100.73	83.884
PK003/58B	OLI	39	1	C	CP	0.000	39.315	18.781	0.012	0.022	0.039	41.696	0.232	0.037	0.166	0.156	0.000	100.457	79.823
PK003/58B	OLI	39	2	I	CP	0.028	39.448	18.612	0.001	0.000	0.022	41.232	0.256	0.033	0.178	0.183	0.000	99.994	79.789
PK003/58B	OLI	39	3	R	CP	0.002	39.217	18.577	0.000	0.000	0.018	41.788	0.247	0.032	0.179	0.155	0.003	100.219	80.034
PK003/58B	OLI	40	1	IC	CP	0.023	39.596	13.214	0.010	0.038	0.030	45.938	0.134	0.027	0.174	0.327	0.000	99.510	86.102
PK003/58B	OLI	40	2	C	CP	0.021	39.647	13.200	0.000	0.069	0.550	46.039	0.155	0.035	0.175	0.351	0.000	99.749	86.140
PK003/58B	OLI	40	3	R	CP	0.005	38.849	15.969	0.005	0.000	0.012	42.971	0.216	0.034	0.351	0.089	0.000	98.502	82.744
PK003/58B	OLI	40	4	R	CP	0.000	39.069	16.245	0.001	0.025	0.002	44.109	0.262	0.022	0.353	0.097	0.014	100.199	82.872
PK003/58B	OLI	41	1	C	CP	0.017	39.958	13.724	0.000	0.023	0.041	45.545	0.114	0.036	0.169	0.287	0.000	99.913	85.536
PK003/58B	OLI	41	2	R	CP	0.020	39.839	16.434	0.014	0.010	0.012	43.286	0.227	0.053	0.303	0.103	0.000	100.300	82.437
PK003/59B	OLI	1	1		CP	0.04	39.65	15.41	0.00	0.00	0.00	45.01	0.20	0.02	0.19	0.21	.	100.73	83.884
PK003/59B	OLI	5	1	IC	CP	0.00	38.91	19.18	0.00	0.00	0.03	42.48	0.28	0.02	0.15	0.16	.	101.21	79.785
PK003/59B	OLI	5	2	R	CP	0.00	39.49	14.86	0.01	0.00	0.03	45.38	0.30	0.08	0.52	0.08	.	100.74	84.477
PK003/59B	OLI	5	3	IC	CP	0.00	38.92	19.17	0.00	0.00	0.02	42.25	0.28	0.03	0.14	0.16	.	100.97	79.706
PK003/59B	OLI	5	4	IR	CP	0.02	38.74	19.41	0.00	0.00	0.01	42.42	0.28	0.04	0.16	0.13	.	101.21	79.569
PK003/59B	OLI	14	1	IR	CP	0.01	39.32	15.88	0.00	0.00	0.02	44.24	0.32	0.04	0.37	0.08	.	100.28	83.234
PK003/59B	OLI	14	2	IR	CP	0.00	39.82	13.82	0.00	0.00	0.03	45.89	0.21	0.02	0.23	0.24	.	100.26	85.543
PK003/59B	OLI	14	3	C	CP	0.03	39.59	15.52	0.00	0.00	0.01	44.55	0.23	0.03	0.29	0.15	.	100.40	83.647
PK003/59B	OLI	14	4	C	CP	0.00	39.30	16.20	0.00	0.00	0.02	44.05	0.27	0.04	0.29	0.12	.	100.29	82.893
PK003/59B	OLI	14	5	C	CP	0.01	39.33	15.43	0.00	0.00	0.03	44.55	0.23	0.03	0.27	0.15	.	100.03	83.727
PK003/59B	OLI	14	6	IR	CP	0.00	39.35	15.89	0.00	0.00	0.03	44.56	0.25	0.03	0.29	0.15	.	100.55	83.326
PK003/59B	OLI	14	7	R	CP	0.00	39.25	15.86	0.11	0.00	0.19	44.13	0.25	0.04	0.45	0.11	.	100.39	83.217
PK003/59B	OLI	14	8	IR	CP	0.03	39.20	15.81	0.00	0.00	0.02	44.34	0.30	0.04	0.41	0.12	.	100.27	83.327
PK003/59B	OLI	14	9	R	CP	0.01	39.35	15.82	0.00	0.00	0.00	44.51	0.29	0.04	0.38	0.09	.	100.49	83.371
PK003/59B	OLI	15	1	C	CP	0.01	39.36	15.74	0.01	0.00	0.02	44.35	0.29	0.06	0.40	0.10	.	100.34	83.392
PK003/59B	OLI	15	2	C	CP	0.01	39.50	15.11	0.00	0.00	0.02	45.45	0.19	0.02	0.12	0.26	.	100.68	84.277
PK003/59B	OLI	15	3	IR	CP	0.03	39.60	14.84	0.00	0.00	0.01	45.87	0.19	0.03	0.12	0.25	.	100.94	84.635
PK003/59B	OLI	15	4	R	CP	0.01	39.74	14.75	0.01	0.00	0.03	45.63	0.19	0.02	0.12	0.23	.	100.73	84.645
PK003/59B	OLI	18	1	IR	CP	0.01	39.43	13.76	0.00	0.00	0.03	45.77	0.19	0.03	0.22	0.25	.	99.69	85.565
PK003/59B	OLI	18	2	C	CP	0.02	39.41	15.11	0.00	0.00	0.02	45.02	0.19	0.02	0.13	0.22	.	100.14	84.151
PK003/59B	OLI	18	3	C	CP	0.10	39.31	15.21	0.02	0.00	0.01	44.97	0.18	0.01	0.13	0.22	.	100.16	84.048
PK003/59B	OLI	18	4	IR	CP	0.04	39.50	15.16	0.00	0.00	0.03	44.73	0.20	0.02	0.12	0.21	.	100.10	84.024
PK003/59B	OLI	18	5	R	CP	0.06	40.43	15.15	0.01	0.00	0.07	43.65	0.23	0.04	0.30	0.15	.	100.09	83.698
PK003/59B	OLI	18	6	R	CP	0.01	39.40	14.24	0.01	0.01	0.02	45.42	0.20	0.06	0.21	0.26	.	99.84	85.031

OCCNUM	MIN	GR	A	PO	PA	NA2O	SIO2	FEO	K2O	CR2O3	AL2O3	MGO	MNO	TIO2	CAO	NIO	V2O5	TOTAL	FO
PK003/59B	OLI	18	7	IR	CP	0.05	39.44	15.22	0.01	0.00	0.02	45.21	0.19	0.02	0.12	0.22	.	100.50	84.110
PK003/59B	OLI	23	1	C	CP	0.01	39.48	14.28	0.00	0.00	0.03	45.16	0.18	0.02	0.12	0.30	.	99.58	84.930
PK003/59B	OLI	23	2		CP	0.00	39.43	14.19	0.01	0.00	0.03	45.71	0.18	0.02	0.16	0.28	.	100.01	85.164
PK003/66D	OLI	2	1	R	CP	.	39.65	13.67	.	0.02	0.02	46.49	0.19	0.05	0.23	0.25	.	100.57	85.836
PK003/66D	OLI	2	2	RI	CP	.	39.68	12.85	.	0.03	0.01	47.14	0.16	0.05	0.20	0.32	.	100.44	86.732
PK003/66D	OLI	2	3	RI	CP	.	39.80	12.00	.	0.03	0.03	47.77	0.15	0.04	0.20	0.34	.	100.36	87.645
PK003/66D	OLI	2	4	IR	CP	.	39.93	15.63	.	0.00	0.01	44.42	0.27	0.04	0.32	0.14	.	99.76	83.510
PK003/66D	OLI	2	5	C	CP	.	39.57	12.93	.	0.02	0.04	46.75	0.15	0.03	0.16	0.31	.	99.96	86.565
PK003/66D	OLI	2	6	C	CP	.	39.71	12.96	.	0.02	0.02	47.11	0.14	0.02	0.18	0.29	.	100.45	86.627
PK003/66D	OLI	2	7	IC	CP	.	39.69	12.29	.	0.03	0.02	47.43	0.16	0.03	0.17	0.30	.	100.12	87.305
PK003/66D	OLI	2	8	R	CP	.	39.12	15.34	.	0.00	0.02	44.70	0.28	0.10	0.42	0.12	.	100.10	83.852
PK003/66D	OLI	2	9	RI	CP	.	39.21	14.33	.	0.01	0.02	45.66	0.22	0.06	0.25	0.21	.	99.97	85.025
PK003/66D	OLI	2	10	RI	CP	.	39.38	13.63	.	0.03	0.02	46.19	0.20	0.04	0.21	0.27	.	99.97	85.793
PK003/66D	OLI	2	11	IR	CP	.	39.95	12.00	.	0.03	0.04	47.70	0.14	0.03	0.20	0.33	.	100.42	87.629
PK003/66D	OLI	2	12	IR	CP	.	39.91	11.93	.	0.02	0.02	47.82	0.15	0.03	0.17	0.34	.	100.39	87.719
PK003/66D	OLI	2	13	IC	CP	.	39.61	11.96	.	0.03	0.02	47.49	0.14	0.03	0.18	0.35	.	99.81	87.617
PK003/66D	OLI	2	14	C	CP	.	39.40	12.44	.	0.03	0.02	47.14	0.14	0.02	0.18	0.31	.	99.68	87.101
PK003/58B	OLI	5	1	C	P	0.020	39.666	15.361	0.000	0.000	0.036	44.081	0.178	0.038	0.118	0.272	0.010	99.781	83.643
PK003/58B	OLI	5	2	R	P	0.002	39.731	14.955	0.000	0.023	0.014	44.128	0.342	0.053	0.569	0.044	0.013	99.874	84.021
PK003/58B	OLI	7	1	C	P	0.000	39.944	14.627	0.012	0.009	0.026	44.633	0.154	0.040	0.122	0.296	0.000	99.863	84.466
PK003/58B	OLI	7	2	R	P	0.012	40.416	14.499	0.000	0.020	0.017	44.633	0.202	0.047	0.141	0.278	0.013	100.280	84.581
PK003/58B	OLI	11	2	R	P	0.011	39.348	18.167	0.000	0.000	0.005	41.561	0.188	0.056	0.157	0.135	0.000	99.628	80.302
PK003/58B	OLI	12	1	C	P	0.000	39.909	15.521	0.012	0.026	0.000	44.209	0.194	0.019	0.133	0.268	0.000	100.292	83.541
PK003/58B	OLI	13	1	C	P	0.021	39.262	16.438	0.007	0.037	0.024	42.958	0.287	0.050	0.353	0.112	0.023	99.573	82.323
PK003/58B	OLI	13	2	R	P	0.012	39.644	15.982	0.000	0.006	0.011	43.507	0.277	0.074	0.457	0.094	0.000	100.065	82.909
PK003/58B	OLI	25	1	C	P	0.006	39.256	16.951	0.009	0.014	0.032	42.668	0.155	0.029	0.114	0.253	0.000	99.487	81.770
PK003/58B	OLI	25	2	R	P	0.018	39.731	14.259	0.000	0.052	0.030	44.928	0.166	0.050	0.243	0.214	0.000	99.693	84.882
PK003/58B	OLI	42	1	C	P	0.007	39.748	15.652	0.000	0.016	0.029	44.080	0.163	0.031	0.127	0.214	0.005	100.072	83.385
PK003/58B	OLI	42	2	R	P	0.000	39.579	15.649	0.006	0.036	0.016	44.555	0.158	0.028	0.135	0.194	0.000	100.356	83.535
PK003/59B	OLI	6	1	C	P	0.03	39.78	15.09	0.00	0.00	0.04	44.99	0.21	0.03	0.13	0.22	.	100.52	84.159
PK003/59B	OLI	6	2	IC	P	0.00	39.68	14.99	0.00	0.00	0.03	45.50	0.19	0.03	0.13	0.24	.	100.79	84.397
PK003/59B	OLI	6	3	IR	P	0.03	39.45	15.57	0.00	0.00	0.02	45.08	0.24	0.04	0.28	0.15	.	100.86	83.765
PK003/59B	OLI	6	4	R	P	0.00	39.44	15.69	0.01	0.01	0.02	44.56	0.29	0.08	0.43	0.09	.	100.62	83.501
PK003/59B	OLI	7	1	C	P	0.01	39.69	15.51	0.00	0.00	0.03	45.77	0.20	0.03	0.13	0.26	.	101.63	84.022
PK003/59B	OLI	7	2	C	P	0.02	39.67	15.48	0.00	0.00	0.02	45.58	0.19	0.03	0.13	0.25	.	101.37	83.992
PK003/59B	OLI	7	3	CI	P	0.01	39.55	15.44	0.00	0.00	0.04	45.02	0.20	0.03	0.13	0.24	.	100.66	83.860
PK003/59B	OLI	7	4	IC	P	0.01	39.50	15.47	0.00	0.00	0.03	45.12	0.20	0.04	0.13	0.24	.	100.74	83.864
PK003/59B	OLI	7	5	IR	P	0.02	39.28	15.45	0.00	0.00	0.02	44.83	0.19	0.03	0.13	0.24	.	100.19	83.794
PK003/59B	OLI	7	6	RI	P	0.02	39.06	15.32	0.00	0.00	0.03	44.62	0.20	0.04	0.13	0.23	.	99.65	83.845
PK003/59B	OLI	7	7	R	P	0.07	39.09	15.22	0.02	0.00	0.02	44.75	0.18	0.05	0.14	0.24	.	99.78	83.973
PK003/59B	OLI	20	1	C	P	0.03	39.35	14.70	0.00	0.00	0.02	45.21	0.18	0.03	0.12	0.32	.	99.96	84.569
PK003/59B	OLI	20	2	R	P	0.00	39.42	15.00	0.01	0.00	0.02	45.03	0.22	0.04	0.24	0.20	.	100.18	84.251
PK003/59B	OLI	21	1	C	P	0.01	39.10	16.19	0.01	0.00	0.02	43.17	0.23	0.02	0.16	0.20	.	99.11	82.614
PK003/59B	OLI	21	2	R	P	0.02	39.42	14.53	0.00	0.00	0.05	44.81	0.19	0.03	0.20	0.18	.	99.43	84.605
PK003/59B	OLI	10	1	C	P	0.12	39.52	12.64	0.02	0.01	0.03	47.22	0.17	0.03	0.17	0.39	.	100.32	86.940
PK003/58B	OLI	10	1	C	MP	0.020	39.587	15.307	0.004	0.015	0.017	44.095	0.187	0.034	0.130	0.247	0.000	99.644	83.696
PK003/58B	OLI	10	2	R	MP	0.015	39.957	15.449	0.006	0.000	0.007	43.124	0.296	0.056	0.490	0.092	0.014	99.507	83.261
PK003/58B	OLI	11	1	C	MP	0.013	39.288	18.164	0.002	0.010	0.035	41.617	0.241	0.005	0.145	0.152	0.000	99.672	80.326
PK003/58B	OLI	15	1	C	MP	0.007	39.715	15.356	0.002	0.000	0.016	44.425	0.131	0.016	0.124	0.262	0.005	100.059	83.754
PK003/58B	OLI	15	2	R	MP	0.012	39.430	16.143	0.008	0.012	0.012	43.491	0.253	0.035	0.389	0.110	0.012	99.907	82.761
PK003/58B	OLI	17	1	C	MP	0.016	39.749	15.001	0.000	0.010	0.009	44.894	0.216	0.037	0.110	0.288	0.018	100.346	84.210
PK003/58B	OLI	17	2	R	MP	0.024	39.406	15.531	0.009	0.012	0.026	43.834	0.168	0.046	0.268	0.117	0.000	99.442	83.415
PK003/58B	OLI	19	1	C	MP	0.003	39.366	16.518	0.004	0.000	0.014	43.288	0.242	0.026	0.135	0.246	0.009	99.851	82.363
PK003/58B	OLI	19	2	R	MP	0.013	39.500	16.265	0.007	0.052	0.010	43.238	0.249	0.061	0.456	0.113	0.028	99.990	82.570
PK003/58B	OLI	24	1	C	MP	0.015	39.330	16.222	0.000	0.026	0.029	42.678	0.189	0.030	0.144	0.251	0.002	98.917	82.420
PK003/58B	OLI	24	2	R	MP	0.003	39.531	16.401	0.002	0.019	0.005	42.593	0.296	0.046	0.385	0.108	0.000	99.362	82.231
PK003/58B	OLI	31	1	C	MP	0.022	39.737	14.875	0.000	0.032	0.036	44.604	0.158	0.021	0.155	0.330	0.000	99.969	84.236
PK003/58B	OLI	31	2	R	MP	0.020	39.975	14.673	0.000	0.028	0.019	44.291	0.209	0.068	0.270	0.231	0.001	99.785	84.324
PK003/58B	OLI	37	1	I	MP	0.000	40.831	11.156	0.003	0.005	0.015	48.112	0.097	0.040	0.089	0.341	0.000	100.688	88.486
PK003/58B	OLI	4	1	C	MP	0.017	39.754	15.795	0.000	0.020	0.018	43.307	0.195	0.044	0.283	0.166	0.013	99.611	83.010
PK003/58B	OLI	6	1	C	MP	0.014	40.833	9.857	0.021	0.088	0.039	48.340	0.120	0.039	0.187	0.400	0.031	99.970	89.732

OCCNUM	MIN	GR	A	PO	PA	NA2O	SIO2	FEO	K2O	CR2O3	AL2O3	MGO	MNO	TIO2	CAO	NIO	V2O5	TOTAL	FO
PK003/58B	OLI	8	1	C	MP	0.023	39.959	15.170	0.004	0.034	0.049	43.926	0.182	0.070	0.267	0.167	0.007	99.859	83.766
PK003/58B	OLI	9	1	C	MP	0.02	40.513	10.986	0.000	0.022	0.038	47.741	0.161	0.059	0.186	0.341	0.006	100.073	88.563
PK003/58B	OLI	9	2	R	MP	0.030	39.523	15.344	0.033	0.051	0.020	43.956	0.189	0.057	0.294	0.164	0.015	99.677	83.620
PK003/58B	OLI	18	1	C	MP	0.014	39.774	13.922	0.000	0.046	0.015	45.099	0.172	0.047	0.236	0.251	0.000	99.577	85.235
PK003/58B	OLI	18	2	R	MP	0.021	39.203	15.662	0.000	0.022	0.030	43.475	0.204	0.071	0.296	0.157	0.000	99.141	83.183
PK003/58B	OLI	20	1	C	MP	0.002	40.476	10.974	0.000	0.092	0.029	47.506	0.129	0.032	0.198	0.408	0.000	99.866	88.524
PK003/58B	OLI	20	2	R	MP	0.019	39.580	16.361	0.000	0.016	0.016	43.188	0.250	0.077	0.305	0.129	0.020	99.961	82.468
PK003/58B	OLI	21	1	C	MP	0.023	40.194	12.645	0.000	0.078	0.036	46.288	0.163	0.020	0.213	0.308	0.006	99.973	86.708
PK003/58B	OLI	26	1	C	MP	0.018	39.988	14.317	0.000	0.010	0.010	44.995	0.149	0.030	0.101	0.350	0.016	99.985	84.849
PK003/58B	OLI	27	1	IC	MP	0.030	39.565	15.521	0.007	0.027	0.022	43.669	0.184	0.058	0.299	0.152	0.017	99.552	83.371
PK003/58B	OLI	30	1	C	MP	0.019	40.989	9.120	0.002	0.000	0.000	49.326	0.117	0.000	0.062	0.321	0.011	99.968	90.600
PK003/58B	OLI	32	1	C	MP	0.007	39.639	14.305	0.010	0.036	0.025	44.687	0.191	0.061	0.263	0.239	0.005	99.469	84.772
PK003/58B	OLI	33	1	C	MP	0.011	39.110	17.138	0.003	0.009	0.020	42.538	0.182	0.074	0.198	0.135	0.019	99.437	81.560
PK003/59A	OLI	26	1	C	MP	0.01	39.06	14.79	0.00	0.01	0.01	45.11	0.19	0.06	0.18	0.22	.	99.64	84.460
PK003/59A	OLI	26	2	R	MP	0.08	39.07	15.54	0.01	0.00	0.02	44.57	0.27	0.11	0.40	0.16	.	100.23	83.636
PK003/59A	OLI	28	1	C	MP	0.00	39.64	12.32	0.00	0.03	0.04	47.35	0.17	0.05	0.23	0.33	.	100.16	87.259
PK003/59B	OLI	22	1	IC	MP	0.00	39.11	16.46	0.01	0.00	0.03	43.83	0.23	0.03	0.15	0.21	.	100.06	82.594
PK003/59B	OLI	8	1	C	MP	0.03	39.41	14.68	0.00	0.00	0.04	45.83	0.30	0.10	0.55	0.09	.	100.63	84.764
PK003/59B	OLI	9	1	C	MP	0.01	39.07	15.58	0.01	0.00	0.03	44.66	0.26	0.08	0.37	0.12	.	100.19	83.628
PK003/59B	OLI	11	1	C	MP	0.01	39.16	16.31	0.00	0.00	0.03	44.04	0.24	0.03	0.22	0.16	.	100.20	82.793
PK003/59B	OLI	11	2	R	MP	0.00	39.37	15.19	0.00	0.00	0.02	45.20	0.28	0.11	0.49	0.10	.	100.76	84.133
PK003/59B	OLI	12	1	C	MP	0.01	39.47	15.03	0.00	0.00	0.03	45.09	0.19	0.02	0.14	0.24	.	100.22	84.242
PK003/59B	OLI	16	1	IR	MP	0.00	39.54	14.77	0.00	0.00	0.02	45.63	0.18	0.02	0.12	0.25	.	100.53	84.628
PK003/59B	OLI	16	2	IR	MP	0.00	40.28	9.38	0.00	0.00	0.01	49.83	0.12	0.00	0.07	0.38	.	100.07	90.446
PK003/59B	OLI	16	3	IR	MP	0.01	40.33	9.40	0.00	0.00	0.01	49.37	0.13	0.00	0.07	0.37	.	99.69	90.347
PK003/59B	OLI	16	4	R	MP	0.01	40.35	9.45	0.00	0.00	0.01	49.53	0.11	0.00	0.07	0.37	.	99.90	90.329
PK003/59B	OLI	17	1	IR	MP	0.02	40.32	9.39	0.00	0.00	0.01	49.93	0.11	0.00	0.07	0.39	.	100.24	90.454
PK003/59B	OLI	17	2	IR	MP	0.00	39.46	14.66	0.01	0.00	0.03	45.23	0.18	0.03	0.14	0.24	.	99.98	84.610
PK003/59B	OLI	19	1	C	MP	0.11	39.22	14.51	0.03	0.00	0.02	45.56	0.19	0.03	0.13	0.26	.	100.06	84.838
PK003/59B	OLI	19	2	R	MP	0.02	39.39	13.84	0.02	0.00	0.02	45.88	0.19	0.07	0.28	0.23	.	99.94	85.523
PK003/59B	OLI	29	1	C	MP	0.01	40.38	9.70	0.00	0.00	0.02	49.42	0.11	0.01	0.09	0.38	.	100.12	90.078
PK003/59B	OLI	29	2	R	MP	0.01	39.39	16.01	0.00	0.01	0.04	44.74	0.30	0.07	0.41	0.10	.	101.08	83.277
PK003/59B	OLI	30	1	C	MP	0.01	39.77	14.51	0.00	0.01	0.06	45.22	0.20	0.04	0.12	0.28	.	100.22	84.741
PK003/59B	OLI	30	2	R	MP	0.02	39.74	14.20	0.00	0.03	0.06	46.30	0.20	0.07	0.27	0.22	.	101.11	85.316
PK003/59B	OLI	31	1	C	MP	0.22	39.29	14.15	0.02	0.04	0.14	45.14	0.20	0.12	0.38	0.17	.	99.87	85.041
PK003/64	OLI	3	1	C	MP	0.043	39.463	15.617	0.004	0.000	0.018	43.325	0.182	0.059	0.180	0.245	0.000	99.136	83.175
PK003/66D	OLI	3	1	C	MP	.	39.39	14.04	.	0.00	0.01	45.75	0.18	0.03	0.20	0.27	.	99.87	85.309
PK003/66D	OLI	3	2	R	MP	.	38.78	14.88	.	0.00	0.01	44.49	0.29	0.15	0.56	0.08	.	99.24	84.197
PK003/66D	OLI	3	3	RI	MP	.	39.08	15.10	.	0.00	0.01	44.77	0.30	0.13	0.53	0.10	.	100.02	84.085
PK003/66D	OLI	4	1	C	MP	.	39.04	15.53	.	0.01	0.03	44.27	0.24	0.07	0.29	0.15	.	99.63	83.552
PK003/66D	OLI	4	2	C	MP	.	39.07	15.43	.	0.02	0.01	44.69	0.24	0.07	0.28	0.16	.	99.97	83.769
PK003/66D	OLI	4	3	R	MP	.	39.36	16.18	.	0.01	0.02	44.92	0.29	0.11	0.42	0.09	.	101.40	83.186
PK003/66D	OLI	5	1	C	MP	.	39.50	15.66	.	0.00	0.03	45.29	0.22	0.06	0.28	0.16	.	101.20	83.750
PK003/66D	OLI	5	3	RI	MP	.	39.04	15.34	.	0.00	0.04	43.83	0.27	0.11	0.88	0.13	.	99.64	83.584
PK003/66D	OLI	6	1	C	MP	.	39.71	13.23	.	0.03	0.03	47.26	0.17	0.04	0.22	0.33	.	101.02	86.423
PK003/66D	OLI	9	1	C	MP	.	39.60	13.37	.	0.04	0.04	47.09	0.16	0.04	0.20	0.29	.	100.83	86.257
PK003/66D	OLI	9	2	R	MP	.	39.42	15.74	.	0.00	0.02	45.26	0.29	0.08	0.41	0.09	.	101.31	83.671

SPINEL ANALYSES

OCCNUM	MIN	GR	A	PO	PA	NA2O	SIO2	FE2O3	FEO	K2O	CR2O3	AL2O3	MGO	MNO	TIO2	CAO	NIO	CORRTOT
PK003/64B	SPI	1	1	C	X	0.002	0.024	14.393	25.100	0.000	34.168	6.364	9.834	0.393	9.022	0.015	0.359	99.674
PK003/64B	SPI	1	2	C	X	0.000	0.009	14.315	25.348	0.000	34.201	6.355	9.823	0.371	9.163	0.007	0.369	99.961
PK003/66D	SPI	1	1	C	X	0.013	0.032	3.578	11.695	0.005	38.225	28.523	15.811	0.166	0.267	0.000	0.209	98.524
PK003/66D	SPI	1	2	C	X	0.000	0.033	3.388	11.758	0.000	38.181	28.681	15.884	0.132	0.312	0.019	0.209	98.597
PK003/66D	SPI	1	3	R	X	0.023	0.032	41.088	30.649	0.014	0.478	4.279	8.309	0.689	13.778	0.145	0.058	99.542
PK003/56D	SPI	1	1	C	X	0.032	0.047	3.885	11.150	0.002	33.220	32.832	16.368	0.167	0.117	0.000	0.237	98.057
PK003/56D	SPI	1	2	I	X	0.006	0.056	3.888	11.433	0.012	33.034	32.652	16.319	0.102	0.249	0.034	0.222	98.008
PK003/56D	SPI	1	3	R	X	0.127	0.152	41.189	31.522	0.021	0.343	4.027	5.997	0.957	13.060	1.041	0.057	98.492
PK003/36C	SPI	1	1	C	X?	0.037	0.075	35.766	35.953	0.012	0.920	3.251	6.465	0.379	16.267	0.064	0.062	99.251
PK003/36C	SPI	1	2	R	X?	0.045	0.095	35.577	35.343	0.001	0.921	2.115	7.045	0.487	17.074	0.119	0.068	98.891
PK003/64	SPI	1	1	C	G	0.025	0.056	33.062	31.692	0.014	5.341	4.699	9.034	0.448	15.471	0.078	0.131	100.050
PK003/64	SPI	1	2	R	G	0.056	0.352	40.839	33.188	0.054	0.295	3.236	6.865	0.791	14.120	0.191	0.033	100.020
PK003/64	SPI	2	1	C	G	0.015	0.043	38.992	32.016	0.019	0.333	4.044	8.694	0.568	15.481	0.133	0.082	100.420
PK003/64	SPI	2	2	R	G	0.059	1.111	40.895	33.409	0.147	0.154	2.974	6.056	0.892	12.829	0.199	0.037	98.763
PK003/64	SPI	3	1	C	G	0.054	0.123	43.734	29.307	0.042	0.191	4.251	8.052	0.720	12.416	0.363	0.064	99.318
PK003/64	SPI	3	2	R	G	0.000	0.085	44.111	32.224	0.072	0.182	3.751	5.742	0.964	11.911	0.367	0.022	99.432
PK003/64	SPI	4	1	C	G	0.029	0.046	35.716	32.475	0.031	2.481	4.131	7.986	0.807	15.455	0.112	0.108	99.377
PK003/64	SPI	4	2	R	G	0.030	0.054	43.215	31.697	0.030	0.054	4.248	6.720	0.792	12.581	0.331	0.032	99.785
PK003/64	SPI	5	1	C	G	0.036	0.053	32.983	32.211	0.009	4.988	4.687	8.994	0.480	15.895	0.079	0.151	100.566
PK003/64	SPI	5	2	R	G	0.001	0.038	41.512	31.668	0.001	0.228	4.112	7.791	0.535	13.650	0.119	0.067	99.722
PK003/64B	SPI	2	1	C	G	0.021	0.039	40.944	30.748	0.020	0.156	3.966	8.441	0.724	14.245	0.163	0.075	99.542
PK003/64B	SPI	2	2	R	G	0.020	0.220	43.263	33.019	0.017	0.080	3.076	5.415	0.980	12.284	0.278	0.093	98.744
PK003/64B	SPI	3	1	C	G	0.031	0.046	35.378	33.390	0.000	1.389	4.122	7.965	0.777	16.219	0.114	0.064	99.494
PK003/64B	SPI	3	2	R	G	0.000	0.125	32.344	31.172	0.031	5.235	4.661	9.183	0.502	15.458	0.112	0.109	98.932
PK003/64B	SPI	4	1	C	G	0.037	0.306	42.251	32.386	0.072	0.149	3.938	6.387	0.842	12.672	0.157	0.068	99.265
PK003/64B	SPI	5	1	C	G	0.042	0.054	35.017	32.358	0.005	1.396	4.099	8.933	0.540	16.678	0.175	0.119	99.416
PK003/64B	SPI	6	1	C	G	0.041	0.116	39.184	30.354	0.032	0.940	4.171	8.979	0.627	14.705	0.252	0.065	99.465
PK003/64B	SPI	6	2	R	G	0.064	0.273	43.085	30.974	0.094	0.127	3.942	6.936	0.852	12.855	0.762	0.095	100.058
PK003/64B	SPI	7	1	C	G	0.049	0.016	38.163	32.188	0.012	0.124	3.294	8.585	0.807	16.289	0.125	0.092	99.745
PK003/64B	SPI	7	2	R	G	0.029	0.044	43.644	29.822	0.011	0.066	4.458	8.003	0.742	12.445	0.130	0.085	99.479
PK003/64B	SPI	8	1	C	G	0.014	0.044	24.310	36.413	0.007	2.636	3.465	9.507	0.638	22.020	0.068	0.141	99.263
PK003/64B	SPI	8	2	R	G	0.010	0.079	41.863	31.863	0.030	0.116	4.228	7.037	0.703	13.007	0.107	0.025	99.068
PK003/64B	SPI	9	1	C	G	0.025	0.006	33.725	36.504	0.013	0.064	2.227	7.300	0.564	18.748	0.095	0.111	99.382
PK003/64B	SPI	10	1	C	G	0.054	0.922	52.423	35.215	0.118	0.146	0.232	1.929	0.523	7.907	0.233	0.000	99.702
PK003/64B	SPI	11	1	C	G	0.027	0.085	35.180	36.720	0.008	1.114	3.363	5.560	0.341	15.750	0.044	0.044	98.235
PK003/64B	SPI	11	2	R	G	0.039	0.133	38.917	32.299	0.015	0.220	4.084	7.829	0.572	14.788	0.163	0.084	99.143
PK003/64B	SPI	12	1	C	G	0.016	0.054	36.322	32.829	0.019	1.161	4.091	8.291	0.665	16.084	0.250	0.067	99.849
PK003/64B	SPI	12	2	R	G	0.113	2.182	42.978	32.198	0.349	0.198	2.662	6.138	1.120	11.203	0.284	0.055	99.480
PK003/66D	SPI	2	1	C	G	0.000	0.041	33.776	32.553	0.006	3.022	4.467	8.516	0.571	15.981	0.157	0.084	99.174
PK003/66D	SPI	2	2	R	G	0.002	0.038	42.035	31.412	0.017	0.115	4.354	7.088	0.690	12.832	0.231	0.093	98.907
PK003/66D	SPI	3	1	C	G	0.021	0.043	34.088	31.955	0.007	4.137	4.312	8.220	0.588	15.106	0.131	0.089	98.697
PK003/66D	SPI	3	2	R	G	0.030	0.042	41.851	31.710	0.028	0.127	4.331	6.671	0.746	12.754	0.233	0.047	98.570
PK003/76	SPI	1	1	C	C	.	0.00	13.432	22.054	.	34.31	11.06	11.32	0.25	6.91	0.00	.	99.336
PK003/76	SPI	2	1	C	C	.	0.00	21.794	30.799	.	19.42	6.67	8.82	0.26	12.85	0.01	.	100.624
PK003/76	SPI	3	1	C	C	.	0.00	16.484	23.467	.	27.58	12.44	10.98	0.19	7.79	0.00	.	98.932
PK003/76	SPI	4	1	C	C	.	0.00	23.096	30.658	.	18.99	6.65	8.49	0.22	12.21	0.00	.	100.314
PK003/76	SPI	5	1	C	C	.	0.00	10.352	15.595	.	37.14	17.10	14.45	0.23	4.07	0.00	.	98.937
PK003/76	SPI	6	1	C	C	.	0.00	19.494	28.209	.	24.48	7.79	9.49	0.29	10.89	0.00	.	100.643
PK003/76	SPI	7	1	C	C	.	0.00	21.230	29.697	.	20.65	6.52	8.81	0.23	12.08	0.00	.	99.217
PK003/76	SPI	8	1	C	C	.	0.00	23.019	30.938	.	19.55	6.63	8.59	0.24	12.37	0.02	.	101.356
PK003/76	SPI	9	1	C	C	.	0.04	17.554	24.845	.	31.16	8.65	9.91	0.25	7.76	0.01	.	100.179
PK004/1	SPI	1	1	C	C	.	0.00	15.892	18.700	.	31.90	14.96	13.41	0.38	5.68	0.00	.	100.922
PK004/1	SPI	2	1	C	C	.	0.00	11.944	19.123	.	39.23	12.09	12.09	0.47	4.85	0.01	.	99.807
PK004/1	SPI	3	1	C	C	.	0.00	3.251	14.235	.	38.48	26.57	13.55	0.32	0.20	0.02	.	96.626
PK004/1	SPI	4	1	C	C	.	0.00	14.428	18.658	.	38.41	10.23	12.78	0.42	5.57	0.01	.	100.505
PK004/1	SPI	5	1	C	C	.	0.00	14.642	19.325	.	36.68	10.71	12.89	0.42	6.27	0.02	.	100.957
PK004/1	SPI	6	1	C	C	.	0.00	6.726	9.408	.	34.03	29.22	17.33	0.29	0.50	0.01	.	97.514
PK004/1	SPI	7	1	C	C	.	0.00	6.816	9.107	.	30.89	33.29	18.15	0.26	0.33	0.00	.	98.843
PK004/1	SPI	8	1	C	C	.	0.00	7.921	8.073	.	31.26	31.82	18.42	0.27	0.23	0.00	.	97.994
PK004/1	SPI	9	1	C	C	.	0.00	7.352	10.145	.	38.44	25.46	16.56	0.33	0.32	0.00	.	98.607
PK004/1	SPI	10	1	C	C	.	0.00	13.151	18.116	.	37.52	13.02	12.48	0.47	4.46	0.01	.	99.228

OCCNUM	MIN	GR	A	PO	PA	NA2O	SIO2	FE2O3	FEO	K2O	CR2O3	AL2O3	MGO	MNO	TIO2	CAO	NIO	CORRTOT
PK004/1	SPI	11	1	C	C	.	0.00	16.382	24.100	.	31.22	10.85	10.34	0.45	7.36	0.02	.	100.721
PK004/1	SPI	12	1	C	C	.	0.00	7.422	10.142	.	34.61	27.92	16.65	0.33	0.44	0.01	.	97.524
PK004/1	SPI	13	1	C	C	.	0.00	18.068	25.192	.	25.26	10.58	11.08	0.43	9.94	0.02	.	100.570
PK004/1	SPI	14	1	C	C	.	0.00	7.144	9.052	.	25.27	37.01	18.59	0.22	0.65	0.00	.	97.936
PK004/1	SPI	15	1	C	C	.	0.00	7.698	7.693	.	25.85	36.79	19.05	0.21	0.14	0.00	.	97.431
PK004/1	SPI	16	1	C	C	.	0.00	10.240	14.956	.	30.51	24.14	15.10	0.34	3.44	0.01	.	98.736
PK004/1	SPI	17	1	C	C	.	0.00	7.655	9.412	.	29.49	32.12	17.52	0.28	0.51	0.01	.	96.997
PK004/1	SPI	18	1	C	C	.	0.00	14.677	19.503	.	37.23	9.88	12.38	0.44	6.04	0.01	.	100.160
PK004/1	SPI	19	1	C	C	.	0.00	14.173	18.447	.	37.00	12.98	12.89	0.41	4.92	0.02	.	100.840
PK004/1	SPI	20	1	C	C	.	0.00	13.415	19.409	.	37.45	11.72	12.31	0.40	5.44	0.02	.	100.164
PK004/1	SPI	21	1	C	C	.	0.00	14.112	18.152	.	36.14	13.54	13.01	0.41	4.89	0.01	.	100.264
PK004/1	SPI	22	1	C	C	.	0.00	4.057	12.070	.	42.07	23.06	14.72	0.34	0.39	0.01	.	96.716
PK004/1	SPI	23	1	C	C	.	0.00	15.377	20.024	.	34.54	11.21	12.42	0.41	6.37	0.02	.	100.371
PK004/1	SPI	24	1	C	C	.	0.00	15.935	17.741	.	32.60	13.19	12.80	0.49	5.11	0.01	.	97.876
PK004/1	SPI	25	1	C	C	.	0.00	13.846	18.961	.	38.30	10.60	12.76	0.41	5.75	0.02	.	100.647
PK004/1	SPI	26	1	C	C	.	0.00	14.388	18.763	.	38.24	9.95	12.78	0.42	5.80	0.02	.	100.362
PK004/1	SPI	27	1	C	C	.	0.00	14.988	19.253	.	34.09	13.03	12.72	0.42	5.74	0.01	.	100.252
PK004/1	SPI	28	1	C	C	.	0.00	14.443	19.094	.	37.28	10.14	12.90	0.42	6.26	0.01	.	100.547
PK004/1	SPI	29	1	C	C	.	0.00	15.543	19.584	.	34.68	11.41	12.47	0.39	6.00	0.01	.	100.087
PK004/1	SPI	30	1	C	C	.	0.00	15.251	19.777	.	37.10	9.57	12.42	0.42	6.24	0.02	.	100.798
PK004/1	SPI	31	1	C	C	.	0.00	25.626	31.762	.	19.33	5.78	7.74	0.44	11.83	0.01	.	102.517
PK004/1	SPI	32	1	C	C	.	0.00	8.167	6.191	.	21.21	38.82	19.57	0.18	0.11	0.00	.	94.248
PK004/1	SPI	33	1	C	C	.	0.00	7.784	5.896	.	23.58	37.36	19.68	0.18	0.10	0.00	.	94.580
PK004/1	SPI	34	1	C	C	.	0.00	13.716	17.528	.	34.60	16.30	13.31	0.37	4.24	0.01	.	100.074
PK004/1	SPI	35	1	C	C	.	0.00	15.140	20.237	.	36.77	9.41	12.34	0.45	6.61	0.02	.	100.977
PK004/1	SPI	36	1	C	C	.	0.00	24.095	29.699	.	20.77	6.57	8.98	0.45	11.62	0.02	.	102.204
PK004/1	SPI	37	1	C	C	.	0.00	15.139	19.118	.	37.05	9.97	12.83	0.42	6.15	0.00	.	100.677
PK004/1	SPI	38	1	C	C	.	0.00	9.462	11.926	.	45.69	15.25	15.46	0.46	1.86	0.00	.	100.108
PK004/1	SPI	39	1	C	C	.	0.00	12.399	18.423	.	43.28	11.70	11.43	0.49	2.80	0.02	.	100.542
PK004/1	SPI	40	1	C	C	.	0.00	15.173	19.157	.	34.85	12.47	12.73	0.42	5.67	0.01	.	100.480
PK004/1	SPI	41	1	C	C	.	0.00	14.201	19.082	.	36.96	11.47	13.05	0.41	6.02	0.01	.	101.203
PK004/1	SPI	42	1	C	C	.	0.00	14.845	18.622	.	35.98	12.28	13.27	0.39	5.75	0.01	.	101.147
PK004/1	SPI	43	1	C	C	.	0.00	14.125	18.640	.	38.61	10.42	12.95	0.43	5.69	0.02	.	100.885
PK004/1	SPI	44	1	C	C	.	0.00	15.251	18.397	.	33.65	14.47	13.06	0.36	5.06	0.02	.	100.268
PK004/1	SPI	45	1	C	C	.	0.00	14.480	19.521	.	37.04	9.89	12.66	0.40	6.40	0.01	.	100.401
PK004/1	SPI	46	1	C	C	.	0.00	15.632	19.864	.	34.85	11.22	12.51	0.42	6.22	0.01	.	100.726
PK004/1	SPI	47	1	C	C	.	0.00	20.259	26.311	.	23.41	7.85	11.22	0.41	11.69	0.01	.	101.160
PK004/1	SPI	48	1	C	C	.	0.00	15.663	19.346	.	33.72	12.84	12.93	0.38	5.98	0.01	.	100.869
PK004/1	SPI	49	1	C	C	.	0.00	7.894	6.907	.	23.67	37.68	19.37	0.20	0.19	0.00	.	95.911
PK004/1	SPI	50	1	C	C	.	0.00	15.221	22.314	.	28.18	13.29	12.63	0.41	8.74	0.01	.	100.795
PK004/1	SPI	51	1	C	C	.	0.00	14.811	19.153	.	35.01	12.33	12.51	0.38	5.53	0.01	.	99.734
PK004/1	SPI	52	1	C	C	.	0.00	5.859	8.808	.	33.38	30.29	17.46	0.26	0.24	0.00	.	96.297
PK004/1	SPI	53	1	C	C	.	0.00	23.658	33.642	.	14.08	5.73	7.88	0.47	14.93	0.02	.	100.410
PK004/1	SPI	54	1	C	C	.	0.00	10.455	20.122	.	41.53	10.68	11.54	0.45	5.17	0.01	.	99.957
PK004/1	SPI	55	1	C	C	.	0.00	16.142	19.576	.	31.81	12.49	12.91	0.39	6.62	0.02	.	99.957
PK004/1	SPI	56	1	C	C	.	0.00	14.070	20.020	.	38.10	9.63	12.05	0.42	6.01	0.01	.	100.310
PK004/1	SPI	57	1	C	C	.	0.00	10.058	19.449	.	42.61	11.99	11.75	0.48	4.33	0.02	.	100.688
PK004/1	SPI	58	1	C	C	.	0.00	12.455	18.083	.	40.83	10.85	12.98	0.42	5.07	0.02	.	100.708
PK004/1	SPI	59	1	C	C	.	0.00	14.540	20.866	.	36.63	9.87	12.02	0.41	6.62	0.01	.	100.967
PK004/1	SPI	60	1	C	C	.	0.00	7.875	10.654	.	41.14	22.29	16.22	0.37	0.69	0.00	.	99.239
PK004/1	SPI	61	1	C	C	.	0.00	6.076	14.633	.	45.32	17.20	13.11	0.40	1.19	0.01	.	97.939
PK005/1	SPI	1	1	C	C	.	0.00	22.161	30.200	.	18.58	7.13	9.60	0.41	13.33	0.02	.	101.430
PK005/1	SPI	2	1	C	C	.	0.00	6.364	13.683	.	33.34	28.93	14.25	0.20	0.16	0.01	.	96.938
PK005/1	SPI	3	1	C	C	.	0.00	4.853	10.654	.	35.84	28.78	16.02	0.29	0.06	0.01	.	96.506
PK005/1	SPI	4	1	C	C	.	0.00	6.771	8.918	.	34.23	29.58	17.35	0.28	0.03	0.00	.	97.158
PK005/1	SPI	5	1	C	C	.	0.00	23.126	30.861	.	17.45	6.93	9.29	0.42	13.53	0.02	.	101.627
PK005/1	SPI	6	1	C	C	.	0.00	21.082	29.110	.	19.49	8.49	9.97	0.40	12.59	0.03	.	101.162
PK005/1	SPI	7	1	C	C	.	0.00	21.830	22.187	.	27.34	18.21	8.05	0.48	0.81	0.01	.	98.917
PK005/1	SPI	8	1	C	C	.	0.00	19.115	23.400	.	40.36	5.24	8.04	0.68	3.94	0.03	.	100.805
PK005/1	SPI	9	1	C	C	.	0.00	25.821	30.676	.	18.69	5.91	8.37	0.47	11.95	0.03	.	101.917
PK005/2	SPI	1	1	C	C	.	0.00	7.081	8.798	.	35.74	27.65	17.25	0.31	0.17	0.01	.	97.009
PK005/2	SPI	2	1	C	C	.	0.00	5.876	8.203	.	28.10	35.28	18.35	0.24	0.21	0.01	.	96.269
PK005/2	SPI	3	1	C	C	.	0.00	22.085	28.607	.	20.49	8.20	10.00	0.43	11.95	0.02	.	101.783

OCCNUM	MIN	GR	A	PO	PA	NA2O	SIO2	FE2O3	FEO	K2O	CR2O3	AL2O3	MGO	MNO	TIO2	CAO	NIO	CORRTOT
PK005/2	SPI	4	1	C	C	.	0.00	6.640	9.015	.	31.37	32.55	17.78	0.26	0.12	0.00	.	97.735
PK005/2	SPI	5	1	C	C	.	0.00	5.827	10.357	.	41.00	24.79	16.39	0.37	0.27	0.01	.	99.014
PK005/2	SPI	6	1	C	C	.	0.00	23.359	29.851	.	19.56	7.43	9.61	0.42	12.47	0.01	.	102.710
PK005/2	SPI	7	1	C	C	.	0.00	15.020	19.925	.	21.68	30.44	10.36	0.39	0.19	0.01	.	98.015
PK005/2	SPI	8	1	C	C	.	0.00	22.167	29.444	.	19.21	8.18	9.58	0.43	12.33	0.03	.	101.371
PK005/2	SPI	9	1	C	C	.	0.00	5.227	9.087	.	31.05	33.81	17.90	0.22	0.20	0.00	.	97.494
PK005/2	SPI	10	1	C	C	.	0.00	22.341	29.967	.	18.09	7.26	9.50	0.42	13.14	0.02	.	100.738
PK005/3	SPI	1	1	C	C	.	0.00	9.092	10.049	.	39.61	22.36	15.86	0.38	0.08	0.01	.	97.441
PK005/3	SPI	2	1	C	C	.	0.00	6.531	8.993	.	37.26	26.82	17.11	0.30	0.19	0.00	.	97.204
PK005/3	SPI	3	1	C	C	.	0.00	7.440	9.166	.	36.32	27.30	17.03	0.32	0.05	0.00	.	97.625
PK005/3	SPI	4	1	C	C	.	0.00	21.030	27.907	.	21.96	8.18	10.37	0.43	11.82	0.03	.	101.727
PK005/3	SPI	5	1	C	C	.	0.00	7.113	8.539	.	37.24	26.77	17.40	0.31	0.11	0.00	.	97.483
PK005/3	SPI	6	1	C	C	.	0.00	7.777	8.262	.	33.26	28.95	17.58	0.31	0.16	0.00	.	96.299
PK005/3	SPI	7	1	C	C	.	0.00	6.422	9.142	.	31.17	32.71	17.82	0.24	0.27	0.01	.	97.783
PK005/3	SPI	8	1	C	C	.	0.00	6.195	9.376	.	33.63	31.08	17.39	0.27	0.04	0.01	.	97.991
PK005/3	SPI	9	1	C	C	.	0.00	5.828	9.126	.	34.32	30.67	17.48	0.28	0.06	0.00	.	97.764
PK005/3	SPI	10	1	C	C	.	0.00	6.733	10.991	.	42.20	22.75	15.76	0.36	0.25	0.01	.	99.055
PK005/3	SPI	11	1	C	C	.	0.00	21.354	27.985	.	21.88	8.43	10.17	0.40	11.49	0.03	.	101.739
PK005/3	SPI	12	1	C	C	.	0.00	8.396	14.955	.	46.00	13.45	12.97	0.47	1.98	0.01	.	98.231
PK005/3	SPI	13	1	C	C	.	0.00	35.377	18.447	.	17.63	8.29	9.81	0.37	3.47	0.02	.	93.414
PK005/3	SPI	14	1	C	C	.	0.00	6.438	10.157	.	34.75	30.00	16.88	0.27	0.03	0.00	.	98.525
PK005/3	SPI	15	1	C	C	.	0.00	17.961	25.709	.	32.91	4.77	9.79	0.57	9.32	0.02	.	101.049
PK005/3	SPI	16	1	C	C	.	0.00	21.844	30.164	.	18.93	7.44	9.60	0.44	13.20	0.03	.	101.649
PK005/3	SPI	17	1	C	C	.	0.00	7.943	12.373	.	39.27	21.32	15.32	0.36	1.61	0.01	.	98.206
PK005/4	SPI	1	1	C	C	.	0.00	17.625	18.270	.	40.09	12.74	10.29	0.50	0.70	0.00	.	100.216
PK005/4	SPI	2	1	C	C	.	0.00	7.542	10.053	.	40.64	22.33	16.31	0.35	0.64	0.01	.	97.876
PK005/4	SPI	3	1	C	C	.	0.00	7.444	11.202	.	34.98	28.38	15.95	0.29	0.03	0.01	.	98.286
PK005/4	SPI	4	1	C	C	.	0.00	5.787	10.092	.	37.56	27.45	16.83	0.31	0.39	0.00	.	98.420
PK005/4	SPI	5	1	C	C	.	0.00	22.842	28.506	.	21.28	9.66	9.14	0.22	9.94	0.00	.	101.588
PK005/4	SPI	6	1	C	C	.	0.00	24.421	29.275	.	20.59	8.49	8.57	0.26	10.07	0.00	.	101.677
PK005/4	SPI	7	1	C	C	.	0.00	9.101	17.901	.	39.18	14.05	14.16	0.29	6.07	0.00	.	100.752
PK005/4	SPI	8	1	C	C	.	0.00	17.024	24.752	.	27.24	10.41	11.84	0.25	10.14	0.00	.	101.656
PK005/4	SPI	9	1	C	C	.	0.00	24.938	32.650	.	20.87	4.26	6.88	0.32	11.76	0.00	.	101.678

WHOLE ROCK

MAJOR ELEMENTS

NUMBER	SIO2	TIO2	AL203	FE203	MNO	MGO	NA2O	CAO	K2O	P2O5	LOI	TOTAL
PK001/3	24.43	3.61	5.36	11.82	0.23	8.96	0.33	20.16	1.36	3.62	19.91	100.00
PK001/4	23.59	3.46	5.06	16.10	0.23	10.13	0.51	20.18	1.15	2.63	16.54	100.32
PK003/55	34.82	3.98	6.78	15.30	0.27	21.43	0.75	6.49	2.43	2.15	6.62	101.28
PK003/56	31.47	3.88	6.65	14.51	0.27	20.46	1.23	9.36	2.59	2.14	8.46	101.24
PK003/58	30.35	3.96	5.78	14.52	0.23	22.00	1.09	10.38	1.64	1.70	9.33	101.15
PK003/59	31.32	3.85	5.80	14.48	0.23	20.73	1.39	10.74	1.90	1.77	8.78	101.15
PK003/64	37.15	3.61	6.08	13.79	0.23	17.00	1.16	11.72	1.56	1.72	6.59	100.92
PK003/66	38.02	3.58	6.00	13.41	0.23	18.10	1.33	11.40	1.44	1.72	5.68	101.17
PK001/3R	24.39	3.60	5.37	11.85	0.23	8.94	0.34	20.08	1.37	3.63	19.91	99.91
PK001/4R	23.59	3.46	5.08	16.08	0.23	9.86	0.55	20.11	1.27	2.63	16.54	100.14
PK003/66R	37.94	3.58	5.96	13.43	0.23	18.06	1.35	11.37	1.48	1.72	5.68	101.06

TRACE ELEMENTS

OCCNUM	AS	CE	CO	CR	GA	LA	NB	ND	NI	PB	RB	SC	SR	TH	U	V	Y	ZN	ZR	BA
PK001/3	4	575	-9	148	10	296	220	230	80	136	31	-7	2671	73	21	294	64	159	881	1791
PK001/4	-1	471	-7	191	-2	241	196	194	222	95	24	-5	2462	71	22	207	252	149	687	6641
PK003/55	4	342	50	671	14	199	322	148	1162	91	75	51	1506	48	17	280	56	138	880	2418
PK003/56	3	352	32	454	13	181	240	136	420	78	69	36	1368	44	15	291	54	137	835	2060
PK003/58	2	378	41	544	12	204	216	166	429	63	43	13	1349	48	16	213	41	133	416	1612
PK003/59	1	371	49	496	13	204	213	154	457	68	48	-7	1481	48	13	217	43	131	428	1433
PK003/64	2	340	39	430	13	179	190	134	366	80	40	-7	1731	46	15	227	41	128	527	2776
PK003/66	2	346	34	414	11	170	190	142	381	77	35	-7	1612	44	13	222	40	125	531	2418
PK001/3R	4	554	-9	150	8	297	222	232	80	138	32	-8	2669	77	24	302	64	159	884	
PK001/4R	2	470	-7	159	6	254	181	206	194	87	22	20	2456	65	15	197	52	141	693	
PK003/66R	2	330	30	414	12	181	191	135	381	77	37	21	1616	45	17	220	40	119	530	

Rb-Sr WHOLE ROCK RESULTS

LOCALITY: EMTILOMBO PK3

No.	^{87}Rb	TOT. Rb	^{86}Sr	TOT. Sr	$^{87}Rb/^{86}Sr$ *	$^{87}/^{86}Sr$	SD	SE	2σ
23	15,6769	55,3863	68,7057	708,0439	0,2255	0,710554	0,000289	0,000038	0,000076
40	17,6157	62,2363	200,2025	2063,9317	0,0870	0,714276	0,000297	0,000020	0,000040
47	10,6858	37,7528	89,5865	924,3113	0,1179	0,722489	0,00184	0,000185	0,000370
48	10,3129	36,4354	63,7475	656,6739	0,1599	0,706312	0,000411	0,000030	0,000060
56	20,7651	73,3630	118,0237	1216,1045	0,1739	0,709016	0,000382	0,000022	0,000040
56 AG	20,5259	72,5179	115,7698	1192,8720	0,1752	0,708941	0,000271	0,000020	0,00004
58	12,3589	43,6638	116,2446	1197,7918	0,1051	0,709021	0,000281	0,000026	0,000059
59	16,6770	58,9198	132,8963	1369,7394	0,1240	0,711912	0,000978	0,000076	0,00015
60	17,1045	60,4301	109,8148	1131,9659	0,1539	0,713026	0,000294	0,000029	0,00005
61	17,9524	63,4257	129,8382	1343,1372	0,1367	0,711809	0,000259	0,000027	0,00005
64	11,4112	40,3157	165,0071	1700,7006	0,0684	0,711916	0,000385	0,000022	0,000044
66	9,9646	35,2049	147,9846	1524,7792	0,0666	0,708755	0,000421	0,000027	0,000050
67	10,7256	37,8936	143,4980	1478,6253	0,0739	0,709266	0,000285	0,000023	0,000046
67AG	10,6972	37,7931	143,2850	1477,0565	0,0738	0,713581	0,000319	0,000032	0,000060

No.	87Rb/86Sr	87/86Sr +/- 2σ		Calculated Ro at 80My
23	0,2255	0,710554	76	0,7103
40	0,0870	0,714276	40	0,7142
47	0,1179	0,722489	370	0,7222
48	0,1599	0,706312	60	0,7061
56	0,1739	0,709016	44	0,7088
56AG	0,1752	0,708941	40	0,7087
58	0,1051	0,709021	52	0,7089
59	0,1240	0,711912	152	0,7118
60	0,1539	0,713126	58	0,7130
61	0,1367	0,711809	54	0,7117
64	0,0684	0,711916	44	0,7118
66	0,0566	0,708755	54	0,7087
67	0,0739	0,709266	46	0,7092
67AG	0,0736	0,713581	64	0,7135

(AG means rock crushed in agate sieb)

APPENDIX 3

1.1 FILES ON DISK

The data is in ASCII format.

Olivine Analyses - OLIVINE.MIN

Spinel Analyses - SPINEL.MIN

Whole Rock Data:

Major Elements - MAJORS.XRF

Trace Elements - TRACE.XRF

1.2 FORMAT OF DATA

The format of the data is shown on the listing overleaf. Abbreviations are as explained in Appendix 2. For the whole rock major element data the variable names occur on the first line and the analyses start on the second line. The data for each sample analysed occupies a single line. A blank row occurs between the samples from different localities. An 'R' attached to the locality/sample number means a replicate analysis.

For the remainder of the data the variable names occur on the first and second lines and analyses start on the third line. The data for each sample/mineral grain analysed occupies two

rows. In the case of the mineral chemistry analyses a blank row separates each paragenetic group.

The original microprobe determined total iron and analytical total (wt%) are included with the spinel data. They occur as the last two numbers in the second row of each analysis. Variable names are FEO and TOTAL respectively.

3.1 OLIVINE DATA

OCCNUM	MIN	GR	A	PO	PA	NA2O	SIO2	FEO	K2O	CR2O3	AL2O3	MGO	MNO
TIO2	CAO	NIO	V2O5	TOTAL	FO	REMARKS							
PK003/59B	OLI	3	4	R	M	0.00	39.75	15.57	0.00	0.01	0.21	43.06	0.29
0.07	0.48	0.11	.	99.55	83.132								
PK003/59B	OLI	3	5	C	M	0.02	39.77	14.86	0.00	0.01	0.03	45.08	0.18
0.04	0.13	0.30	.	100.42	84.389								
PK003/59B	OLI	3	6	C	M	0.02	39.50	14.86	0.00	0.01	0.03	45.62	0.17
0.04	0.13	0.28	.	100.66	84.546								
PK003/58B	OLI	2	1	R	CP	0.022	39.272	14.157	0.021	0.000	0.013	44.756	0.356
0.036	1.043	0.050	0.006	99.732	84.925								
PK003/58B	OLI	2	2	R	CP	0.005	39.484	14.613	0.001	0.000	0.003	44.459	0.310
0.048	0.719	0.059	0.000	99.702	84.428								
PK003/58B	OLI	20	2	R	MP	0.019	39.580	16.361	0.000	0.016	0.016	43.188	0.250
0.077	0.305	0.129	0.020	99.961	82.468								
PK003/58B	OLI	21	1	C	MP	0.023	40.194	12.645	0.000	0.078	0.036	46.288	0.163
0.020	0.213	0.308	0.006	99.973	86.708								

3.2 SPINEL DATA

OCCNUM	MIN	GR	A	PO	PA	NA2O	SIO2	FE2O3	FEO	K2O	CR2O3	AL2O3	MGO
MNO	TIO2	CAO	NIO	CORRTOT	FEO	TOTAL						REMARKS	
PK003/64B	SPI	1	1	C	X	0.002	0.024	14.393	25.100	0.000	34.168	6.364	9.834
0.393	9.022	0.015	0.359	99.674	38.051	98.232	DUNITE						
PK003/64B	SPI	1	2	C	X	0.000	0.009	14.315	25.348	0.000	34.201	6.355	9.823
0.371	9.163	0.007	0.369	99.961	38.229	98.527	DUNITE						
PK003/66D	SPI	1	1	C	X	0.013	0.032	3.578	11.695	0.005	38.225	28.523	15.811
0.166	0.267	0.000	0.209	98.524	14.915	98.166	DISCRETE						
PK003/64	SPI	1	1	C	G	0.025	0.056	33.062	31.692	0.014	5.341	4.699	9.034
0.448	15.471	0.078	0.131	100.050	61.441	96.738							
PK003/64	SPI	1	2	R	G	0.056	0.352	40.839	33.188	0.054	0.295	3.236	6.865
0.791	14.120	0.191	0.033	100.020	69.936	95.929							
PK003/64	SPI	2	1	C	G	0.015	0.043	38.992	32.016	0.019	0.333	4.044	8.694
0.568	15.481	0.133	0.082	100.420	67.101	96.513							

3.3 MAJOR ELEMENT WHOLE ROCK DATA (WT%)

NUMBER	SIO2	TIO2	AL2O3	FE2O3	MNO	MGO	NA2O	CAO	K2O	P2O5	LOI	TOTAL
PK001/3	24.43	3.61	5.36	11.82	0.23	8.96	0.33	20.16	1.36	3.62	19.91	100.00
PK001/4	23.59	3.46	5.06	16.10	0.23	10.13	0.51	20.18	1.15	2.63	16.54	100.32
PK003/55	34.82	3.98	6.78	15.30	0.27	21.43	0.75	6.49	2.43	2.15	6.62	101.28
PK003/56	31.47	3.88	6.65	14.51	0.27	20.46	1.23	9.36	2.59	2.14	8.46	101.24
PK003/58	30.35	3.96	5.78	14.52	0.23	22.00	1.09	10.38	1.64	1.70	9.33	101.15
PK001/4R	23.59	3.46	5.08	16.08	0.23	9.86	0.55	20.11	1.27	2.63	16.54	100.14

3.4 TRACE ELEMENT WHOLE ROCK DATA (PPM)

OCCNUM	AS	CE	CO	CR	GA	LA	NB	ND	NI	PB	RB	SC	SR	TH	U	V	Y	ZN
ZR	BA																	
PK001/3	4	575	-9	148	10	296	220	230	80	136	31	-7	2671	73	21	294	64	159
881	1791																	
PK001/4	-1	471	-7	191	-2	241	196	194	222	95	24	-5	2462	71	22	207	252	149
687	6641																	
PK003/55	4	342	50	671	14	199	322	148	1162	91	75	51	1506	48	17	280	56	138
880	2418																	
PK003/56	3	352	32	454	13	181	240	136	420	78	69	36	1368	44	15	291	54	137
835	2060																	